Molecular and phenotypic characterisation of zebrafish mutants displaying defects in axonal development in the central nervous system.

Maryam Mangoli

A thesis submitted for the degree of Doctor in Philosophy

in the University of London

Department of Paediatrics and Child Health

Royal Free and University College Medical School

University College London

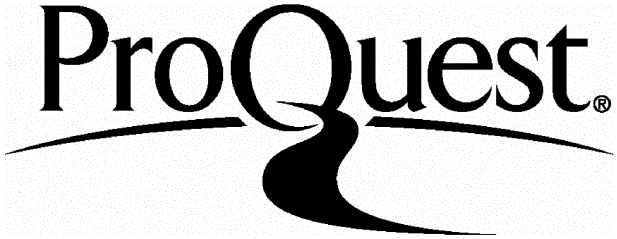

Abstract

Zebrafish mutants isolated from large-scale chemical mutagenesis screens display defects in various aspects of embryonic development (Driever, 1996; Haffter, 1996). The aim of this project was to investigate the role of *monorail*^{tv53a}, *eisspalte*^{ty77e}, *otter*^{ta76b} and *shrink*^{U41} in central nervous system (CNS) development, both by characterisation of mutant phenotypes and by genetic mapping and identification of the mutated genes. It was anticipated that the findings would provide new insights into early vertebrate brain development by increasing knowledge of the components involved in neuronal patterning and axon pathfinding in the CNS.

Phenotypic analysis of homozygous *monorail*^{tv53a} mutant embryos revealed a reduction in the width of the floor plate in the ventral CNS as well as defects in induction and patterning of adjacent neurons in the midbrain and hindbrain. The gene was mapped to linkage group 17 in a region harbouring two *fork head* genes, *foxA1* and *foxA2*, both of which are expressed in the floor plate. Sequence analysis of *foxA1* revealed no significant changes in amino acid sequence between *monorail* and wild-type siblings. Sequence analysis of *foxA2* identified a nonsense mutation in the conserved fork head DNA binding domain in *monorail*. This change creates a stop codon and results in absence of 84 % of the DNA binding domain, complete loss of transactivating domains II and III and is predicted to render the FoxA2 protein non-functional.

Phenotypic characterisation and genetic mapping of *shrink*^{U41}, *otter*^{ta76b} and *eisspalte*^{ty77e} was undertaken and revealed defasciculation of forebrain commissural axons and abnormal retinotectal projections in all mutants. These genes were mapped to linkage groups 6 (*shrink*) and 14 (*otter* and *eisspalte*). Further investigation of possible candidates for the *shrink*, *otter* and *eisspalte* phenotypes is underway.

Acknowledgements

Firstly I would like to thank my supervisor Michele Rees for her expert guidance and immense amounts of advice and support that she has given me throughout my PhD studies. Thank you Michele for your help and for being such a good friend and listener.

I am grateful to Mark Gardiner for allowing me to undertake this project in his lab and to everyone in the department of Paediatrics at UCL for their support. In particular thank you to Alicia White, Nichole Taske, Tonia Wilkinson, Morwenna Porter, Hannah Mitchison, Julie Sharp and Keith Parker for their technical assistance and for making the lab such an enjoyable place to work in. I will always be grateful to Alicia for all her encouragement, enthusiasm and expert guidance and for always making me laugh. Thank you also to Morwenna for our friendly chats!

I am very grateful to everyone in the zebrafish group at UCL for their help during my PhD. I would like to thank Stephen Wilson for all his expert guidance and Corinne Houart, Zsolt Lele, Will Norton, Jacqui Hoyle, Paul Chandwani, Lucy Kinton and Diz for teaching me lots of techniques and providing helpful suggestions. Thank you to Carole Wilson for helping me out with fish care on numerous occasions.

I would like to thank Robert Geisler, Gerd Rauch, Silke Geiger-Rudolph and Maria Bühl in Tübingen for all their help and technical advice.

I am very grateful to my family and friends for all their love and encouragement. Thank you to Mahnaz and Nasrin joon and family in Iran for being so understanding and supportive throughout the past four years.

I would like to say a special thank you to the person who has always given me hope, support, encouragement and lots of love, my wonderful Mum. Thank you for all the opportunities that you have given me. I could not have done this without you.

To Mum, Babi, Maman Sima and Baba Mohammad

Table of contents

Figures

Tables

Abbreviations

aa	amino acid
APS	ammonium persulphate
BLAST	Basic Local Alignment Search Tool
bp	base pair
BSA	bovine serum albumin
cDNA	complementary DNA
cM	centiMorgan
cR	centiRay
DEPC	diethylpyrocarbonate
DiI	1,1'-dioctadecyl-3,3,3',3'-tetramethyl indocarbocyanine perchlorate
DiO	3,3'-dioctadecyl oxacarbocyanine perchlorate
DMSO	dimethylsulphoxide
DNA	deoxyribonucleic acid
dNTP	deoxynucleoside triphosphate
DTT	dithiothreitol
ECL	enhanced chemiluminescence
EDTA	ethylene diaminetetra acetic acid
ENU	ethylnitrosurea
EST	expressed sequence tagged site
EtBr	ethidium bromide
FAM	5-carboxyfluorescein

fox	*forkhead box*
GFP	green fluorescent protein
HNF	hepatocyte nuclear factor
hpf	hours post fertilisation
HRP	horseradish peroxidase
IPTG	β-D-isopropyl-thiogalactopyranoside
kb	kilobase
kDa	kiloDalton
LB	Luria-Bertani (medium)
LOD	logarithm of odds
M	molar
Mb	megabase
min	minutes
mRNA	messenger RNA
NBT	nitro-blue tetrazolium
NCBI	National Centre for Biotechnology Information
NP40	Nonidet P40
nt	nucleotide
O/N	overnight
OD	optical density
ORF	open reading frame
PAGE	polyacrylamide gel electrophoresis
PBS	phosphate buffered saline

PBTriton	phosphate buffered saline with Triton X-100
PBTween	phosphate buffered saline with Tween-20
PCR	polymerase chain reaction
PMSF	phenylmethylsulphonylfluoride
PTU	1-phenyl-2-thiourea
RFLP	restriction fragment length polymorphism
rpm	revolutions per minute
RT	reverse transcription
RT-PCR	reverse transcription PCR
SDS	sodium dodecyl sulphate
SSLP	simple sequence length polymorphism
TAMRA	6-carboxy-tetramethylrhodamine
TBE	tris, orthoboric acid, EDTA buffer
TBS	tris buffered saline
TCA	trichloroacetic acid
TE	tris, EDTA buffer
TEMED	N,N,N', N' –tetramethylethylenediamine
Tm	melting temperature
Tricaine	3-amino benzoic acid ethylester
Tris	tris (hydroxymethyl)methylamine
Triton X-100	iso-octylphenoxypolyethoxyethanol
TUNEL	Terminal deoxynucleotidyl transferase mediated dUTP nick end labelling

Tween-20	polyoxyethylenesorbitan monolaurate
U	unit of enzyme activity
UTR	untranslated region
UV	ultraviolet
v/v	volume per volume
vol	volume
w/v	weight per volume
X-gal	5-bromo-4-chloro-3-indolyl β-D-galactopyranoside
ZFIN	The Zebrafish Information Network

1. Introduction

1.1 Zebrafish biology

The zebrafish (*Danio rerio*; formerly known as *Brachydanio rerio*) is the first vertebrate organism used in large-scale mutagenesis screens to identify genes involved in embryonic development (Driever *et al.*, 1996). It has many advantages as a model organism including external development and optical transparency during embryogenesis, allowing for direct observation of tissue movements, cell behaviour and interactions; small size, about 4 cm in length, which allows maintenance of large numbers of animals in a small area; short generation time, 2-3 months and prolific reproduction, females generate hundreds of eggs per week. Development of embryos occurs through a series of morphologically distinct stages, which include the zygote (0-0.75 hours post fertilisation; hpf); cleavage (0.75-2.25 hpf); blastula (2.25-5.25 hpf); gastrula (5.25-10 hpf); and segmentation (10-24 hpf) periods. At 35 hpf the larva hatches from the chorion and becomes free-swimming (Kimmel *et al.*, 1995; Fig.1.1).

In the early 1980s, George Streisinger and colleagues developed methods to manipulate the ploidy and parental origin of zebrafish genes (Streisinger *et al.*, 1981, 1986) e.g. gynogenetic haploid embryos are generated by fertilisation of secondary oocytes with UV-irradiated sperm. It is also possible to produce both homozygous and 'half-tetrad' gynogenetic diploid adult fish (Postlethwait and Talbot, 1997). The availability of thousands of mutant lines has identified novel genes, which regulate various aspects of development and enable mechanisms involved in early embryonic patterning to be elucidated (Mullins *et al.*, 1994; Driever *et al.*, 1994).

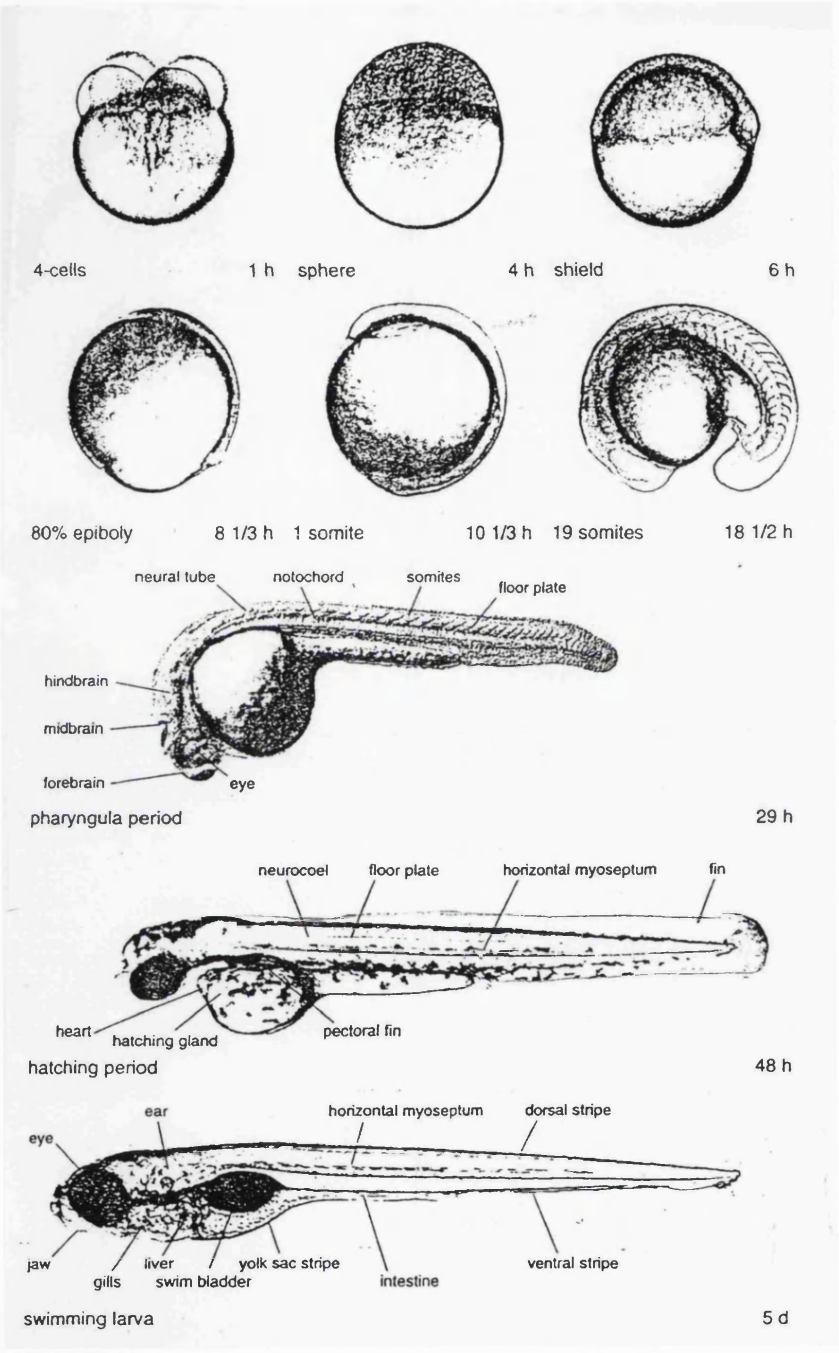

Fig. 1.1 Zebrafish anatomy during the first five days of development. Source: Kimmel *et al.*, Dev. Dyn. (1995) 203:253.

1.2 Mutagenesis screens

Chemical mutagenesis is the most efficient and widely used means of inducing mutations in zebrafish. The chemical N-ethyl-N-nitrosourea (ENU) is used to mutagenise zebrafish spermatogonial stem cells, the sperm from which are then used to fertilise eggs *in vitro*. This method induces single nucleotide mutations by alkylating guanine residues resulting in GC- to AT transitions. Mutations producing developmental phenotypes are then recovered in an F_2 breeding scheme (Mullins *et al.*, 1994; Solnica-Krezel *et al.*, 1994; Fig. 1.2). In 1996, an entire issue of the journal *Development* published the results of the characterisation of almost two thousand mutations derived from two large chemical mutagenesis screens (Driever *et al.*, 1996; Haffter *et al.*, 1996).

Many of the mutants currently being studied were first identified in these two large-scale screens. More recently, a further large-scale genetic screen ('Tübingen 2000') has been carried out by collaboration between Artemis Pharmaceuticals and laboratories at the Max Planck Institutes of Developmental Biology and Immune Biology, the University of Heidelberg, the Howard Hughes Medical Institute in Boston and University College London. These screens have focussed on specific aspects of development, including hindbrain patterning, neural crest migration, heart function, and bone formation. A third of the mutants have developmental defects that primarily affect one or more organs, body shape and the rest show more widespread abnormalities. Many of the cloned genes encode transcription factors, ligands and their receptors and many were identified as important developmental genes in other species. All the genes so far identified have orthologues or clearly related genes in human.

Apart from chemical mutagenesis, other methods of inducing mutations in the zebrafish genome include insertional mutagenesis, whereby a Moloney murine

leukaemia-based retroviral vector is used as the mutagen (Golling *et al.*, 2002). Retrovirally mutated genes can generally be identified within two weeks and the ease of gene cloning has allowed isolation of genes required for early development, which encode a wide range of proteins. The other technique is gamma irradiation (Walker *et al.*, 1999), which uses the mutagen γ-$_{200}$ to introduce large deletions into the zebrafish genome.

The zebrafish therefore provides a 'forward genetic' approach for assigning function to genes and positioning them in developmental and/or disease-related pathways. As many of the zebrafish mutant phenotypes identified in genetic screens are reminiscent of human disorders, it is possible to gain insight into their corresponding pathophysiology. Many vertebrate specific and clinically relevant developmental processes are being investigated using the zebrafish. For instance the *one-eyed pinhead* (*oep*) mutant displays cyclopia and lacks ventral neuroectoderm, a phenotype that resembles the human congenital disorder, holoprosencephaly (Dooley and Zon, 2000).

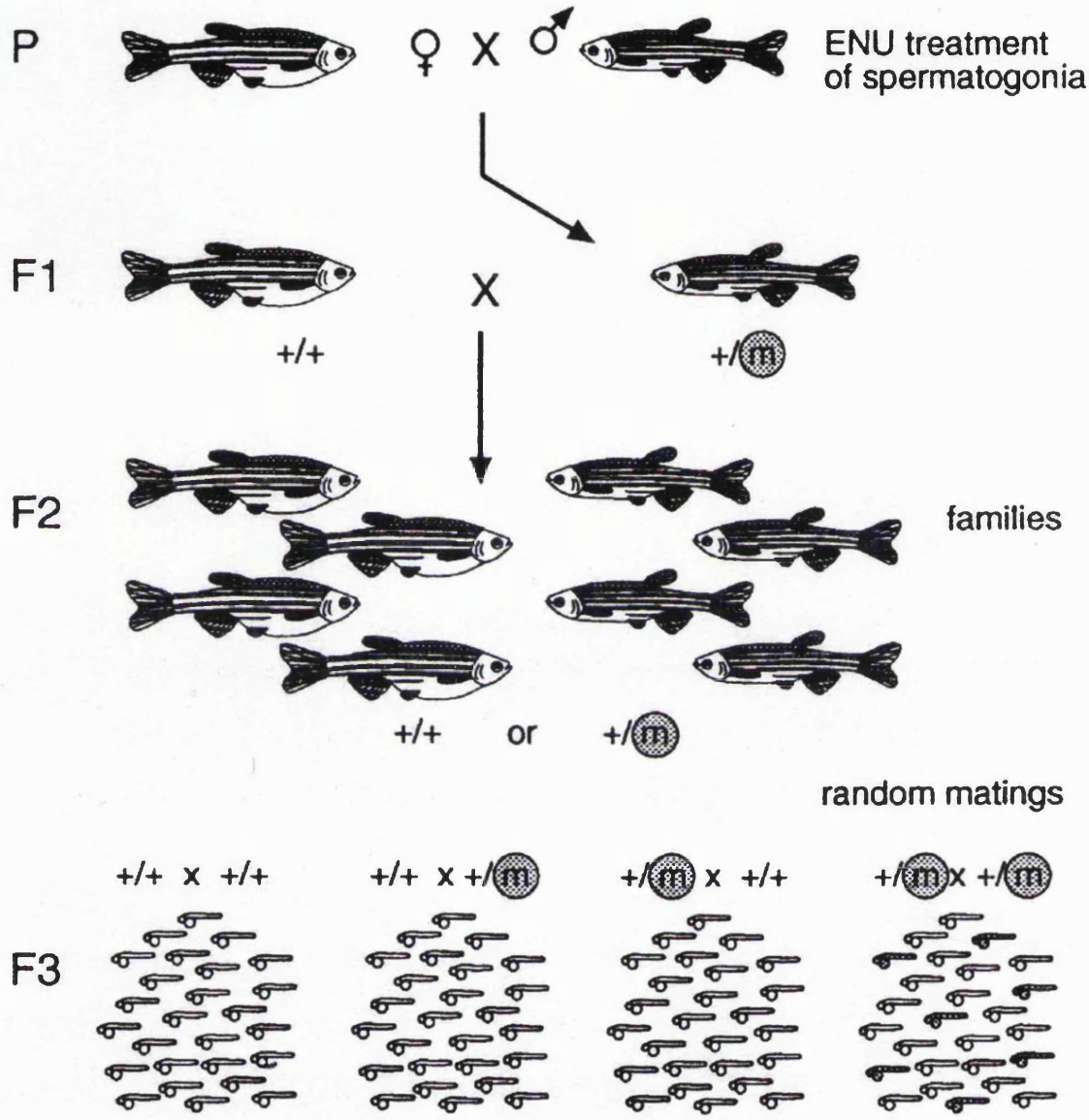

Fig. 1.2 The three-generation crossing scheme for production of homozygous mutant zebrafish.
Source: Haffter *et al.*, (1996) Development (123) 1-36.

1.3 Zebrafish models of human diseases

Many studies have shown that zebrafish is a powerful vertebrate model of human diseases (for review see Penberthy *et al.*, 2002). These include the zebrafish *sauternes* (*sau*) mutant, which has microcytic, hypochromic anaemia, significant reduction in haemoglobin levels and immature circulating erythrocytes (Brownlie *et al.*, 1998). *Sau* was shown to be due to a defect in the erythroid δ-aminolevulinate synthase (ALAS-2) gene, an essential enzyme that regulates the first step in haem biosynthesis in embryonic erythrocytes. In humans, mutations in ALAS-2 cause X-linked congenital sideroblastic anaemia with many features that resemble the *sau* phenotype.

Using the candidate gene approach, a second human haematopoietic disease gene was found in zebrafish (Wang *et al.*, 1998). This was a photosensitive porphyria mutant called *yquem* (*yqe*). Biochemical analyses of the *yqe* photosensitive erythrocytes showed an accumulation of porphyrins in the cells, which suggested a deficiency of uroporphyrinogen decarboxylase (UROD) in the mutant. A missense UROD mutation was identified in *yqe* mutant DNA. This phenotype resembles that of human hepatoerythropoietic porphyria (HEP).

There are several zebrafish disease models for human neurological diseases. These include congenital fibrosis of the extraocular muscles (CFEOM2). The zebrafish mutant *soulless* has a mutation in the *phox2a* gene and shows defects in oculomotor cranial nerve III and abducens cranial nerve IV formation (Guo *et al.*, 1999a). CFEOM2 patients have been identified with mutations in the human homologue of the *PHOX2A* gene (Nakano *et al.*, 2001). Other neurological disease models include Waardenburg-Shah syndrome/Hirschsprung disease, for which a mutation in the *sox10* gene has been identified in mouse and the zebrafish mutant *colourless*. The defect results in extensive loss of pigment cells and enteric nervous system, in addition to a

significant reduction in sensory and sympathetic neurons and glial cells (Dutton *et al.*, 2001). Holoprosencephaly (HPE) is the most common developmental defect of the forebrain in humans and in severe cases, results in a complete lack of separation of the telencephalic ventricles. Several genes involved in the development of human HPE have been identified and these include *SONIC HEDGEHOG* (Belloni *et al.*, 1996). Morpholino-based knockdown of both *sonic hedgehog* and *tiggy-winkle hedgehog* gene expression in zebrafish phenocopies HPE, resulting in mutants with cyclopic eyes with very little brain between them (Nasevicius *et al.*, 2000). The zebrafish *slow muscle omitted* (*smu*) mutant exhibits patterning defects in the anterior neural plate, which is correlated with reduced hypothalamic tissue and interocular distance. The *smu* mutant alleles affect zebrafish *smoothened* (Varga *et al.*, 2001). Smoothened and Patched are transmembrane proteins that mediate Hedgehog signalling intracellularly. Smoothened interacts with Patched and is needed for transduction of Hedgehog signals (Ingham, 1998).

High-resolution analysis of zebrafish mutant phenotypes allows elucidation of mechanisms that control various developmental processes. Ultimately, the genes that cause the mutant phenotypes have to be cloned and analysed. One way this can be achieved is by mapping mutations in a genetic linkage map and isolating the gene by chromosome walking from nearby cloned markers (Postlethwait and Talbot, 1997).

1.4 Genetic linkage mapping

The zebrafish genome has a genetic length of approximately 2900 cM and a physical length of about 1700 Mb, which means that 1 cM in zebrafish corresponds to only 600 kb, compared with 1 Mb in human and 2 Mb in mice. The highly recombinogenic nature of the zebrafish genome therefore makes it a highly favourable model organism for mapping purposes.

1.4.1 Genetic markers

1.4.1.1 Random Amplified Polymorphic DNA Analysis

The first genetic linkage map developed for the zebrafish contained more than 400 markers most of which were random amplified fragments of polymorphic DNA or RAPDs (Postlethwait *et al.*, 1994). These RAPD markers were generated by using the polymerase chain reaction (PCR) to amplify DNA fragments using zebrafish genomic DNA as a template and primers consisting of 10 nucleotides of random sequence.

The pattern of fragments generated by PCR differed consistently between strains of zebrafish, and was therefore inherited in a Mendelian fashion in crosses between strains. The segregation of these markers was then scored in the haploid offspring of a single hybrid female to generate the linkage map. The advantage of using haploid embryos is that they can develop through much of embryogenesis and both a dominant allele representing the presence and a recessive allele representing the lack of a fragment can be detected. This strategy was used to map mutations including *cyclops* and *no tail* (Rebagliati *et al.*, 1998; Schulte-Merker *et al.*, 1994).

1.4.1.2 Amplified Fragment Length Polymorphism Analysis

Amplified fragment length polymorphism (AFLP) is a strategy of DNA fingerprinting shown to be useful for genetic mapping in zebrafish (Vos *et al.*, 1995). This method uses many of the advantages of RAPD analysis but is more amenable to diploid organisms. Genomic DNA is digested with restriction enzymes, ligated to oligonucleotide adapters and selectively amplified. Restriction sites that are polymorphic between strains result in a generation of strain-specific bands and segregation of these bands with a mutation can be scored.

1.4.1.3 Simple Sequence Length Polymorphism Analysis

Simple sequence length polymorphisms (SSLPs) are tracts of short repeated sequences, often $[CA]_n$ dinucleotides, in which the number of repeats varies among different strains of fish. They are also known as microsatellite markers, simple sequence repeats (SSRs) or short tandem repeat polymorphisms (STRPs). These markers are the standard starting point for positional cloning and serve as anchors for other types of maps. SSLPs present several advantages over other types of markers, including:

- Abundance and relatively uniform distribution throughout the 25 linkage groups of the zebrafish genome (Goff *et al.*, 1992).
- Polymorphism between outbred strains.
- Reliability and ease in use, making them ideal tools for small laboratories or high-throughput facilities.
- High incidence of co-dominance allowing all four alleles to be traced.
- Easily assayable by PCR.

1.4.2 Zebrafish genetic map with microsatellite markers

A low-density genetic map comprising around 4000 SSLPs (Shimoda *et al.*, 1999) and covering 2350 cM of the zebrafish genome is currently available; see website http://zebrafish.mgh.harvard.edu/. The zebrafish genome has a haploid DNA content of 1.7×10^9 base pairs (Hinegardner and Rosen, 1972) located on 25 linkage groups (LGs), so called because it is difficult to distinguish between chromosomes (Daga *et al.*, 1996). Positional cloning enables identification of mutated genes on the basis of their chromosomal location, without previous information about the biochemical and molecular properties of genes.

1.4.2.1 Mutation mapping resources

Polymorphic markers have two important functions in a positional cloning project. Firstly as a means to genetically localise a mutation to a specific recombinant interval and secondly as an entry point for identifying large-insert genomic clones e.g. yeast artificial chromosome (YACs), bacterial artificial chromosome (BACs) and P1-derived artificial chromosome (PAC) that can be used for chromosome walking (Kelly *et al.*, 2000). At present two YAC libraries are available, one comprising 36,000 clones with an average insert size of 280 kb and the other containing 17,000 clones with an average insert size of 470 kb (Zhong *et al.*, 1998). A PAC library consisting of 75,600 clones with an average insert size of 120 kb and a BAC library have also been generated in zebrafish (Amemiya *et al.*, 1999). These genomic libraries can be used to isolate genomic clones containing a mutant locus. Partial rescue of mutant phenotypes by injection of genomic clones containing the wild-type gene is also possible (Yan *et al.*, 1998).

DNA pooling methods and the huge number of anonymous polymorphisms available by microsatellites, RAPDs, and AFLPs permit the identification of DNA polymorphisms very closely linked to zebrafish mutations. As the resolution of the genetic map improves, it will become possible to identify a marker that lies within 0.5 cM (300 kb) of a mutation.

1.4.2.2 A divergent zebrafish line useful for genetic mapping

A laboratory line of zebrafish was established for genetic mapping and termed WIK, which derives from a wild catch in India. Several sublines were gained from single pair matings (WIK2, WIK3, WIK4, WIK9, WIK10, WIK11 and WIK20). Of 314 SSLP primer pairs tested, 43 % showed polymorphism between the Tü and WIK11 lines and

47 % showed only one shared allele (Rauch *et al.*, 1997). Therefore the WIK11 line is polymorphic relative to the Tü line, making it useful for genetic mapping purposes.

1.4.2.3 SSLP analysis on pooled samples

The first step in cloning a gene underlying a mutant phenotype involves genetic mapping to localise the gene to a linkage group (rough mapping). Previously placed polymorphic markers e.g. SSLPs are then used to increasingly narrow the region of interest (fine mapping). Linkage mapping is necessary until the region between a flanking marker and the mutant gene is small enough to initiate physical mapping. Rough mapping of many mutant lines is being carried out in the laboratory of Robert Geisler at the Max-Planck Institute in Tübingen. Tü mutant carriers are crossed to wild-type (WIK) fish; 240 SSLPs are amplified from pools of 48 mutant F2 embryos and their wild-type siblings, and separated on agarose gels. A difference in band intensity between the mutant and sibling pools indicates a potential linkage, which is confirmed and refined by genotyping up to 2000 single embryos (Fig. 1.3).

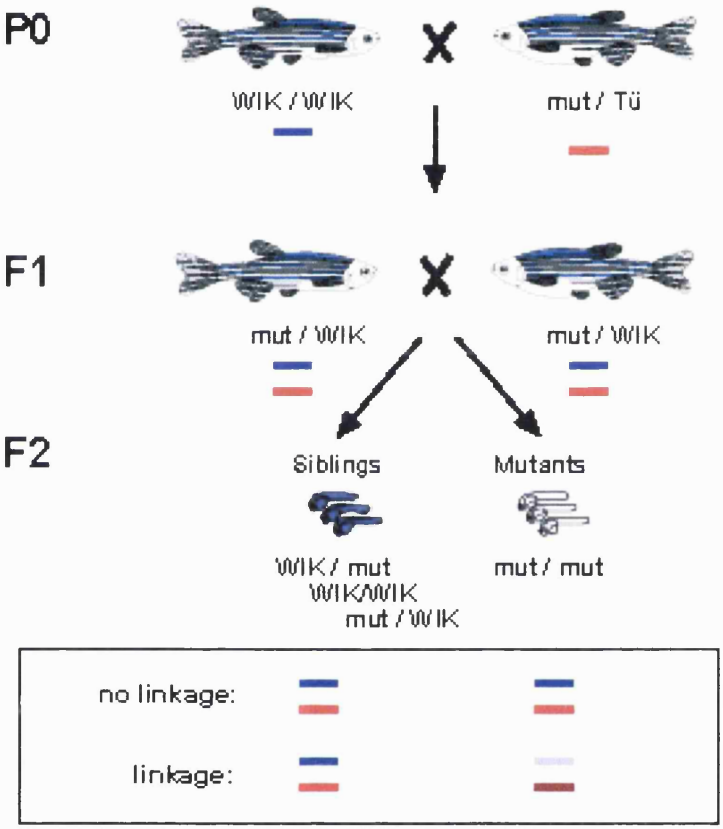

Fig. 1.3 Mapping Cross diagram to show the generation of homozygous mutants and identification of linkage using SSLP markers.
Source: Geisler, R. (2002). Mapping and cloning in Zebrafish, A Practical Approach, C. Nüsslein-Volhard and R. Dahm, eds. (Oxford: Oxford University Press).

1.5 Genomic resources

1.5.1 The Zebrafish Gene Map

The laboratory of William Talbot is meiotically localising 3000 zebrafish genes on an integrated genetic map to create a resource that will enhance comparative and functional analysis of the vertebrate genome. The genes are mapped by scoring single-strand conformational polymorphism (SSCPs) in the 3' untranslated (UTRs) and other non-conserved regions. This is an efficient PCR-based method to detect sequence variation.

The laboratory of Stephen Johnson at Washington University is using EST sequencing to develop sequence tagged sites (STSs) that are used to identify single nucleotide polymorphisms (SNPs) between inbred strains and mapped on radiation hybrid and meiotic mapping panels.

A SNP map of the zebrafish genome containing 2035 SNPs and 178 insertions/deletions and a method for mapping mutations in which many SNPs can be scored in parallel together with an oligonucleotide microarray have been developed (Stickney *et al.*, 2002), which will accelerate the mapping and molecular analysis of zebrafish mutations.

1.5.2 Radiation hybrid map

The radiation hybrid (RH) maps of zebrafish can be used to place cloned or candidate genes on genetic maps. A whole-genome radiation hybrid panel for the zebrafish has been generated by the Goodfellow lab, in which an irradiated zebrafish donor cell line is fused with a recipient hamster cell line (Kwok *et al.*, 1998). Random fragments of the donor chromosomes are integrated into recipient chromosomes or retained as separate minichromosomes. The radiation-induced mutations can be used for mapping in a similar way to genetic mutation mapping but at higher resolution and without a need for

polymorphism. DNA from each of the radiation hybrid lines is tested for the presence or absence of a marker by PCR, and a map is constructed by positioning markers next to each other if they are retained by many of the same lines. About 1300 markers were mapped on the Goodfellow T51 panel at a resolution of approximately 350 kb; 82 % of the expressed sequences tags (ESTs) tested had significant linkage (Geisler *et al.* 1999). The LN54 panel is another radiation hybrid map, made by fusing irradiated zebrafish cells with mouse cells and has a resolution of 500 kb (Ekker *et al.*, 1999).

The NCBI Map Viewer presents a graphical view of the zebrafish radiation hybrid (T51 and LN54) maps, the genetic maps (MGH, HS, MOP, GAT) and the SNP variation map. These maps contain an increasing numbers of cloned and mapped zebrafish genes and ESTs, which facilitate molecular identification of mutated genes by the candidate gene approach. The availability of an increasing number of PCR based polymorphic markers, e.g. SSLPs, makes positional cloning more feasible (for review see Talbot and Hopkins, 2000).

1.5.3 Zebrafish genome sequencing

The sequencing of the zebrafish genome was initiated in February 2001 at the Sanger Institute and funded by the Wellcome Trust. Two methods were used, the first was whole genome shotgun sequencing and involved extraction of DNA from Tübingen embryos, which was used to generate plasmid libraries with 2-10 kb inserts. These were then sequenced and the traces obtained used to assemble the genome sequence. The second approach was clone-based sequencing. The BAC libraries CHORI211 and DanioKey were used and fingerprinted to generate a map covering the genome sequence clone by clone (www.ensembl.org/Danio_rerio). To date (July 2003) the whole genome shotgun approach has produced 11.7 million traces, which amounts to 7.64 Gbp and covers the genome 4.5 times. The clone-based approach has covered 410,582,005 bp.

The sequencing project is predicted to finish by the end of 2005 and updates can be found at www.ensembl.org/Danio_rerio. Complete knowledge of the zebrafish genome sequence will allow greater understanding of zebrafish biology and in the absence of any known candidates will allow the application of gene prediction programs to identify novel genes.

1.6 Zebrafish genome duplication

Approximately 30 % of zebrafish genes are duplicated as a result of a whole-genome duplication event in the fish lineage leading to teleosts about 300-450 million years ago. This was followed by selection pressure on duplicated genes and divergent expression pattern of genes within the same family, which led to redundancy or loss of gene function during evolution.

Many multigene families potentially comprise more members in fish than in mammals, e.g. seven *homeobox* (*hox*) gene clusters have been found in zebrafish compared to four in mammals (Postlethwait *et al.*, 1999). Comparative genomics amongst teleost fish suggests that genome-wide duplication in zebrafish occurred before the divergence of zebrafish, pufferfish, and medaka lineages (Amores *et al.*, 1998; Meyer and Malaga-Trillo, 1999; Naruse *et al.*, 2000). Despite this duplication, zebrafish has about the same number of chromosomes as human (25 versus 23 pairs), rather than twice as many as expected in the absence of chromosome rearrangements. This could be due to either an excess of chromosome fusions in the fish lineage compared to the human lineage or an excess of chromosome fission events in the human lineage (Postlethwait *et al.*, 1998).

A group of genes that are syntenic in human tend to have orthologues that are syntenic in zebrafish. Analysis of zebrafish genes and their mammalian counterparts has revealed more than forty groups of syntenic genes in both zebrafish and human

(Postlethwait and Talbot, 1997; Amores *et al.* 1998; Postlethwait *et al.* 1998; Gates *et al.* 1999; O'Brien *et al.* 1999). Some of these regions are relatively large (for review see Talbot and Hopkins, 2000) and facilitate the use of comparative gene mapping to provide candidates for genes disrupted by various zebrafish mutations and hence aid cloning projects. Therefore if a zebrafish mutation maps to a conserved chromosome segment, genes in this corresponding human chromosomal region could become candidates for the zebrafish mutation. Alternatively, the phenotype of a zebrafish mutation may provide information regarding the function of the human gene (Postlethwait *et al.*, 1998).

Comparative mapping identified a candidate gene for the *you-too* (*yot*) mutation (Karlstrom *et al.* 1999), which was mapped to zebrafish LG 9. This linkage group contains genes with orthologues on human chromosome 2. Analysis of human genes on chromosome 2 and the prediction that the Hedgehog signalling pathway is affected in *yot*, revealed *gli2 as* a candidate for *yot*. Similarly, conservation of synteny between zebrafish LG 11 and human chromosome 20 as well as knowledge that the *snailhouse* (*snh*) mutation interferes with the bone morphogenetic protein (BMP) signalling pathway, revealed *bmp7* as a candidate for *snh* (Schmid *et al.* 2000).

1.7 Technologies developed to study gene function

Knockdown of gene expression using morpholinos is widely used (Nasevicius and Ekker, 2000). Morpholinos (MO; Gene-Tools®) are chemically modified oligonucleotides that bind to and inhibit translation of mRNA both *in vitro* and in tissue culture. They are molecularly characterised by the presence of a morpholine moiety instead of a ribose and a phosphorodiamidate linkage resulting in a neutral charge backbone (Summerton, 1999). These modifications result in the formation of a highly soluble polymer, which can hybridise single-stranded nucleic acid sequences with high

affinity, a relatively low amount of cellular toxicity and non-specific side effects. Zebrafish showing phenotypes induced by injection of Mos are termed morphants and are listed in a database (http://beckmancenter.ahc.umn.edu/). The human diseases hepatoerythropoietic porphyria and holoprosencephaly, as well as several cloned mutant genes, including *chordin*, *no tail*, *one-eyed pinhead*, *nacre*, *sparse* and *gridlock* have been phenocopied in zebrafish using MOs (for review see Penberthy *et al.*, 2002).

Gain of function analysis by ectopic expression of genes in a temporal and spatial manner has become possible by development of a technique called RNA/DNA caging. This involves covalent attachment of a photo-removable 'caging' group (6-bromo-4-diazomethyl-7-hydroxycoumarin; Bhc-diazo) with the phosphate moiety of the sugar-phosphate backbone of RNA causing inactivation of RNA. Bhc-caged mRNA is re-activated ('uncaged') by exposure to ultraviolet light of a specific wavelength (Ando *et al.*, 2001). This method has been successfully applied in zebrafish; uncaging *eng2a*, which encodes a transcription factor Engrailed2a, in the head, results in development of small eyes, enhanced midbrain and midbrain-hindbrain boundary at the expense of the forebrain (Ando *et al.*, 2001).

1.8 Development of the zebrafish central nervous system

Over the past century, developmental neurobiologists have extensively studied the formation of commissural axon tracts in the brain and spinal cord (Mihalkovics, 1877; His, 1889; Langelaan, 1908; Von Szily, 1912; Johnston, 1913; Suitsu, 1920; Katz *et al.*, 1983; Silver, 1993). Zebrafish are amenable to these studies and their developmental advantages and CNS formation will be discussed below.

1.8.1 The advantages of zebrafish for the study of early neural development

The zebrafish has many advantages for the study of vertebrate neural induction and patterning mechanisms, some of which are listed below:

- Relatively small brain size, which measures about 300 μm from the rostral tip to the boundary between the tectum and cerebellum and is approximately 250 μm thick.
- Relatively rapid development; neural patterning starts during gastrulation at 6-7 hpf and a functional nervous system is established by 24 hpf (Wilson *et al.*, 1990).
- The brain is optically transparent during embryogenesis as a result of sequestration of yolk granules into a single, large sac rather than being dispersed as platelets intracellularly where they can scatter light (as in amphibians). Therefore individual cells, neurons, outgrowth of processes and formation of synaptic connections can be visualised and studied *in situ* and their fate followed during development.
- Early tracts develop superficially directly beneath the presumptive pia and this is an advantage in terms of microscopic analysis, as these structures are separated from the microscope objective by a few micrometers only. Differential interference contrast optics is used to analyse the expression of genes following *in situ* hybridisation or proteins after antibody labelling.

1.8.2 Axis formation and patterning

The basic body plan of the vertebrate embryo is formed at the start of gastrulation and results in formation of three germ layers; endoderm, mesoderm and ectoderm as well as development of the three main body axes, anterior-posterior (A-P), dorsal-ventral (D-V) and left-right (L-R). The vertebrate CNS forms as a result of inductive interactions between the ectoderm and mesoderm. Patterning of the neuroectoderm is a progressive process and, at the end of gastrulation, A-P and D-V axes are organised into broad domains that can be characterised morphologically and molecularly. As neurulation continues, these domains become more evident and include development of rhombomeres (Keynes and Lumsden, 1990) and regional subdivisions of the anterior neural plate into telencephalon, hypothalamus, diencephalon, and eyes (Ruiz i Altaba and Jessell, 1993). A complex network involving members of the bone morphogenetic protein (Chordin, Noggin, Follistatin), Nodal, Wnt (Frzb/Dickkopf-1/Crescent), Hedgehog, Fibroblast growth factor (FGF), Delta/Notch, Slit/Robo, retinoic acid and lipid signalling pathways, provide molecular cues that interact to pattern the early embryo (De Robertis *et al.*, 2000; for review see Schier, 2001).

Investigation of regional patterning of the neural plate requires information about the location of the various CNS primordia before, during and after this process. Fate maps of different vertebrates, including zebrafish, have been constructed by analysing the location of a cell at the onset of gastrulation and by monitoring its development, establish its resulting fate (Kimmel *et al.*, 1990; Woo and Fraser, 1995).

In 1924, Hans Spemann and Hilde Mangold transplanted tissue from the dorsal blastopore lip of a developing *Xenopus* embryo to the future ventral domain of another embryo. The result of their experiment was an exact copy of head structures at the region of the implant, which contained cells mostly from the host embryo. Hence cells

from a specific region of an embryo can change and reprogram cell differentiation in other parts of the embryo. The dorsal blastopore lip was consequently termed the 'organiser' (Spemann and Mangold, 1924).

The organiser is responsible for the establishment of the body axes and is a source of signals that can induce and pattern new neural tissue and re-specify existing mesoderm structures. It gives rise to the notochord, which is an important source of signals for D-V patterning of the spinal cord and somites (Johnson *et al*, 1994). Transplant experiments have revealed a region of the embryo with the same properties as the classic organiser, the shield (Shih and Fraser, 1996); in chick, Hensen's node (Storey *et al.*, 1992); and in mouse, the node (Davidson and Tam, 2000). Hence the organiser is a conserved structure in embryonic patterning in vertebrates. When shield mesoderm is transplanted to the ventral side of a host embryo, it generates a complete secondary axis by inducing adjacent cells to form dorsal and lateral, instead of ventral fates. The zebrafish shield can induce axis duplication in amphibia as well, indicating that the function of molecular cues from the organiser region is conserved (Oppenheimer, 1936; Saude *et al.*, 2000). The development of the embryonic zebrafish brain is a dynamic process and involves morphogenetic movements as described below.

1.8.3 Neurulation

The process of neurulation is different in zebrafish to that in other vertebrates, which involves primary neurulation i.e. invagination of the neural plate to form a hollow tube by fusion of its lateral edges at the dorsal midline. However, convergent extension movements in the zebrafish neural plate result in formation of a solid rod-like structure, the neural keel, which develops at about 12 hpf and subsequently hollows to form the lumen of the neural tube during the process of secondary neurulation (Papan and Campos-Ortega, 1994).

1.8.4 Segmentation

Segmentation of the zebrafish CNS is visible at 16 hpf by the formation of ten neuromeres along the rostro-caudal axis of the neural tube. These include the seven most caudal neuromeres of the hindbrain compartments, known as rhombomeres (r), and three anterior neuromeres, which correspond to the anlagen of the telencephalon, diencephalon and midbrain respectively (Kimmel *et al.*, 1995). The expression of *homeobox* (*hox*) genes in rhombomere-specific patterns is required for segment identity within the hindbrain (for review see Lumsden and Krumlauf, 1996).

1.8.5 The major subdivisions of the brain

There are five major subdivisions of the zebrafish brain. The rostral neural tube forms the forebrain and midbrain. The forebrain includes two of these subdivisions, the telencephalon; located in a dorso-rostral position above the optic stalk, and the adjacent diencephalon, which occupies a domain from below the optic stalk to the ventral flexure. The ventral flexure is the position of the future mid-diencephalic boundary and dorsally positioned epiphysis (Ross *et al.*, 1992).

The midbrain (mesencephalon) forms another subdivision and is characterised by the dorsally located tectum and the ventrally positioned tegmentum. The cerebellum appears as two folds in the neuroepithelium in the region of the midbrain/hindbrain boundary. The hindbrain includes two subdivisions, the metencephalon and myelencephalon and rhombomere 1 is ventrally located adjacent to the cerebellum (Kimmel *et al.*, 1995).

1.8.6 The development of axonal tracts and commissures

By 24 hpf, the first neuronal clusters develop and together with their axons, form a simple scaffold of five bilaterally symmetrical axonal tracts and four commissures connecting adjacent subdivisions (Wilson *et al.*, 1990, Fig. 1.4). The first neurons that form are primary neurons, many of which express the LIM homeobox gene *islet-1* and extend axons over long distances (Korzh *et al.*, 1993). Signalling from factors secreted by the axial mesoderm, including *sonic hedgehog*, *shh* from the notochord, is required for specification of primary motor neurons (Beattie *et al.*, 2000).

Post-mitotic neurons start to develop at 16 hpf in the ventral midbrain and form the ventrocaudal cluster (vcc) or the nucleus of the medial longitudinal tract. In the ventral diencephalon, they form the ventrorostral cluster (vrc). The first neurons in the telencephalon develop after those of the vcc and form the dorso-rostral cluster (drc). At 18 hpf, a small cluster of neurons forms in the dorsal forebrain, which later develop into the epiphysis. By 24 hpf, additional neuronal clusters have developed in the midbrain, which later extend axons from the vcc to the roof of the midbrain to form the nucleus of the tract of the posterior commissure, nTPC (Chitnis and Kuwada, 1990).

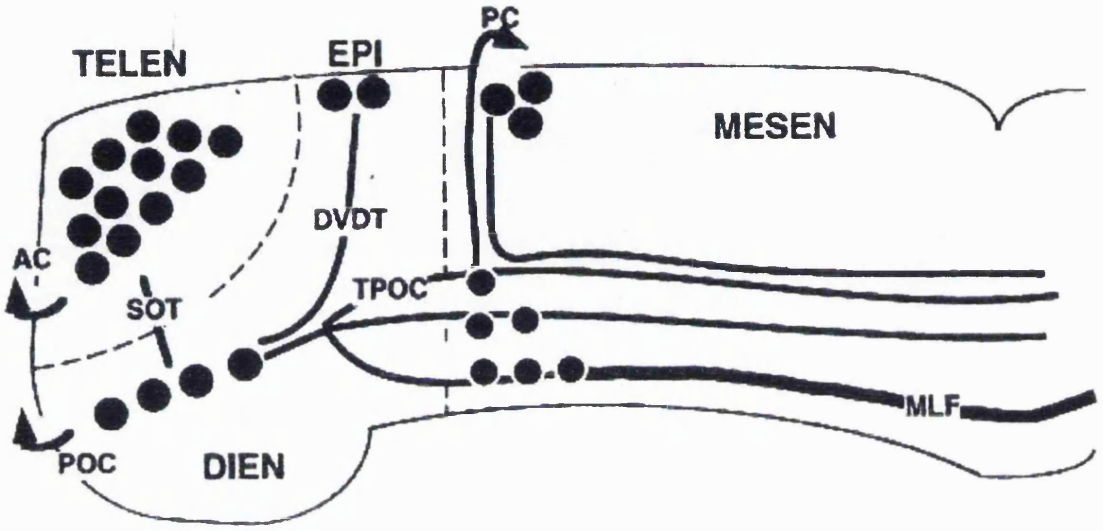

Fig. 1.4 Early zebrafish brain tracts. The axon tracts (dark lines) shown are the anterior commissure (AC), dorsoventral diencephalic tract (DVDT), medial longitudinal fasciculus (MLF), posterior commissure (PC), postoptic commissure (POC), supraoptic tract (SOT), and tract of the postoptic commissure (TPOC). Filled circles indicate neuronal bodies.
TELEN indicates telencephalon, DIEN indicates diencephalon, EPI indicates epiphysis, MESEN indicates mesencephalon.
Source: Chitnis and Dawid (1999) Methods in Cell Biology (59) 369.

1.8.7 Axonogenesis in the forebrain and midbrain

At 16 hpf, the first axons emerge from the vcc and either extend caudally to the medial longitudinal fasciculus (MLF) or project rostrally to the tract of the post-optic commissure (TPOC). By 18 hpf, the first axons emerge from the vrc and extend rostrally to the post-optic commissure (POC); whose axons cross the rostral surface of the diencephalon and grow into the contralateral TPOC. At the same stage, neurons of the drc extend axons ventrally from the telencephalon, through the caudal optic stalk, into the region of the vrc and TPOC to target the supra-optic tract (SOT). Axons from the drc also pioneer the anterior commissure (AC), which then cross the rostral surface of the telencephalon in a thick tight fascicle. At 20 hpf, axons project ventrally from neurons of the epiphyseal cluster and grow to the dorsoventral diencephalic tract (DVDT). At the same time, neurons from the nTPC project axons ventrally that target the tract of the posterior commissure (TPC) and dorsally to establish the posterior commissure, PC (Chitnis and Kuwada, 1990; Wilson *et al.*, 1990).

1.8.7.1 Regulatory gene expression domains

Boundaries of expression domains of members of the *ephrin*, *hedgehog*, *fork head*, *pax*, and *wnt* gene families correlate with regions where neurons differentiate and extend axons e.g. nuclei of the tract of the post-optic commissure (nTPOC) and medial longitudinal fasciculus (nMLF) develop and project along the ventral boundary of *pax6* and *rtk1* expression. Also, the transcription factor *noi/pax2a* is expressed in cells located at the dorsal border of axons in the POC (Macdonald *et al.*, 1994, 1997).

1.8.8 Axonogenesis in the hindbrain

Major neuronal subclasses that develop in the hindbrain include the reticulospinal and branchiomotor neurons. By 8 hpf, the first reticulospinal neuron, the Mauthner neuron,

forms in r4 of the hindbrain and at about 21 hpf, extends an axon that projects ventrally, crosses the midline and turns caudally to grow along axons of the contralateral MLF (Mendelson, 1986). By 24 hpf, two more neuronal clusters form at each rhombomere boundary and extend axons ventrally. The formation of their commissural axon bundles is dependent upon expression of L1-related CAMs and polysialic acid on NCAMs (Marx *et al.*, 2001).

The branchiomotor (motor) neurons develop in specific rhombomeres and extend axons out of the CNS to innervate muscles that differentiate in the pharyngeal arches. The anterior located mandibular and hyoid arches give rise to the lower jaw and associated structures, whereas the other pharyngeal arches give rise to the gills (Kimmel *et al.*, 1995). In zebrafish, the first motor neurons develop at 21 hpf and begin to extend axons at 24 hpf. They include, trigeminal (V) motor neurons in r2 and r3, which extend axons via r2 to innervate the mandibular pharyngeal arch muscles; motor neurons of the facial (VII) nerve located in r4 and r5 that migrate to r6 and r7 and project axons that exit the CNS via r4 to innervate muscles of the hyoid pharyngeal arch; glossopharyngeal (IX) motor neurons located in r7 that project axons which exit via r6 and innervate the first gill arch; vagus (X) motor neurons in the caudal region of r7, which innervate gill arches 2-5 (Chandrasekhar *et al.*, 1997). Transgenic zebrafish expressing green fluorescent protein (GFP) under the control of the *isl-1* promoter have been used to study the projection of branchiomotor axons (Higashijima *et al.*, 2000) and they show that specific branchiomotor nuclei innervate particular muscle groups, to form a simple stereotypical pattern of neurons and axons in the hindbrain.

1.8.9 Floor plate development in zebrafish

The floor plate in zebrafish extends along the ventral neural tube from the *zona limitans intrathalamica* into the spinal cord of the tail. It is composed of non-neuronal, epithelial cells with cuboidal morphology, which are easily visualised and distinguished from other cell types in the living embryo using differential interference optics. It is three to four cells wide and consists of a single row of medial floor plate (MFP) cells flanked by lateral floor plate (LFP) cells (Odenthal *et al.*, 2000). These two cell populations can be distinguished by gene expression analysis. The expression of the genes *foxA1*, *shh* (Krauss *et al.*, 1993), *netrin-1* (Strähle *et al.*, 1997) and *col2α1* (Yan *et al.*, 1995) is restricted to the MFP cells, whereas *foxA2* and *foxA* are expressed in both MFP and LFP cells (Odenthal and Nüsslein-Volhard, 1998; Odenthal *et al.*, 2000). The *nk2.2* gene (Barth and Wilson, 1995) is expressed in LFP cells only.

The floor plate functions as an organising centre that controls D-V patterning of the neural tube at early stages of development. Later on in development it acts as an intermediate target in commissural and longitudinal axon guidance (for review see Kaprielian *et al.*, 2001). The floor plate orientates commissural axon growth towards and across the midline through expression of a range of secreted guidance signals. These include Netrin-1 and Sonic hedgehog (Shh), which have been identified as chemoattractants in midline axon guidance (for review see Kaprielian *et al.*, 2001; Charron *et al.*, 2003). Analysis of *Netrin-1*$^{-/-}$ mutant mice, which lack the floor plate, has identified foreshortened commissural axons and failure to target the ventral spinal cord. In addition, axons project medially toward the ventricle with fewer reaching the midline and there is absence of the ventral commissure (Charron *et al.*, 2003). This compares to the highly fasciculated pattern of axon growth towards the midline in wild-type embryos (Serafini *et al.*, 1996).

Morphogens are signalling molecules produced in a restricted area of a tissue, which form a long-range concentration gradient from their source of origin and result in differentiation of specific cell types. The morphogen Shh specifies distinct classes of neurons in the ventral neural tube (for review see Jessell, 2000). As well as Shh, other signalling molecules exist, which are implicated in specification of neuronal cell types as well as axon guidance (for review see Osterfield *et al.*, 2003). These cues include members of the bone morphogenetic protein family e.g. BMP7 repels commissural axons in the spinal cord roof plate (Butler and Dodd, 2003). In *Drosophila*, members of the vertebrate homologue of the *wingless* gene, Wnt e.g. Wnt-5 guide commissural axons in the ventral nerve cord (Yoshikawa *et al.*, 2003). Members of the fibroblast growth factor (FGF) family also play a role in axon guidance e.g. Fgf8 is a chemoattractant for trochlear axons *in vitro* (Irving *et al.*, 2002).

Genetic screens in the zebrafish have identified a number of mutations in which various aspects of floor plate development are affected. These 'midline' mutants include *cyclops, squint, one-eyed pinhead, chameleon, detour, iguana, you-too, sonic-you, you, uboot, schmalhans, schmalspur and monorail* (Brand *et al.*, 1996). Further phenotypic and molecular characterisation of these mutants has revealed genes involved in induction and patterning of the zebrafish midline and surrounding structures.

1.8.9.1 The role of the organiser in floor plate induction

The zebrafish organiser induces midline precursor cells that give rise to the floor plate; hence this structure can be induced independent of notochord specification. Evidence to support this is shown by zygotic mutations in the zebrafish *cyclops* (Hatta *et al.*, 1991) and *one-eyed pinhead* (Gritsman *et al.*, 1999) genes, which lack floor plate cells despite the presence of an intact notochord, expressing *shh* (Strähle *et al.*, 1997). Also mutations in the zebrafish *floating-head* and *no-tail* genes, which are required for

formation of the notochord, develop a patchy or wider floor plate respectively (Halpern *et al.*, 1997).

Analysis of a temperature sensitive mutation in the zebrafish *cyclops* locus, cyc^{sp1}, has revealed that floor plate induction occurs during gastrulation and requires continuous and high levels of Cyclops/Nodal signalling to specify the ventral neural tube completely (Tian *et al.*, 2003). At 22°C, embryos homozygous for the cyc^{sp1} mutation develop variable fused eyes, ventral curvature of the body axis, a patchy to complete floor plate and motor neurons that are sometimes located in their normal positions. However at 28.5°C the phenotype of cyc^{sp1} mutants is the same as *cyclops* null embryos with fused eyes, lack of medial floor plate cells and ventral curvature of the body axis (Tian *et al.*, 2003).

1.8.10 Midline signalling pathways

Specialised axial mesodermal structures, including the notochord and prechordal plate, underlie the midline of the neural plate and regulate patterning along the D-V axis. The notochord induces floor plate cells, which secrete diffusible factors that regulate differentiation of basal plate cells, including motor neurons (Yamada *et al.*, 1993); which develop on both sides of the floor plate in the ventral neural tube.

Midline signalling involves components of both Hh and Nodal signalling pathways, which interact to differentially regulate floor plate induction and maintenance. These will be described below.

1.8.10.1 Nodal signalling pathway components

Two classes of the transforming growth factor-β (TGF-β) superfamily provide important morphogenetic signals during early patterning processes in vertebrates. These are the BMPs that pattern the gastrula embryo along the D-V axis and are required to define ventral cell fates and Nodal-related proteins, which have important

roles in formation of the gastrula organiser, induction of mesoderm and endoderm, patterning of the anterior neural plate and determination of bilateral asymmetry in vertebrates (for review see Schier and Shen, 2000).

Nodal was first identified as an essential gene for gastrulation in mouse; *Nodal* mutant embryos exhibit severe reduction of mesoderm formation and abnormal migration of residual mesodermal cells (Zhou *et al.*, 1993). In zebrafish, two *nodal*-related genes, *squint* (*sqt*) and *cyclops* (*cyc*) have been identified. Mutant embryos homozygous for either *cyc* or *sqt* show partial loss of axial mesoderm and ventral neuroectoderm, whereas *cyc;sqt* double mutants lack most mesendodermal tissues (Feldman *et al.*, 2000).

The *one-eyed pinhead* (*oep*) gene encodes a member of the extracellular CFC family of membrane-bound epidermal growth factor (EGF)-like proteins, an essential mediator of Nodal signals (Gritsman *et al.*, 1999). Zebrafish maternal and zygotic *oep* mutants and embryos lacking the *oep* orthologues, *cripto* and *cryptic* in mouse, show absence of endodermal and mesodermal tissue and hence exhibit phenotypes similar to the *nodal* mutants *cyc* and *sqt* (Ding *et al.*, 1998).

Antagonists of the Nodal signalling pathway include Lefty and its orthologue Antivin, which are members of the TGF-β superfamily. Overexpression of Lefty blocks endoderm and mesoderm formation and development of posterior neuroectoderm and leads to phenotypes resembling *cyc;sqt* or maternal-zygotic *oep* mutants (Thisse *et al.*, 2000). The extracellular protein Cerberus, a member of the cystein knot family and its truncated form ('Cer-short') bind and inactivate Nodal-related proteins (Agius *et al.*, 2000; Cheng *et al.*, 2000).

The transcription factor FoxH1/FAST1 associates with Nodal pathway signals and is disrupted by mutations in the zebrafish *schmalspur* locus (Sirotkin *et al.*, 2000;

Pogoda *et al.*, 2000). Maternal-zygotic *schmalspur* mutants exhibit defects in formation of the dorsal mesoderm but their phenotype is less severe than *cyc;sqt* or maternal-zygotic *oep* mutants. This has also been shown in mouse *FoxH1/FAST1* mutants, which show less severe defects than *Nodal* mutants (Yamamoto *et al.*, 2001).

The mechanisms involved in transduction of Nodal signals include ligand binding and activation of the Activin-like serine/threonine receptor complex to phosphorylate the intracellular signal transducer Smad2 and form a complex with Smad4. The Smad2/Smad4 complex then translocates to the nucleus where it interacts with DNA binding proteins, including FoxH1/Fast1 and paired class homeobox proteins of the Mix/Bix family, to initiate transcriptional activation of downstream genes (for review see Schier and Shen, 2000).

1.8.10.2 Nodal signalling and medial floor plate development

Mutations in the zebrafish *nodal*-related genes *squint* and *cyclops* (Hatta *et al.*, 1991; Feldman *et al.*, 1998; Sampath *et al.*, 1998), their extracellular membrane-associated cofactor gene *one-eye pinhead* (Schier *et al.*, 1997; Zhang *et al.*, 1998) and the transcriptional effector of Nodal signalling *schmalspur* (Pogoda *et al.*, 2000; Sirotkin *et al.*, 2000) show cyclopia, defects in MFP induction, loss of posterior prechordal plate, failure to establish cardiac asymmetry and ventral curvature of the body axis. The zebrafish *spadetail* (*spt*)/*VegT* and *no tail* (*ntl*)/*Brachyury* T-box genes are also required for MFP development. Studies of $spt^{-};ntl^{-}$ double mutants, which lack posterior MFP but have normal anterior development, suggest that Nodal signalling is not affected in this anterior region. However single *ntl* or *spt* mutations enhance posterior MFP development; *spt* and *ntl* are required together in a non-cell autonomous manner for MFP formation (Amacher *et al.*, 2002). In addition, studies of enhancer elements of

several genes expressed in the floor plate show dependence on Nodal signals for their activity (Müller *et al.*, 2000; Rastegar *et al.*, 2002).

In zebrafish, MFP differentiation occurs as a result of two temporally distinct signalling mechanisms. During the first day of development, *cyclops* mutants lack MFP cells. However by day two, differentiation of MFP cells in the hindbrain and spinal cord region is evident. The latter induction of MFP specification is dependent on intact Hh signalling. Hh signalling maintains floor plate differentiation following specification of the floor plate by Nodal related signals (Albert *et al.*, 2003).

1.8.10.3 Hedgehog signalling pathway components

Ventral differentiation in the CNS depends on Shh signalling mediated by the Gli family of zinc finger transcription factors (Methot and Basler, 2001). The secreted protein Sonic hedgehog (Shh), which is the vertebrate *Drosophila hedgehog* homologue, begins to be expressed at 60 % epiboly in the embryonic shield during gastrulation (Krauss *et al.*, 1993). Its expression continues in the notochord and floor plate (Krauss *et al.* 1998) and is required for induction of the floor plate, motor neurons and ventral interneurons in the spinal cord (Lewis and Eisen, 2001). Unlike other vertebrates, zebrafish express two additional *hedgehog* genes in overlapping domains to that of *shh* expression and at the time when motor neurons are specified. *Tiggy-winkle hedgehog* (*twhh*) starts to be expressed in the embryonic shield from 50 % epiboly and continues its expression in the floor plate and ventral brain (Ekker *et al.*, 1995); *echidna hedgehog* (*ehh*) is only expressed in the notochord and from late gastrulation (Currie and Ingham, 1996).

Mouse loss-of function *Shh* mutants are characterised by single fused telencephalic and optic vesicles and do not develop motor neurons (Chiang *et al.*, 1996). Human patients with mutations in the orthologous *SHH* gene exhibit a variable range of

facial defects including cyclopia, proboscis and microcephaly with normal development of the rest of the body (Belloni *et al.*, 1996). Such patients are heterozygous for *SHH* mutations, a condition that does not result in a detectable phenotype in mice. Zebrafish *sonic-you* (*syu*) mutants homozygous for the t4 allele of *syu* completely lack the *shh* locus but develop normal numbers of motor neurons. Redundant function with Ehh and Twhh, which are normally expressed in the body axis of syu^{t4} mutants, may explain the formation of motor neurons in the absence of Shh (Schauerte *et al.*, 1998). Ehh has been found to have a less of a critical role than Twhh or Shh in motor neuron specification (Lewis and Eisen, 2001).

A number of components of the Hh signalling pathway are conserved between *Drosophila* and vertebrates (v), these include the Hh receptors *Drosophila* Patched (Ptc) and vPtc, the receptor coupled seven transmembrane proteins *Drosophila* Smoothened (Smo) and vSmo and the downstream Hh transcription factor *Drosophila* Cubitus interruptus, Ci and vGli (Sasaki *et al.*, 1997; Ingham, 1998).

Gli proteins can act in both activator and repressor forms to regulate D-V patterning of the neural tube in response to Hh signals. For instance in the spinal cord, Shh signalling is responsible for establishment of ventral cell identity in part by antagonising Gli3 or Gli2 mediated repression of intermediate and ventral cell specification respectively (Persson *et al.*, 2002). In mouse, Gli3 is not involved in floor plate formation; however Gli2 acts as an activator of Hh targets and is essential for floor plate induction (Karlstrom *et al.*, 2003). This is shown by mutations in the *Gli2* gene, which result in absence of the floor plate with normal development of motor neurons and interneurons (Ding *et al.*, 1998). In zebrafish, it is Gli1 rather than Gli2 that is required for activating ventral CNS gene expression (Karlstrom et al. 2003). Analysis of the *detour* mutation, which encodes loss-of-function alleles of the *gli1* gene, has

shown that Gli1 activates ventral CNS patterning through Hh regulated genes. These results show conservation as well as divergence of Gli function in mouse and zebrafish (Karlstrom *et al.*, 2003).

1.8.10.4 Hedgehog signalling and lateral floor plate development

In zebrafish, Hh signalling is responsible for induction of LFP cells. None of the mutations that impair the Hh signal pathway affect differentiation of the MFP (Barresi *et al.*, 2000; Odenthal *et al.*, 2000; Etheridge *et al.*, 2001). However although MFP cells form in Hh pathway mutants, Hh signalling is required for the survival of MFP cells (Varga *et al.*, 2001; Chen *et al.*, 2001). Loss of hedgehog signalling in zebrafish results in a wide range of defects including ventral curvature of the body, deficiencies in ventral forebrain specification, ventral spinal cord abnormalities and absence of the optic chiasm (Brand *et al.*, 1996; Karlstrom *et al.*, 1999; Varga *et al.*, 2001).

Other genes involved in Hh signalling have been revealed by the study of the 'U' mutants, so-called due to their characteristic u-shaped somites; which include *you-too*, the zebrafish homologue of the Hh pathway transcription factor Gli2 (Karlstrom *et al.*, 1999), *detour*, *chameleon*, *you* and *iguana* (van Eeden *et al.*, 1996; Odenthal *et al.*, 2000) and *slow muscle omitted* (*smu*; Barresi *et al.*, 2000; Varga *et al.*, 2001) which encodes a zebrafish orthologue of Smoothened that transduces Hedgehog signals. The *smu* mutant has a more severe phenotype than the other 'U' mutants in terms of somite morphology. It also shows a greater reduction of primary motor neurons and complete loss of secondary neurons. Its phenotype is similar to that of *cyclops;floating head* (*cyc;flh*) double mutants, which show reduced Hh signalling, lack both notochord and floor plate and hence do not express *ehh* or *twhh* and show transient expression of *shh* in post-somitogenesis stages (Chen *et al.*, 2001).

1.9 Axon Guidance

1.9.1 History of axon guidance research

Santiago Ramón y Cajal first observed neuronal growth cones over a century ago and predicted their function in guiding the axons and dendrites of differentiating neurons towards their targets (Ramón y Cajal, 1892). Since then many neuroscientists have tried to elucidate the mechanisms by which growth cones function.

In the 1940s and 50s, Roger Sperry proposed that growth cones are guided by chemical cues that might be distributed in concentration gradients (Sperry, 1963). In the 1970s and 80s, Friedrich Bonhoeffer investigated growth cone migration using *in vitro* assays and showed that they detect and respond to gradients that differ as little as 1-2 % across their diameter (Baier and Bonhoeffer, 1992). Since then, large numbers of biochemical and genetic studies in invertebrates and vertebrates have led to the identification of several families of guidance molecules, all of which can act as graded cues to guide axonal growth cones and are dynamically regulated (for reviews see Tessier-Lavigne and Goodman, 1996; Yu and Bargmann, 2001).

1.9.2 Role of the midline in axon guidance

The formation of a complex network of neuronal connections during the development of the nervous system is based on axons navigating precisely to their appropriate targets (Tessier-Lavigne and Goodman, 1996). In insects and vertebrates, the two symmetric halves of the nervous system are separated by a specialised group of cells located at the ventral midline. These are termed midline cells in *Drosophila* and form the floor plate in vertebrates. In the *Drosophila* nerve cord, as in the vertebrate spinal cord, many neurons extend axons across the midline to select targets on the opposite (contralateral) side. These axons form the commissures that connect the two sides of the nervous

system. Other axons (about 10 % in *Drosophila*) never cross the midline and instead reach targets on their own (ipsilateral) side (Klambt *et al.*, 1991; Colamarino and Tessier-Lavigne, 1995). The midline therefore acts as an intermediate target, providing choice points by secreting guidance cues to control and regulate neuronal growth cone behaviour (Stoeckli and Landmesser, 1998; Tear, 1999).

1.9.3 Cellular mechanisms of axon guidance

Growth cones are guided to their targets by attractive and repulsive extracellular cues, which include members of the Netrin, Semaphorin, Ephrin, and Slit protein families (Brose *et al.*, 1999; Harris *et al.*, 1996; Kennedy *et al.*, 1994; Kidd *et al.*, 1999; Mitchell *et al.*, 1996; Serafini *et al.*, 1994; Stoeckli *et al.*, 1997; Zou *et al.*, 2000, Fig. 1.5). Evidence is accumulating that several of these ligands are bifunctional, attracting some growth cones, whilst producing repulsive effects on others (for review see Seeger and Beattie, 1999) and that receptors and receptor complexes play an important role as effectors for different guidance cues (for review see Seeger and Beattie, 1999).

The principal mechanisms involved in signalling, interaction and function of these ligands and their receptors have been conserved throughout evolution from nematodes to mammals (Chisholm and Tessier-Lavigne, 1999) and will be discussed below in greater detail.

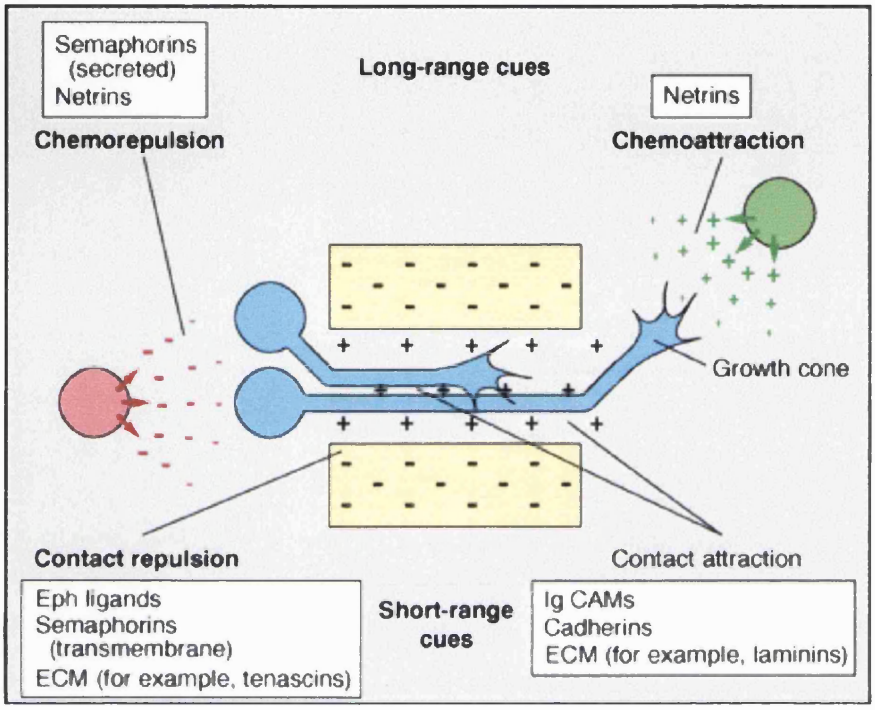

Fig. 1.5 The mechanisms contributing to axon growth cone guidance. Individual growth cones might be 'pushed' from behind by a chemorepellent (red), 'pulled' from afar by a chemoattractant (green), and 'hemmed in' by attractive (grey) and repulsive (yellow) local cues.
Source: Tessier Lavigne and Goodman (1996) Science (274) 1123-1133.

1.9.3.1 Slits and their receptors

Drosophila Slit is a large extracellular matrix protein that is expressed by midline glia cells and acts as a long-range chemorepellent for axons (Kidd *et al.*, 1999).

The transmembrane receptor Roundabout (Robo) mediates the repulsive cues elicited by slits (Kidd *et al.*, 1998, Kidd *et al.*, 1999). Robo was identified in a genetic screen for mutations affecting axon pathfinding in *Drosophila* (Seeger *et al.*, 1993). The commissural axons of r*obo* mutants cross and re-cross the ventral midline multiple times (Kidd *et al.*, 1998). So far, three Robo genes, Robo-1, 2 and 3 have been identified in *Drosophila* (Kidd *et al.*, 1998; Rajagopalan *et al.*, 2000; Simpson *et al.*, 2000), *C. elegans* (Zallen *et al.*, 1998; Yu *et al.*, 2002), zebrafish (Challa *et al.*, 2001; Lee *et al.*, 2001), mouse (Taguchi *et al.*, 1996; Brose *et al.*, 1999; Yuan *et al.*, 1999) and human (Kidd *et al.*, 1998).

Zebrafish Slit2 and Slit3 are Robo2 ligands and their expression pattern in the ventral diencephalon indicates that they have important roles in guiding retinal axons. Slit2 is expressed in the optic stalk, along the midline rostral to the optic recess; across the path of the anterior commissure and regulates optic nerve fasciculation (Niclou *et al.*, 2000). Slit3 is expressed in three domains in the ventral forebrain, rostral to the anterior commissure, between the anterior and post-optic commissure, and caudal to the post-optic commissure (Ringstedt *et al.*, 2000).

Drosophila and human Robo1 contain four conserved cytoplasmic domains named CC0-CC3, whereas human Robo2 and Robo3 only have the CC0 and CC1 motifs. Genetic studies in *Drosophila* have revealed the CC1 and CC2 domains interact with the Enabled (Ena) protein and the CC3 motif binds to Abelson (Abl), a cytoplasmic tyrosine kinase (Smith and Mayer, 2002). Tyrosine phosphorylation of the

CC1 domain of Robo by Abl inhibits Robo-mediated repulsion. Over-expression of Abl causes midline guidance defects that are similar to the *robo* mutant phenotype (Bashaw *et al.*, 2000). Enabled binds to the CC2 domain of Robo and regulates actin dynamics in response to signalling from the cell membrane. Repulsive responses via Robo are disrupted in *enabled* loss of function mutants; therefore Ena is another modifier of Robo signalling, but unlike Abl, acts by enhancing repulsion (Reinhard *et al.*, 2001).

The Rho GTPase family members Cdc42 and RhoA regulate Robo signalling in a similar manner to their involvement in plexin receptor function. Upon binding of Slit to Robo, Slit-Robo GTPase-activating proteins directly interact with the CC3 domain of Robo and induce repulsion (Wong *et al.*, 2001).

1.9.3.2 Netrins and their receptors

Netrins are a conserved family of secreted proteins that primarily act as long-range chemoattractants but can also elicit short and long-range repulsive signals, hence act as bifunctional guidance cues (Kennedy *et al.*, 1994). Their name is derived from the Sanskrit 'netr', meaning 'one that guides'.

Netrin-induced attraction is mediated by the DCC (deleted in colorectal cancer) family of receptors, which include Frazzled in *Drosophila* (Kolodziej *et al.*, 1996), UNC40 in *C. elegans* and DCC and neogenin in vertebrates (Yu *et al.*, 2001; Shen *et al.*, 2002). Netrin-induced repulsion is mediated by the UNC5 receptor family and also by DCC co-receptors as described below.

DCC activates mitogen-activated protein kinase (MAPK) signalling via an extracellular signal-regulated kinase (ERK)-1 and -2 to mediate netrin-1 binding in commissural neurons. Inhibition of ERK-1/2 antagonises netrin-dependent axon

outgrowth and orientation; hence MAPK signalling is required for netrin function during axon guidance (Forcet *et al.*, 2002).

A zebrafish gene, *netrin-1a*, most closely related to *netrin*-1 in other vertebrates, has been cloned and characterised. It is widely expressed in the CNS during axonogenesis in domains that implicate that it guides specific growth cones and influences their behaviour. Axon tracts correlate with *netrin-1a* expression and include the anterior commissure, supraoptic tract, tract of the post-optic commissure, the dorsoventral diencephalic tract, the ventral tegmental commissure, the medial longitudinal fasciculus, hindbrain commissures and the ventral spinal cord (Lauderdale *et al.*, 1997).

Zebrafish *floating head* (*flh*) mutants lack a notochord and certain floor plate cells in the caudal spinal cord are missing (Halpern *et al.*, 1995). These embryos show reduced expression of *netrin-1a* in regions of the spinal cord lacking floor plate cells. Spinal commissural neurons located at the border or in between islands of *netrin-1a* expression abnormally extend their axons caudally towards regions that do express *netrin-1a*. However commissural neurons situated within *netrin-1a* expression domains have normal ventral projections (Lauderdale *et al.*, 1997).

A zebrafish homologue of DCC, *zdcc*, has been identified and characterised. Sequence analysis of *zdcc* reveals that it is highly homologous to human, mouse, rat and *Xenopus* DCC but is not a Neogenin homologue. Between 12 and 33 hpf, *zdcc* is expressed in a dynamic spatiotemporal pattern and corresponds to the location of the first neuronal nuclei of the zebrafish brain which develop during neurogenesis. These include the ventro-caudal, dorso-rostral and ventro-rostral clusters, which later become interconnected by outgrowing axons (Hjorth *et al.*, 2001).

1.9.3.3 Initial guidance decisions made by growth cones

Axons display an initial differential sensitivity to guidance cues, which allows them to choose a path to attract them towards the midline or keep them away e.g. axons expressing the DCC/frazzled group of receptors alone on their growth cones are receptive to the attractive activity of the netrin molecules secreted from the midline (Keino-Masu *et al.*, 1996; Kolodziej *et al.*, 1996). Conversely the expression of Robo on growth cones makes them sensitive to the midline repellent Slit and turns axons away from the midline (Kidd *et al.*, 1998).

Transmembrane receptors determine whether a growth cone detects a cue as attractive or repulsive. The cytoplasmic domains of receptors are important effectors for initiating an attractive or repulsive response. The formation of heteromeric receptor complexes is important in regulating the response of growth cones to complex bifunctional guidance cues (Bashaw and Goodman 1999, Hong *et al.*, 1999). Netrin-induced attraction is switched to repulsion by the interaction of the cytoplasmic domains P1 in DCC and DCC-binding (DB) in UNC5 (for review, see Seeger and Beattie, 1999).

1.9.3.4 Robo, Comm and Slit interactions at the midline

Commissural growth cones are able to adapt their sensitivity to midline signals. Before crossing the midline, commissural neurons express *robo* mRNA but not Robo protein on their surface in contrast to ipsilateral neurons, which do express Robo protein. After crossing the midline, Robo protein levels on these neurons increase and they become responsive to Slit. These switches in sensitivity explain why commissural axons do not re-cross the midline and remain away from it (Kidd *et al.*, 1998; Kidd *et al.*, 1999).

The *Drosophila* transmembrane protein Comm downregulates Robo protein levels to allow commissural axons to cross the midline. Once across the midline, Robo

levels increase, suggesting Comm acts only at the midline (Tear *et al.*, 1996; Kidd *et al.*, 1998). In the absence of Comm, commissural growth cones are unable to cross the midline (Seeger *et al.*, 1993; Tear *et al.*, 1996). When Comm is overexpressed in all neurons, Robo protein levels are downregulated and the *robo* phenotype is observed (Kidd *et al.*, 1998). Comm protein accumulates at the axon surface within the commissural region by a mechanism involving Comm in the midline glia. However expression of Comm protein at the midline alone is not sufficient for commissure formation. Midline crossing errors occur when Comm expression is inhibited specifically in neurons and at the midline, therefore Comm is present and required in both commissural neurons and midline glia. The lack of any guidance errors in ipsilateral neurons means that Comm activity is not required at this location (Georgiou and Tear, 2002).

Comm regulates Robo protein levels by binding to DNedd4, a *Drosophila* ubiquitin ligase. Interference of Comm/DNedd4 interaction impairs Comm's regulation of Robo localisation and results in gain-of function activity at the midline (Myat *et al.*, 2002; Rosenzweig and Garrity, 2002). Ubiquitination of Comm by DNedd4 leads to Robo protein sequestration away from the cell surface by transferring Robo from the Golgi apparatus to endosomes (Keleman *et al*, 2002).

The *Drosophila* gene *lola* (*longitudinals lacking*) is responsible for the longitudinal extension of axons and their repulsion away from the midline (Seeger *et al.*, 1993; Giniger *et al.*, 1994; Cavarec *et al.*, 1997). It interacts with and increases levels of the midline repellent Slit and its receptor Roundabout. In the absence of *lola*, Slit and Robo levels are reduced and excessive midline crossing occurs (Crowner *et al.*, 2002). Lola balances signals from multiple guidance molecules and regulates the precise timing, location and level of their expression. It inhibits axon growth across the

midline and promotes their longitudinal projections (Giniger *et al.*, 1994; Madden *et al.*, 1999).

Drosophila Derailed (Drl) is a member of the 'related to tyrosine kinase' (RYK) subfamily of receptor tyrosine kinases (RTKs) that include mammalian RYK, a single *C. elegans* member, and two additional members in *Drosophila* (Hovens *et al.*, 1992; Callahan *et al.*, 1995; Oates *et al.*, 1998; Savant-Bhonsale *et al.*, 1999). Drl receptor is expressed and required in growth cones and axons of neurons that extend into and through the anterior commissure and is down regulated as they leave this domain. Absence of its expression causes abnormal projections into the posterior commissure. Misexpression of Drl in the posterior commissure neurons forces them to cross in the anterior commissure, indicating that a repulsive ligand in the posterior commissure is recognised by the Drl receptor. In *drl* mutants many axons still project normally to and through the anterior commissure, indicating that Drl is part of a multicomponent system that regulates correct commissure choice (Bonkowsky *et al.*, 1999; Yoshikawa *et al.*, 2001). Derailed and Wnt5 act together to guide axons into the anterior commissure. A reduction in the activity of *wnt5* gene activity decreases the ability of misexpressed Derailed to switch axons into the anterior commissure. In addition *wnt5* mutants have similar axon guidance defects to *derailed* mutants (Yoshikawa *et al.*, 2003).

1.9.3.5 Silencing of Netrin attraction by Slit

An increase in Robo levels also silences the attractive response by commissural neurons to netrin signalling via a direct interaction between the cytoplasmic domains CC1 in Robo with P3 in DCC (Shirasaki *et al.*, 1998). When growth cones are simultaneously exposed to a gradient of netrin-1 and Slit2, the attractive response of netrin-1 is silenced. The silencing effect of Slit2 is specific for attraction by netrin-1, as Slit2 does

not block the attractive effect of brain-derived neurotrophic factor (BDNF) (Stein and Tessier-Lavigne, 2001).

Replacement of the P3 domain in DCC by a SAM (sterile alpha) motif in EphB1 and of the CC1 domain in Robo by a SAM domain results in receptors that are functional in attraction and repulsion respectively. When SAM substituition is performed in only one of the two receptors, both the cytoplasmic domain interaction and the silencing effect is abolished. But when SAM replacement is carried out simultaneously in both receptors, their interaction and silencing response are restored. When an exogenous Robo1 comprising its ectodomain and transmembrane domain but with a truncated cytoplasmic domain is expressed, Slit2 no longer silences the attractive effect of netrin-1. Hence silencing is mediated by direct interaction of receptor cytoplasmic domains (Stein and Tessier-Lavigne, 2001).

Slit2 does not repel growth cones expressing full-length Robo1, hence additional signalling molecules are required in the growth cone for repulsion to occur. When a chimeric receptor comprising a Met ectodomain (Met receptor tyrosine kinase is a receptor for hepatocyte growth factor, HGF), and the DCC transmembrane and cytoplasmic domain are expressed in cells, an attractive response is elicited. But Slit2 does not silence the attractive response to HGF mediated by wild-type Met receptor tyrosine kinase. Hence Slit2 can induce silencing when netrin is replaced by another ligand, e.g. HGF, but this effect is only specific for attraction caused by activation of the DCC cytoplasmic domain (Stein and Tessier-Lavigne, 2001). Attractive responses elicited by activation of a DCC cytoplasmic domain, whether by netrin-1 or a heterologous ligand acting on a chimeric receptor such as the cytoplasmic domain of Robo1 and the ectodomain of either the trkA receptor tyrosine kinase, a receptor for nerve growth factor, NGF, or Met can be silenced by activation of a Robo cytoplasmic

domain. An exogenously expressed truncated Robo receptor blocks silencing, therefore the presence of Slit protein is not sufficient to block netrin attraction and the effect of this ligand is mediated by an endogenously expressed Robo receptor.

The phenotypes in *Robo* and *Slit* loss-of-function mutants reflect loss of a repulsive and silencing function so that axons are abnormally attracted to the midline by netrin signalling. Deletion of the CC1 domain in Robo leads to impaired receptor binding of Enabled protein; inhibition of Robo mediated repulsion and hence partial rescue of the *robo* phenotype. As mentioned above, the CC1 domain is also the site of Abelson tyrosine kinase binding. Phosphorylation of a conserved tyrosine by Abl impairs Robo function, and mutation of this tyrosine to phenylalanine leads to a hyperactive Robo receptor (Bashaw *et al.*, 2000). Genetic studies in *Drosophila* on Robo2 and Robo3, which both contain a CC1 domain, have provided evidence that they function to repel axons away from the midline as well as silencing attraction (Simpson *et al.*, 2000; Rojagopalan *et al.*, 2000).

Experiments in *Xenopus* have shown that guidance signals are integrated hierarchically. Stage 22 spinal neurons are responsive to the silencing effect of netrin1 attraction by Slit. But they are not repelled by Slit, hence Slit-Robo function is relevant only as a modifier of the netrin response. However stage 28 neurons are repelled by Slit, but do not respond to netrin signalling, hence the interactions between guidance receptors are intrinsically regulated by other factors too (Stein and Tessier-Lavigne, 2001).

Slit-mediated interaction between the cytoplasmic domains of Robo1 and DCC is reminiscent of the netrin-gated interaction between DCC and UNC5 cytoplasmic domains (Hong *et al.*, 1999). The cytoplasmic domains of receptors are important in

altering the function of DCC; interaction with UNC5 switches its attractive response to repulsion and binding to Robo leads to silencing (Stein and Tessier-Lavigne, 2001).

1.9.3.6 Semaphorins and their receptors

Semaphorins (Semas) comprise a large family of secreted and cell-surface proteins that function in axon repulsion. Each family member is characterised by a conserved, 500 amino acid long 'Sema' motif in their extracellular domains. The first semaphorins were identified in grasshopper (Sema-1a/fasciclin IV) and chicken (Sema3a/collapsin-1/Sema III). To date, more than 30 Sema members have been isolated. They exhibit strong evolutionary divergence and act on many neuronal cell types, including sympathetic, motor, cerebellar, hippocampal, olfactory, corticospinal and dorsal root ganglion neurons (for review see Chisholm and Tessier-Lavigne, 1999).

Semaphorins are divided into transmembrane (classes 1, 4 and 6), glycosylphosphatidyl inositol (GPI; class 7) and secreted (classes 2, 3 and V) protein subfamilies. Classes 1 and 2 are found in invertebrates, classes 3 to 7 in vertebrates and class V in viruses. Examples of evidence for the repulsive activities of semaphorins include secreted Sema3A (collapsin-1/Sema III), an inducer of sensory growth cone collapse that can repel their axons, secreted vertebrate class 3 and *Drosophila* Sema-2a (for review see Culotti *et al.*, 1996). Certain classes of semaphorins regulate axon fasciculation depending on where they are expressed, e.g. grasshopper Sema-1a and vertebrate Sema3A in the surrounding environment cause fasciculation of axons through repulsion (for review see Culloti *et al.*, 1996; Keynes *et al.*, 1997; Taniguchi *et al.*, 1997), whereas *Drosophila* transmembrane Sema-1a is required for defasciculation of motor axons (Yu *et al.*, 1998).

Two receptors families, the plexins (Plexs) and neuropilins (NPs), which are found on specific growth cones, mediate the repulsive cues elicited by semaphorins.

NPs are divided into subfamilies NP1 and NP2 and Plexs into PlexA1-4, PlexB1-3. PlexC1, and PlexD1 on the basis of their structural similarities (for review see Tamagnone *et al.*, 2000). Plexins usually bind directly to semaphorins to activate intracellular signalling cascades. However class 3 semaphorins (Sema3A-3F) use neuropilins as coreceptors for signalling through plexin receptor subunits (for review see Tamagnone *et al.*, 2000).

Plexins are a large family of transmembrane proteins that function as repulsive receptors for most if not all semaphorins. They contain a Sema domain at their amino terminus, a cysteine-rich motif in their extracellular region and a conserved plexin-specific domain at their carboxy terminus (for review see Tamagnone *et al.*, 2000). Members of the GPI-linked, viral and transmembrane Sema classes bind to Plexs, which become phosphorylated upon ligand activation (Tamagnone *et al.*, 1999) and initiate Plex-dependent signalling pathways e.g. *Drosophila* PlexA1, human PlexB1 and PlexC1 are receptors for Sema1A, Sema4D and Sema7A respectively (Winberg *et al.*, 1998, Takahashi *et al.*, 1999, Tamagnone *et al.*, 1999). Plexins do not have intrinsic kinase activity (Maestrini *et al.*, 1996) and this led to investigations of potential kinases responsible for phosphorylation of these receptors upon ligand binding.

Studies in *Drosophila* have revealed that the receptor tyrosine kinase Off-track (OTK, formerly known as Dtrk) associates with PlexinA1, a receptor for Sema 1A. Mutations in the *otk* gene lead to defects in guidance of the ISNb motor axon as it defasiculates and branches at specific choice points along its trajectory. These guidance defects are similar to the phenotypes seen in loss-of-function mutations of *Sema1A* that mediates axon defasciculation (Yu *et al.*, 1998), or its receptor, Plexin A1, suggesting that they may all act in the same pathway. Genetic interactions between the three

mutations (*Sema1A*, *plexinA1*, and *otk*) suggest that they function coordinately, with OTK and Plexin A1 acting downstream of Sema 1A (Winberg *et al.*, 2001).

Biochemical and genetic studies in *Drosophila* have shown that members of the Rho GTPase family (primarily Cdc42, Rac, and RhoA) integrate guidance cues and mediate local regulation of the actin cytoskeleton (Hall, 1998) by co-localising with ligand-associated semaphorin receptors and activating their effectors to transduce signals downstream. For example, Rac1-GTPase acts downstream of the Sema3A/Neuropilin-1-PlexA1 complex and activates its downstream effector p21-activated kinase (PAK; Manser *et al.*, 1994). By activating LIM kinase and inhibiting myosin light chain kinase (MLCK), PAK inhibits actin turnover, which results in axonal growth cone collapse (Jin *et al.*, 1997, Fournier *et al.*, 2000). PlexB binds to and inhibits Rac-GTP output by blocking its access to PAK and, at the same time, binds to and increases activation of RhoA, leading to growth cone retraction via LIM kinase signalling, which phosphorylates and inactivates cofilin, an actin depolymerising factor (Hu *et al.*, 2001). Plex-B1 has been shown to interact with PDZ-RhoGEF and LARG, two members of the Dbl family of guanine nucleotide exchange factors (GEFs) that activate RhoA, to induce cell repulsion (Swiercz *et al.*, 2002).

Neuropilin receptors are expressed by commissural neurons and are required to navigate commissural axons across the CNS midline to their rostral targets after midline crossing (Zou *et al.*, 2000). These receptors bind class 3 semaphorins and together with slit proteins, prevent commissural axons from re-crossing the midline. Neuropilin-1 binds all secreted semaphorins, whereas neuropilin-2 binds SemaE (collapsin-3) and Sema IV but not Sema III (collapsin-1) (Chen *et al.*, 1997). *Neuropilin*-deficient mice exhibit defasciculation in certain branchiomotor nerves and in the segmental nerves

innervating the limb buds and this phenotype is consistent with the role of neuropilins as semaphorin receptors (Kitsukawa *et al.*, 1997).

Several semaphorins have been cloned in zebrafish (SemaZ) and their sequence homology to other semaphorins and expression patterns identified (Halloran *et al.*, 1998). SemaZ1a is highly homologous to Sema III/D/collapsin-1 (Yee *et al.*, 1999). Its expression pattern during axonogenesis and the findings that SemaZ1a repels peripherally extending growth cones of posterior lateral line ganglia neurons and causes collapse of chick dorsal root ganglia growth cones indicate that it has potential roles in axon guidance (Shoji *et al.*, 1998). SemaZ2 is highly homologous to collapsin-2 and is expressed in a number of neuroectodermal and mesodermal tissues. Its expression domains in the forebrain and midbrain include the rostral diencephalon spanning the midline at the base of the optic stalks and the caudoventral diencephalon extending into the midbrain tegmentum. Interestingly, the axons that form the initial scaffold of tracts in the brain, including those of the nucleus of the posterior commissure and the epiphysial neurons, grow around but not through the domains of *semaZ2* expression, suggesting that SemaZ2 acts as an inhibitory guidance molecule (Halloran *et al.*, 1999). In the hindbrain, domains of *semaZ2* expression include the floor plate cells at the ventral midline of the CNS and clusters of commissural neurons present in rhombomere boundary regions. *SemaZ2* is also expressed in a subset of cranial neural crest cells, pharyngeal arches and placode derivatives as well as the notochord, pectoral fin and tail buds. The domains of *semaZ2* expression in the diencephalon and floor plate of the midbrain and hindbrain are reduced in *whitetail* and completely absent in *cyclops* and correlate with axon guidance defects in these mutants (Halloran *et al.*, 1999; Yee *et al.*, 1999). SemaZ7 encodes a transmembrane class IV semaphorin that is most similar to human CD100 (Hall *et al.*, 1996) and its expression domains include the dorsal optic

tectum, rhombomeres 5 to 7 of the hindbrain, dorsal and ventral spinal cord, pharyngeal arches and the pectoral fin bud. SemaZ8 encodes the carboxy half of a secreted class III semaphorin (Luo *et al.*, 1995; Püschel *et al.*, 1995) and its expression domains includes the somites and two bilateral rows of cells in the ventral lateral tegmentum in the midbrain. SemaZ9 is likely a class III semaphorin and shows greatest sequence similarity to mouse SemaA (Püschel *et al.*, 1995) and human SemaV (Sekido *et al.*, 1996). SemaZ10 and Z11 are likely to be class IV semaphorins with SemaZ10 showing highest sequence similarity to M-Sema G (Furuyama *et al.*, 1996) and SemaZ11 to mouse SemaC (Püschel *et al.*, 1995).

1.9.3.7 Ephrins (Eph) and their receptors

The Eph family of receptor tyrosine kinases and their ligands, the ephrins, are involved in short-range chemorepulsive and chemoattractive axon guidance. Invertebrates have only one Eph receptor (Dearborn *et al.*, 2002), whereas vertebrates contain 14 Eph receptors and 9 ligands that are further divided into two classes based on the receptor(s) they interact with. Class one consists of EphA receptors (EphA1-A8) that bind to glycosyl-phosphatidyl-inositol (GPI)-anchored ephrin-As and class two is made up of EphB receptors (EphB1-B4) that interact with transmembrane attached ephrin-Bs; which have a highly conserved cytoplasmic domain containing a single catalytic tyrosine kinase region (Tuzi and Gullick, 1994; Flanagan and Vanderhaeghen, 1998). The binding specificity of both receptor types is low; each receptor binds to most ligands of its corresponding subclass and conversely each ligand binds to multiple receptors (Brambilla *et al*, 1995; Gale and Yancopoulos, 1997).

Functional studies have revealed important roles for ephrins in the patterning of the forebrain and hindbrain (Xu *et al.*, 1995, 1996) and formation of certain commissures (Henkemeyer *et al.*, 1996; Oriolo *et al.*, 1996). At the cellular level,

ephrins function as contact-dependent repulsive signals for retinal axons, motor axons, cortical neurons and neural crest cells (for review see Drescher, 1997). *In vitro* experiments have shown a role for ephrin-A5 in axon fasciculation and the formation of axon branches of cortical neurons (Winslow *et al.*, 1995; Caras, 1997).

Class B ephrins are expressed in the dorsal spinal cord and the floor plate and their corresponding receptor(s) is expressed on commissural axons that project longitudinally between these ephrin domains. Interference with endogenous EphB-ephrinB interactions in intact spinal cord explants results in repulsion and abnormal projection of commissural axons away from the floor plate into dorsal regions of ephrinB expression; hence class B ephrins function in commissural axon pathfinding on the contralateral side of the floor plate (Imondi and Kaprielian, 2001). Mice deficient for the EphB2 receptor (Nuk) show aberrant formation of the anterior commissure; these fiber tracts are misdirected to the ventral forebrain instead of crossing the midline (Henkemeyer *et al.*, 1996). Mice deficient for the EphB3 receptor (Sek4) show defects in the formation of the corpus callosum; these fiber tracts accumulate near the midline on the ipsilateral side instead of crossing the midline (Orioli *et al.*, 1996). Mice deficient for the EphA8 receptor (Eek) show defects in the fiber tract that normally connects the superior colliculus of the midbrain with the contralateral inferior colliculus; the fibers follow the aberrant ipsilateral path to the cervical spinal cord instead (Park *et al.*, 1996).

Both classes of ephrin ligands and Eph receptors signal bidirectionally i.e. the interaction of a receptor-expressing cell with a ligand-expressing cell initiates a signalling response in both cells. Ephrins are inactive in their monomeric form and require membrane attachment via their cytoplasmic SAM motif for receptor activation. Binding of ephrins to Eph receptors results in receptor tetramerisation, initiation of their

intrinsic tyrosine kinase activity and autophosphorylation of specific tyrosine residues in their cytoplasmic domains. This creates binding sites for phospho-tyrosine binding motifs of downstream target proteins, which include Src family kinases, RasGAP and phospholipase Cγ (Henkemeyer *et al.*, 1996; Holland *et al.*, 1996, Bruckner and Klein, 1998). Activation of EphA by ephrinA interaction results in downregulation of mitogen-associated protein kinase (MAPK) levels. MAPK normally signals to the cytoskeleton and its inhibition explains why Ephs are unable to induce cellular growth and proliferation (Miao *et al.*, 2001). EphA receptors also bind to Eph-interacting exchange protein (Ephexin) and in turn activate RhoA GTPases but inhibit the activity of Rac-1 and Cdc42; resulting in growth cone collapse (Shamah *et al.*, 2001).

The retinotectal map is a well-studied model system for the study of axon guidance. The ephrins and Eph receptors play an important role in the development of this projection and show graded expression patterns in both the retina and the tectum (Drescher *et al.*, 1997). The EphA family determine the formation of the antero-posterior (A-P) retinotectal projection. EphA receptors are highly expressed in the temporal retina and anterior tectum, whereas ephrin-As are highly expressed in the nasal retina and posterior tectum. Due to repulsive interactions, axons with high Eph receptor concentrations target regions of the tectum with low ephrin concentrations and axons with low Eph concentrations project to areas of the tectum with high ephrin concentrations (for review see Knöll and Drescher, 2002). EphBs are expressed in a low to high dorso-ventral (D-V) gradient in the retina, and a low to high D-V gradient in the tectum and its mammalian homologues, the thalamus and superior colliculus (SC). Ephrin-Bs are expressed in a high to low D-V gradient in the retina and a high to low D-V gradient in the tectum/SC. Axons expressing high levels of EphB project to targets with high levels of ephrin-B by reverse signalling and vice versa by forward signalling.

EphrinB/EphB bi-directional signalling is therefore important in determining D-V mapping and mediating attractive responses (Hindges *et al.*, 2002; Mann *et al.*, 2002; Pittman *et al.*, 2002; for review see Grunwald and Klein, 2002).

A glycoprotein purified from tectal membranes of embryonic chicken called repulsive guidance molecule (RGM), has recently been identified as a repulsive guidance molecule for retinal axons. It shares no sequence homology with known guidance cues but its messenger RNA is expressed, similar to the Eph family, in a gradient with increasing concentration from the anterior to posterior axis of the tectum. Recombinant RGM has been shown to induce collapse of temporal retinal axon growth cones (Monnier *et al.*, 2002).

1.9.3.8 The retinotectal projection in zebrafish

Retinal ganglion cell (RGC) axons exit the eye through the optic nerve head (papilla) in the central retina and grow along the ventral surface of the optic stalk. They then cross the ventral midline of the forebrain alongside pre-existing axon bundles of the tract of the post-optic commisure, turn dorso-caudally and target the contralateral optic tectum in the dorsal midbrain. Their final position depends on their original location in the retina. Axons from the nasal (anterior) retina project to the posterior tectum and those from the temporal retina target the anterior tectum. Dorsal and ventral retinal axons project to the ventral and dorsal tectum respectively. In addition to the contralateral tectum, zebrafish RGC axons also normally target several nuclei located in the ventral diencephalon, dorsal to the optic tract. The first RGC axons extend during the second day of development and the retinotectal map develops over the next 5 days (Burrill and Easter, 1995).

Zebrafish mutants were screened by labelling retinal ganglion cells of 5-day-old larvae with DiI and DiO and their axonal projections to the tectum analysed. They were classified and grouped according to the position of their axonal defects. In class I mutants (*belladonna, detour, you-too, iguana, umleitung, blowout*) axons leave the eye and project to the ipsilateral tectum. Class II mutants (*chameleon, bashful*) also show ipsilateral projecting axons as well as pathfinding defects within the eye. Class III mutants (*esrom, tilsit, tofu*) have fewer axons than normal crossing the midline but some do target the contralateral tectum. Class IV mutants (*boxer, dackel, pinscher*) show axon sorting defects after crossing the midline and pathfinding errors once the retinal axons have reached the tecta. The final group, class V mutants (*bashful, grumpy, sleepy, cyclops, astray*) have anterior-posterior pathfinding defects at or after the midline. Analysis of these mutants has shown that a sequence of guidance cues direct axons to their final target and has identified the ventral midline as a critical and complex choice point during this process (Baier *et al.*, 1996; Karlstrom *et al.*, 1996).

The zebrafish *astray* (*ast*) mutant exhibits pathfinding defects, particularly in the ventral diencephalon, excessive midline crossing and defasciculation of the retinal projection. The pathfinding errors in *ast* correlate with Slit2 and Slit3 expression in the ventral diencephalon, suggesting that they are responsive to these repulsive cues in the surrounding environment. *Astray* is defective in the gene encoding Robo2, a homologue of the *Drosophila* axon guidance receptor Roundabout (Fricke *et al.*, 2001). The midline of the ventral diencephalon is a critical choice point for retinal axons. At this location, growth cones in wild-type zebrafish migrate slower and become more complex and those in *ast* alter their morphology and make most of their pathfinding errors. However, these defects in *ast* are also observed both before and after the midline hence Robo2 function is required in growth cones before reaching the midline (Hutson

and Chien, 2002). Interestingly, the role of Robo in zebrafish is different to its function in *Drosophila*, which has low expression in commissural axons during midline crossing and is upregulated upon leaving the midline to prevent re-crossing (Kidd *et al.*, 1998). But it is similar to mutations in the *C. elegans* Robo homologue *sax-3* and its ligand slit, which cause midline crossing defects (Zallen *et al.*, 1998; Hao *et al.*, 2001).

Zebrafish brain patterning mutants show retinotectal pathfinding defects similar to *ast*. They include *no isthmus* (*noi*), which has a mutation in the gene *pax2.1* (Brand *et al.*, 1996) and *acerebellar* (*ace*), which is defective in the *fgf8* gene (Shanmugalingam *et al.*, 2000). In *noi*, retinal axons project anteriorly, ipsilaterally and occasionally into the opposite eye (Macdonald *et al.*, 1997).

1.9.3.9 Non-axon guidance functions of signalling cues

Slits also function in mesodermal cell migration (Hedgecock *et al.*, 1990; Kramer *et al.*, 2001), ephrins in somitogenesis, vasculogenesis (for review see Wilkinson, 2001) and synaptic plasticity (Grunwald *et al.*, 2001; Henderson *et al.*, 2001; Takasu *et al.*, 2002) and semaphorins in heart and bone development (Behar *et al.*, 1996). Neuropilin-1 is a cell-surface receptor for vascular endothelial growth factor (VEGF) and is required for angiogenesis in mice and zebrafish (Lee *et al.*, 2002). Sema 4D is also implicated in metastatic processes through activation of the Met pathway (Giordano *et al.*, 2002).

1.10 Local guidance at the midline and regulation of axon fasciculation

Cell adhesion molecules (CAMs) also regulate axon guidance by altering their adhesion to the extracellular matrix (ECM) and other cells (for review see Tessier-Lavigne and Goodman, 1996). The neural cell adhesion molecule (NCAM) belongs to the immunoglobulin (Ig) superfamily, was the first member to be identified in vertebrates

and is widely expressed in the developing and adult brain. It is involved in fasciculation and pathfinding of axons and mediates its function by interacting with a variety of ligands, including the neural adhesion molecule, L1 (Walsh and Doherty, 1997; Kiss and Muller, 2001). L1 interacts with neuropilin-1 and is a component of a Sema3A receptor complex that converts Sema3A-mediated repulsive signals to cortical neuron growth cones (Castellani *et al.*, 2000). NCAM interacts with polysialic acid, PSA, which attaches to its cell surface and inhibits NCAMs ability to promote adhesion and cell-cell interactions mediated by other molecules (for review see Rutishauser, 1989; Rutishauser and Landmesser, 1996). Elongation and pathfinding of corticospinal axons are impaired in NCAM and L1- deficient mice (Cohen *et al.*, 1998; Rolf *et al.*, 2002). These defects are phenocopied in wild-type mice by removal of PSA by a PSA-specific endosialidase, endosialidase N (EndoN; Ono *et al.*, 1994). In the chick, removal of PSA results in defects in fasciculation and pathfinding of retinal axons (Landmesser *et al.*, 1990; Monnier *et al.*, 2001).

In zebrafish, PSA is not expressed in hindbrain commissural axons but controls midline crossing by acting on floor plate cells, where it is expressed (Marx *et al.*, 2001). PSA-NCAM expression is selective and only found in a small set of axon tracts, unlike that found in other vertebrates. Injection of EndoN into the developing CNS causes defasciculation of the posterior commissure. This is because commissural axons and the surrounding CNS express PSA and its removal increases interactions that attract growth cones into paths not normally chosen by these axons.

Heparan sulphate proteoglycans are carbohydrate modifications of some proteins found on the cell surface or in the extracellular matrix (ECM). They enhance binding of Slit2 to its receptor Robo-1 and are involved in Slit2-mediated repulsion (Hu *et al.*, 2001). Other ECM molecules involved in the control of axonal growth include laminin,

fibronectin, collagen, nidogen, vitronectin, tenascin and thrombospondin and the main receptors for these ligands are integrins, proteoglycans and Ig superfamily members (for review see Tessier-Lavigne and Goodman, 1996).

1.11 Aims

Zebrafish mutants isolated from large-scale chemical mutagenesis screens display defects in various aspects of embryonic development (Driever, 1996; Haffter, 1996). The aim of this project was to carry out molecular and phenotypic characterisation of four such mutants with defects in axonal development in the CNS.

The mutants *monorail*^{tv53a}, *shrink*^{U41}, *otter*^{ta76b} and *eisspalte*^{ty77e} (Brand *et al.*, 1996; Jiang *et al.*, 1996; Corinne Houart, personal communication) were studied (see Table 1.1). Phenotypic characterisation of each mutant was carried out using a variety of molecular markers and dissecting and compound microscopes with Nomarski optics to reveal defects in various aspects of CNS development. Initial investigation involved wholemount labelling of embryos with an antibody to acetylated α-tubulin to reveal early axon pathways in the brain (Piperno and Fuller, 1985). Further immunohistochemical techniques were then used to reveal other structures and identify new phenotypes. It was anticipated that re-screening of these mutant lines together with genetic mapping and identification of the affected genes would provide new insights into early vertebrate brain development and increase knowledge of the processes and components involved in neuronal patterning and commissural axon pathfinding in the central nervous system.

Table 1.1 Original phenotypes of the mutant lines investigated:

Mutant name and allele	Gross morphological phenotype	Specific CNS abnormality
monorail (*mol*^{tv53a})	Curly tail down. Patchy floor plate. Irregular notochord.	Absence of ventral tegmental commissure. Reduction of floor plate width in the hindbrain region. Ventral midbrain and hindbrain disorganisation of axon trajectories and neurons.
eisspalte (*ele*^{ty77e})	Thicker hindbrain and notch in hindbrain posterior to cerebellum. Small eyes and head. Enlarged brain ventricles.	Defasciculated anterior commissure. Very poor tectum. 'Disorganised' hindbrain. Thicker optic nerve.
otter (*ott*^{ta76b})	Reduced brain ventricles. Obscure midbrain-hindbrain boundary. Smaller eyes and otic-vesicles.	Defasciculated anterior and post-optic commissures. Ectopic axons in the ventral forebrain.
shrink (*sik*^{U41})	Small eyes. Cell death in the head by embryonic day three.	Defasciculated post-optic commissure. No tecta. Disorganised axon trajectories and neurons in the hindbrain.

2. Materials and Methods

2.1 Materials

2.1.1 Standard buffers and reagents

All reagents were purchased from SIGMA® unless otherwise stated.

Agarose Gel	0.8-3.5 % (w/v) agarose (GibcoBRL®)
	100 ml of 1.0 X TBE buffer
	0.005 % (v/v) ethidium bromide (10 mg/ml)
RNA Gel	1.0 % (w/v) agarose
	37 ml distilled water
	8 ml formaldehyde
	5 ml 10 X MOPS
	0.005 % (v/v) ethidium bromide (10 mg/ml)
Ammonium persulphate	10 % w/v
Blue dextran loading buffer	5 parts de-ionised formamide
	1 part 50 mM EDTA (pH 8.0)
	30 mg/ml Blue Dextran
	Stored at -20°C in aliquots.
Ficoll 400 solution	20 % (w/v) in distilled water

Loading buffer (10 X)	28.5 % (w/v) Ficoll 400 (Pharmacia®)
	1.4 % (w/v) SDS
	28.5 % (w/v) 0.5 M EDTA (pH 8.0)
	0.5 % (w/v) Orange G
	made up with distilled water
	Stored at room temperature.
Molecular weight ladder	10 % (v/v) 1 kb ladder
(Gibco BRL®)	80 % (v/v) TE buffer
	5 % (v/v) 10 X loading buffer
	5 % (w/v) Ficoll 400 solution
	0.4 % (w/v) 5 M NaCl
	Stored at -20°C in aliquots.
MOPS (10 X)	0.2 M MOPS acid
	dissolved in DEPC treated water (pH 7.0)
	5 M NaOH
	50 mM Sodium acetate (pH 7.0)
	10mM EDTA (pH 8.0)

RNA loading buffer (10 X)	50 % (v/v) glycerol 1.0 mM EDTA 0.25 % (w/v) Bromophenol blue 0.25 % (w/v) Xylene cyanol. Stored at room temperature
RNA sample running buffer	1 X MOPS 17.5 % (v/v) formaldehyde, 50 % (v/v) formamide.
dNTP mix (10 mM)	100 µl of each 100mM stock solution of dATP, dCTP, dGTP and dTTP (GibcoBRL®) made up to 1.0 ml with distilled water.
TBE (10 X)	10.8 % (w/v) Tris-base 5.5 % (w/v) Boric acid 0.9 % (w/v) EDTA made up to 1.0 litre with distilled water
TBE (0.5-1.0 X)	50-100 ml of 10 X TBE made up to 1.0 litre with distilled water

TE buffer (TE)	10mM Tris-HCl (pH 8.0) 1.0 mM EDTA
PBS (1 X)	1 tablet (pH 7.4; Oxoid®) dissolved in 1.0 litre of distilled water.
PBTriton (1 X)	0.8 % (v/v) Triton X-100 in 1 X PBS
PBTween (1 X)	0.8 % (v/v) Tween-20 in 1 X PBS
Embryo lysis buffer	10 mM Tris-HCl (pH 8.3) 50 mM KCl 0.3 % (v/v) Tween-20 0.3 % (v/v) Nonidet P40
Proteinase K	Working dilution of 10 mg/ml
Disruption buffer	100 mM NaCl 50 mM Tris (pH 8.0) 100 mM EDTA (pH 8.0) 1.0 % (w/v) SDS

LB broth	10 g Bacto tryptone 5 g yeast extract 10 g NaCl made up to 1.0 litre with distilled water, adjusted to pH 7.5, autoclaved and stored at room temperature.
L-agar	1.5 % (w/v) agar in LB broth.
Protease inhibitor solution	1 protease inhibitor cocktail tablet (Roche®) dissolved in 700 µl of distilled water
Protein extraction buffer	0.1 % Triton X-100 0.1 % Nonidet P40 0.1 M PMSF 10 X protease inhibitor cocktail tablet (Roche®) solution made up to 1.0 ml with PBS. Stored at -20°C in aliquots.
Running buffer	0.025 M Tris-base 0.192 M glycine 0.1 % (w/v) SDS made up to 1.0 litre with distilled water

Transfer buffer	25 mM Tris-HCl (pH 8.3) 150 mM glycine
Destaining solution	7.0 % (v/v) acetic acid 40 % (v/v) methanol made up to 1.0 litre with distilled water
PBS-Tween	0.05 % (v/v) Tween-20 in 1 X PBS
Blocking buffer	5.0 % (w/v) non-fat dried milk in PBS-Tween
TBS (1 X)	10 mM Tris (pH 8.0) 150 mM NaCl
TBS-Tween	0.05 % (v/v) Tween-20 in 1 X TBS
Coomassie blue stain	0.1 % (w/v) Coomassie brilliant blue R-250 25 % (v/v) methanol 10 % (v/v) acetic acid made up to 1.0 litre with distilled water
Ponceau S staining solution	0.2 % (w/v) Ponceau S in 3.0 % (w/v) TCA

Resolving gel mixture	6.0 ml 30 % (v/v) acrylamide/bisacrylamide-37.5:1 (Bio-Rad®),
	3.8 ml of 1.5 M Tris (pH 8.8)
	150 µl of 10 % (w/v) SDS
	150 µl of 10 % (w/v) APS
	6.0 µl TEMED
	made up to 15 ml with distilled water
Stacking gel mixture	830 µl of 30 % (v/v) acrylamide/bisacrylamide-37.5:1 (Bio-Rad®),
	630 µl of 1.0 M Tris (pH 6.8)
	50 µl of 10 % (w/v) SDS
	50 µl of 10 % (w/v) APS
	5.0 µl TEMED
	made up to 5.0 ml with distilled water
SDS sample buffer (2 X)	0.6 % (v/v) 1M Tris-HCl (pH 6.8)
	0.8 % (w/v) SDS
	0.5 % (v/v) β-mercaptoethanol
	1.0 % (v/v) glycerol
	1.0 % (w/v) bromophenol blue
	made up to 10 ml with distilled water
	Stored at -20°C in aliquots.

2.1.2 Maintenance of zebrafish, embryo collection and staging

Breeding zebrafish (*Danio rerio*) were maintained at 28.5°C on a 14 hour light/10 hour dark cycle (Westerfield, 1993).

Wild-type embryos were generated from the lines WIK (Rauch *et al.*, 1997); Tübingen, Tü (Haffter and Nüsslein-Volhard, 1996); *AB (Chakrabarti *et al.*, 1983); and Tup Longfin, TL (Haffter *et al.*, 1996 (a)). ENU-induced mutant embryos were obtained from the lines *shrink*, sik^{U41} (Corinne Houart, unpublished results); *monorail*, mol^{tv53a} (Brand *et al.*, 1996); *otter*, ott^{ta76b} and *eisspalte*, ele^{ty77e} (Jiang *et al.*, 1996).

Mutant carriers were identified by random intercrosses, and outcrossed to wild-type fish to maintain the stock. For genetic mapping purposes mutant carriers were outcrossed to the WIK line (see Figure 1.3). To obtain mutant embryos, two heterozygous carriers were mated. Typically, the eggs spawned synchronously at dawn, embryos were collected in water supplemented with methylene blue to prevent growth of mould in the water, sorted, observed and fixed either in 4.0 % (w/v) paraformaldehyde (PFA) or 2.0 % (w/v) TCA after different stages of development at 28.5°C. In addition, morphological features were used to determine the age of embryos (Westerfield, 1994; Kimmel *et al.*, 1995). Throughout this thesis, the developmental age of the embryos will correspond to the number of hours elapsed since fertilisation, hpf. To inhibit pigmentation and maintain optical transparency, embryos were transferred to fish water containing 0.2 mM PTU between 18 and 22 hpf (Burrill and Easter, 1994). PTU acts by inhibiting tyrosinase activity (Westerfield, 1993).

Caution: PTU is extremely toxic and protective clothing must be worn upon handling.

2.1.2.1 Observation of live embryos

Differential Interference Contrast microscopy / Nomarski Optics

Embryos were observed in fish system water and manually dechorionated with #5 watchmaker's forceps. When required, embryos were anaesthetised in 0.02 % (w/v) tricaine and immobilised for viewing in 3.0 % (w/v) methyl cellulose in fish system water (40 g Instant Ocean in 1.0 litre of distilled water).

2.1.2.2 Generation of transgenic fish

The *monorail*-Islet1-GFP line was generated by crossing a heterozygous *monorail* carrier with a homozygous Islet1-GFP fish (Higashijima *et al.*, 2000). The resulting progeny were homozygous for Islet1-GFP and 25 % of the fish were heterozygous *monorail* carriers.

Fluorescent signals in both live and fixed embryos were assayed under a fluorescence microscope (Leica).

2.2 Methods

2.2.1 Immunohistochemistry

2.2.1.1 Antibodies used

The primary monoclonal antibodies used were anti-acetylated α-tubulin (1:1000; Piperno and Fuller, 1985) and anti-zrf-1 (1:4; Institute of Neuroscience, University of Oregon; Trevarrow *et al.*, 1990). The primary polyclonal antibody used was anti-GFP (1:1000; AMS Biotechnology®). The secondary antibody used was horseradish peroxidase (HRP)-conjugated anti-mouse IgG (1:200) for all reactions except for anti-GFP, for which anti-rabbit IgG-HRP (1:200) was used.

2.2.1.2 Whole-mount antibody labelling of 24-72 hpf embryos

Up to twenty PTU-treated, dechorionated embryos were transferred to a microcentrifuge tube with a Pasteur pipette. The embryo medium was removed and embryos were fixed either for 3 hours at room temperature or at 4°C overnight in 1.0 ml volume of 4.0 % (w/v) PFA if 30 hpf or younger. Embryos older than 30 hpf were fixed in an equivalent volume of 2.0 % (w/v) TCA in phosphate-buffered saline, PBS (Oxoid®) for exactly 3 hours at room temperature. After fixation, the embryos were washed 3 x 5 min in an equivalent volume of PBS. Embryos could be stored for up to a week at 4°C in PBS before antibody labelling. Prior to labelling, embryos were washed 3 x 5 min in PBS and 2 x 10 min in PBTriton (PBS with 0.8 % (v/v) Triton X-100 (BDH®)) at room temperature to remove all traces of fixative. Embryos older than 48 hpf were permeabilised by incubation in chilled trypsin (Gibco BRL®) solution (0.25 % (w/v) in PBTriton) and incubated on ice for 4 min. The trypsin solution was immediately replaced with PBTriton and the embryos were washed 5 x 5 min at room temperature. The embryos were then incubated in 1.0 ml of 10 % (v/v) normal goat serum in PBTriton (blocking solution) for at least 1 hour at room temperature to block non-specific binding sites for immunoglobulins and other types of background protein interactions. The blocking solution was replaced with primary antibody diluted in 1.0 ml of 1.0 % (v/v) normal goat serum in PBTriton and incubated overnight at 4°C on a rocking table with gentle agitation. The following day the primary antibody solution was removed and the embryos were washed over several hours in PBTriton with gentle agitation at room temperature. The buffer was changed at least five times and the final wash was in PBS. The background staining was significantly reduced by longer washes. For embryos older than 30 hpf, endogenous peroxidases were quenched by washing the embryos in the following solutions at room temperature:

- 5 min in 50 % (v/v) methanol/PBS solution,
- 5 min in 100 % (v/v) methanol,
- 10 min in 1.0 ml of 100 % (v/v) methanol/50 µl 6 % (v/v) hydrogen peroxide (H_2O_2).
- 5 min in 50 % (v/v) methanol/PBS solution,
- 10 min in PBS,
- 10 min in PBTriton.

The embryos were then incubated in secondary antibody diluted 1.0 ml of 1.0 % (v/v) normal goat serum in PBTriton and incubated overnight at 4°C on a rocking table with gentle agitation. The following day the primary antibody solution was removed and the embryos were washed over several hours in PBTriton with gentle agitation at room temperature. The buffer was changed at least five times and the final wash was in PBS. Embryos were transferred to a multiwell plate, excess PBS was removed and 0.5 ml of 2 mM diaminobenzidine (DAB) in PBS was added per well.

Caution: DAB is a potential carcinogen, protective clothing must be worn and it should be dispensed in a fume cupboard. Solutions containing DAB should be disposed of in bleach waste.

The embryos were pre-incubated for 20 min at room temperature before the addition of 1-2 µl of 6.0 % (v/v) H_2O_2 per well. The reaction was monitored at low magnification under a microscope. Upon completion, as seen by the appearance of a brown reaction product, the reaction was stopped by PBS washes. The embryos were then post-fixed in 4.0 % (w/v) PFA overnight at 4°C and washed in PBS at room temperature. They were cleared through graded glycerol (AnalaR ®) solutions:

- 30 % (v/v) glycerol/PBS,
- 50 % (v/v) glycerol/PBS,

- 70 % (v/v) glycerol/PBS until the embryos sink.

The embryos were stored in 70 % (v/v) glycerol/PBS at 4°C ready for observation, dissection and microscopy.

Variation of the antibody protocol for anti-GFP antibody labelling

The blocking solution (incubation buffer) contained PBTriton, 10 % (v/v) normal goat serum as well as 1.0 % (v/v) dimethyl sulfoxide (DMSO). The secondary antibody was also diluted in incubation buffer.

2.2.2 Detection of Apoptotic Cells

Detection of apoptotic cells was carried out by the *in situ* terminal deoxynucleotidyl transferase (TdT)-mediated dUTP nick-end labelling (TUNEL) assay (ApopTag *in situ* Apoptosis Detection Kit-Peroxidase; Oncor, Inc.; Cole and Ross, 2001). Dechorionated 72 hpf embryos were fixed in 4.0 % (w/v) PFA in PBS for 1 hour at room temperature. They were washed 3 x 5 min in PBS and stored in methanol at 4°C overnight. The embryos were re-hydrated by washing:

- 5 min in 75 % (v/v) methanol/25 % (v/v) PBTween (1 X PBS in 0.1 % (v/v) Tween-20),
- 5 min in 50 % (v/v) methanol/50 % (v/v) PBTween,
- 5 min in 25 % (v/v) methanol/75 % (v/v) PBTween,
- 3 x 5 min in PBTween.

The embryos were permeabilised by proteinase K treatment (10 μg/ml in PBS) at room temperature for 20 min, washed 2 x 5 min in PBTween and postfixed in 4.0 % (w/v) PFA for 20 min at room temperature. Following 5 x 5 min washes in PBTween, the embryos were postfixed in a prechilled solution of ethanol:acetone (2:1) at -20°C for 10 min and washed 3 x 5 min in PBTween at room temperature. The embryos were

incubated for one hour at room temperature in 75 µl of equilibration buffer (provided in the ApopTag kit). The equilibration buffer was removed and 17 µl working strength TdT enzyme solution (Reaction buffer:TdT enzyme, 2:1; provided in the ApopTag kit) in 0.3 % (v/v) PBTween added to the embryos which were incubated overnight at 37°C. The reaction was stopped by washing the embryos in working strength stop/wash buffer (1 ml stop/wash buffer added to 17 ml distilled water) for 3 hours at 37°C. The embryos were then washed 3 x 5 min in PBTween, incubated in 4.0 % (v/v) BSA in PBTween for at least one hour at room temperature to block non-specific immunoreactivity and incubated in a 1:2000 dilution of preabsorbed sheep anti-digoxigenin-alkaline phosphatase conjugated Fab fragments for 2 hours at room temperature or overnight at 4°C. The antibody was removed and the embryos washed several times with PBTween and equilibrated with 3 x 5 min washes in freshly prepared NTMT buffer (0.1 M Tris-HCl (pH 9.5), 50 mM $MgCl_2$, 0.1 M NaCl, 0.1 % (v/v) Tween-20). The colour reaction was performed with 3.5 µl of 50 mg/ml X-phosphate in dimethylformaldehyde and 4.5 µl of 75 mg/ml NBT in dimethylformamide in 1.0 ml NTMT buffer in the dark for 15 min. The reaction was stopped with washes in PBTween and embryos were fixed in 4.0 % (w/v) PFA for 30 min at room temperature and washed in PBS. They were cleared through graded glycerol (AnalaR ®) solutions:

- 30 % (v/v) glycerol/PBS,
- 50 % (v/v) glycerol/PBS,
- 70 % (v/v) glycerol/PBS until the embryos sink.

The embryos were stored in 70 % (v/v) glycerol/PBS at 4°C ready for observation, dissection and microscopy.

2.2.3 Lipophilic Dye Labeling of the Retinotectal Projection

Three to five day old, PTU-treated larvae were fixed in 4.0 % (w/v) PFA at 4°C overnight. Larvae were washed in 1 x PBS and placed on a large Petri dish against a vertically positioned glass slide with watchmaker's forceps. To prevent them from drying out they were coated with 1 x PBS which also held them in position by surface tension. The larvae were orientated under a dissecting microscope against the glass slide with their trunk under the glass slide and their head sticking out ready for injection. The tip of an injection needle was carefully broken off under a dissecting microscope using watchmaker's forceps. A micropipette was filled with 5 µl of 1.0 % (v/v) DiI (1,1'-dioctadecyl-3,3,3',3'-tetramethyl indocarbocyanine perchlorate or 1.0 % (v/v) DiO (3,3'-dioctadecyl oxacarbocyanine perchlorate) (Molecular Probes) in chloroform and the dye was dispensed into the needle. The needle was mounted in the holder of a Narishige micromanipulator connected to a Picospritzer injection system and brought down to the larvae at an angle. The embryo was injected intraocularly into the gap between the retina and the lens. Each eye was filled with a different dye. Injected larvae were placed in a 1.5 ml microcentrifuge tube filled with 0.5 ml of 1 x PBS and left overnight at 4°C so that the dyes diffused within membranes by a passive process which stained axons of retinal ganglion cells (Godement *et al.*, 1987). Injected larvae were mounted for confocal microscopy analysis as described in section 2.5.2.

2.2.4 Mounting of labelled embryos

Whole embryos were dissected in 70 % (v/v) glycerol to remove the yolk for flat mounting and the skin and eyes to reveal internal labelling. Dissection was carried out using a dissecting microscope (Nikon). Embryos were pinned to small Petri dishes coated with Sylgard silicone elastomer (BDH®) with fine pins. Sharpened tungsten needles and fine forceps were used to dissect the yolk sac and eyes. Embryos were

mounted in wells formed by attaching layers of one to four 22 x 22 mm cover slips on both ends of a 22 x 64 mm glass slide with a drop of 70 % (v/v) glycerol. A long cover slip was placed on top and the embryo viewed at high magnification. After microscopic analysis, embryos were stored indefinitely in 70 % (v/v) glycerol at 4°C.

2.2.4.1 Differential Interference Contrast (DIC) microscopy, photography and image analysis

Labelled, dissected whole-mount embryos were analysed and photographed at 10x or 20x magnification using either a dissecting microscope (Nikon) or compound microscope (Nikon) coupled to a digital camera (Polaroid). Live embryos were anaesthetised in 0.02 % (w/v) tricaine and analysed and photographed using the dissecting microscope (Nikon). Images were compiled and labelled using Adobe Photoshop software (Adobe, version 5.5).

2.2.4.2 Confocal microscopy

Larvae were dissected by removing the yolk and trunk and mounted by embedding in 1.0 % (w/v) low melting point temperature agarose in PBS and placed in a glass ring (Fisher®) fixed with Vaseline on a glass slide. They were orientated dorsal side up. Mounted larvae were covered with distilled water before being placed under water immersion lenses and analysed using a Leica DMRE fluorescence microscope and a Leica DMLFS fluorescence microscope with a TCS SP confocal head and TCSNT software. Images were compiled and labelled using Adobe Photoshop software (Adobe version 5.5).

2.2.5 DNA techniques

2.2.5.1 DNA extraction from single zebrafish embryos

Embryos were dechorionated, placed individually into wells of a 96 well plate and stored in 100 % (v/v) methanol at -70°C. Prior to DNA extraction, as much methanol as possible was removed from the wells. All incubation steps were carried out on a PCR machine. The plates were incubated at 50°C for 10 min to remove any residual methanol. Fifty µl of embryo lysis buffer was added to each well and the embryos incubated at 98°C for 10 min to lyse the cells and then quenched on ice. Five µl of proteinase K (10 mg/ml) was added to each well to remove proteins and the embryos incubated overnight at 55°C. Proteinase K was deactivated by incubating the embryos at 98°C for 10 min. After quenching on ice, the lysed embryo debris was centrifuged at 4, 000 rpm for 10 min and the supernatant from each embryo preparation drawn off into a clean 96 well plate. The final concentration of each sample was approximately 50 ng/µl. The samples were stored at -70°C and diluted as necessary before use.

Table 2.1A *Monorail*^{tv53a} mutant and sibling DNA plates

Single embryo genomic DNA plates from Tübingen

Plate	Family/Cross	Contents
*T1461	34	48 Muts, 48 Sibs
*T1462	34	48 Muts, 48 Sibs
T2081	34	48 Muts, 48 Sibs
T2090	1718	48 Muts, 48 Sibs
T2089	1718	48 Muts, 48 Sibs
T2084	12	48 Muts, 48 Sibs
T2085	78	48 Muts, 48 Sibs

T2086	1314	48 Muts, 48 Sibs
T2087	1516	48 Muts, 48 Sibs
T2088	1516	48 Muts, 48 Sibs

Parental DNA:
Monorail 1384 and 1382
WIK 1473 and 1471

Single embryo genomic DNA plates prepared at UCL

Plate	Contents
1	60 Sibs
2	48 Muts, 48 Sibs
3	48 Muts, 48 Sibs
4	48 Muts, 48 Sibs
5	36 Muts, 60 Sibs
6	96 Sibs
7	96 Sibs

Table 2.1B *Shrink*^{U41} mutant and sibling DNA plates

Single embryo genomic DNA plates prepared at UCL

Plate	Contents
1	48 Muts, 48 Sibs
2	96 Muts
3	96 Sibs
4	96 Sibs
5	72 Muts
6	96 Sibs
7	96 Sibs

Table 2.1C *Otter*^{ta76b} mutant and sibling DNA plates

Single embryo genomic DNA plates prepared in Tübingen

Plate	Family/Cross	Contents
T1047	34	48 Muts, 48 Sibs
T1180	12	48 Muts, 48 Sibs
T1180	12	48 Muts, 48 Sibs
T1466	12	48 Muts, 48 Sibs

Single embryo genomic DNA plates prepared at UCL

Plate	Contents
1	48 Muts, 48 Sibs
2	48 Muts, 48 Sibs
3	48 Muts, 48 Sibs

Parental DNA:
Otter 763
WIK 329

Table 2.1D *Eisspalte*^{ty77e} mutant and sibling DNA plates

Single embryo genomic DNA plates prepared in Tübingen

Plate	Family/Cross	Contents
T1465	12	48 Muts, 48 Sibs
T1465	12	48 Muts, 48 Sibs
T1464	34	48 Muts, 48 Sibs
T1463	78	48 Muts, 48 Sibs
T1465	12	48 Muts, 48 Sibs
T1463	78	48 Muts, 48 Sibs
T1464	34	48 Muts, 48 Sibs

T1463	78	48 Muts, 48 Sibs
T1465	12	48 Muts, 48 Sibs
T1463	78	48 Muts, 48 Sibs

Single embryo genomic DNA plates sent from Tübingen

Plate	Family/Cross	Contents
T2080	12	48 Muts, 48 Sibs

Parental DNA:
Eisspalte 1,2,3, 4 and 33
WIK 770

Single embryo genomic DNA plates prepared at UCL

Plate	Contents
1	48 Muts, 48 Sibs
2	72 Muts, 24 Sibs
3	72 Muts, 24 Sibs
4	60 Muts, 36 Sibs
5	72 Muts, 24 Sibs
6	84 Muts, 12 Sibs
7	96 Sibs
8	96 Sibs
9	60 Muts

KEY:
Muts- mutants in tup longfin background
Sibs- siblings
WIK- wild-type strain
*- DNA plates I prepared in Tübingen, sent to UCL

2.2.5.2 DNA extraction from zebrafish finclips

Finclips were stored at -70°C until needed for use. Each finclip was cut into small pieces and transferred to a 1.5 ml microcentrifuge tube before the addition of 500 µl of disruption buffer. The tissue was homogenized using an autoclaved pellet homogeniser. Twenty-five µl of proteinase K (20 mg/ml) was added to the sample, which was then incubated overnight in a 55°C water bath. Five hundred µl of phenol/ chloroform/isoamylalcohol (25:24:1; pH 7.5) was added to the sample, which was then inverted several times for 1 min and centrifuged at 12, 000 x g for 5 min. The supernatant was transferred to a fresh 1.5 ml microcentrifuge tube before the addition of an equal volume of phenol (pH 7.5). The sample was inverted several times for 1 min and centrifuged at 12, 000 x g for 5 min. The supernatant was transferred to a fresh 1.5 ml microcentrifuge tube before the addition of an equal volume of chloroform/isoamylalcohol (24:1). The sample was inverted several times for 1 min and centrifuged at 12, 000 x g for 1 min. The supernatant was transferred to a fresh 1.5 ml microcentrifuge tube before the addition of 0.1 vols. 3.0 M sodium acetate (pH 5.2) and 2 vols. 100 % (v/v) cold ethanol. The sample was mixed up and down for 1 min and centrifuged at 12, 000 x g for 1 min. The precipitated DNA was then washed with 1000 µl of 70 % (v/v) ethanol and dried on a PCR machine at 60°C for 5 min. The DNA was resuspended in 250 µl of TE (pH 8.0) and left to rotate and mix overnight. The optical density of the suspension was measured on a spectrophotometer and this value was used to calculate the DNA concentration of the sample (section 2.2.1.2), which was subsequently stored at -70°C.

2.2.5.3 Quantification of Nucleic Acid samples

DNA samples were quantified using a spectrophotometer (model M302; Camspec®) at absorbances of 260 nm (A_{260}) and 280 nm (A_{280}). Five µl of the concentrated nucleic acid sample was added to 95 µl of distilled water in a cuvette. Three readings were taken per sample at the two wavelengths and compared to a reference reading obtained from a sample of distilled water alone. The average reading for each sample was obtained and the purity of the nucleic acid preparation determined by calculating the ratio of the average absorbance at 260 nm to the average absorbance at 280 nm. The expected ratio (A_{260}:A_{280}) was in the range of 1.7 - 1.9, as determined for pure DNA.

Concentration of DNA = A_{260} x dilution factor x 50

(For double stranded DNA, an absorbance ratio of 1.0 is equivalent to 50 µg/ml)

Concentration of RNA = A_{260} x dilution factor x 40

Purity of sample = A_{260}/A_{280}

2.2.5.4 Polymerase Chain Reaction (PCR)

The *Taq* DNA Polymerase (recombinant) kit (Invitrogen®) contained:

10 X PCR buffer (200 mM Tris-HCl (pH 8.4), 500 mM KCl),

50 mM of magnesium chloride,

500 units of *Taq* DNA Polymerase.

Amplification of single embryo genomic DNA using microsatellite markers

A 25 µl reaction mix containing the following components was made up in a sterile 1.5 ml microcentrifuge tube on ice:

PCR component	Volume per reaction /µl	Final concentration
10 X PCR buffer	2.5	1.0 X
50 mM $MgCl_2$	0.75	1.5 mM
dNTP Mix (10mM of each dNTP)	0.5	0.2 mM each

DMSO	2.5	10 % (v/v)
Sense primer (20 μM)	1.0	0.8 μM
Antisense primer (20 μM)	1.0	0.8 μM
Taq DNA Polymerase (5 U/μl)	0.2	1.0 unit
Distilled water	added to achieve a final reaction volume of 25 μl	

A master mix was prepared for multiple reactions to minimise pipetting errors and reagent loss. The master mix reaction was vortexed and centrifuged at 12, 000 x g for 1 min to collect the contents to the bottom.

Two μl of single embryo mutant or sibling genomic template DNA (50 ng/ml) was placed in a well of a 96 well plate and 25 μl of master mix reaction added to each sample. Each sample was overlaid with a drop of mineral oil, the plate was sealed with a pre-cut transparent microplate sealer (Greiner Labortechnik®) and placed in a PCR machine (OmniGene, Hybaid®). The amplification program used was as follows:

36 cycles of:

- denaturation at 94°C for 2 min 30 s
- annealing at 60°C for 1 min
- extension at 72°C for 30 s

1 cycle of:

- extension at 72°C for 5 min

The amplified products were stored at 4°C until use. Five μl of 10 X gel loading dye was added to each reaction. Fifteen μl of the reaction was loaded on a 3.5 % (w/v) agarose gel. Five μl of 1 kb molecular weight ladder (Gibco BRL®) was loaded alongside the samples. The samples were run by agarose gel electrophoresis at 200 V for 2 hours and visualised using a UV transilluminator (Model 750-M; International Biotechnologies®).

Amplification of gene fragments from single embryo genomic DNA or cloned cDNA using gene specific primers

Gene specific primers were designed using the program PRIMER. They were generally 21 bp in length, had a GC content of 50 % and a C or G bp at the 3' end. These primers were purchased from Invitrogen® (unlabelled primers) and MWG-BioTECH® (labelled primers). They were resuspended in an appropriate volume of distilled water and stored at -20°C until needed.

The PCR components were the same as those described in the amplification section above using microsatellite markers except that gene specific primers were used instead at a concentration of 50 nmoles. The annealing temperature and extension time of the PCR reaction varied for each primer pair depending on their melting temperature and expected product size respectively.

Five µl of the reaction product was run on a 2.0 % (w/v) agarose gel. If optimal reaction conditions had been achieved, the rest of the product was purified and used in sequencing, restriction digestion and/or genescan experiments.

Optimisation of reaction conditions

Varying the $MgCl_2$ concentration and annealing temperature achieved optimal reaction conditions for each primer pair.

Some reactions were optimised using a PCR optimisation kit (Invitrogen®), which contained PCR buffers with varying $MgCl_2$ concentrations and pH values.

2.2.5.5. Purification Techniques

After PCR amplification, the reaction product was purified to remove contaminants that affect restriction enzyme digestion or sequencing reaction specificity. Contaminants include other types of DNA, nucleases, salts and inhibitors of restriction enzymes such

as DMSO. The purification procedures were followed according to the manufacturer's specifications.

Microcon PCR purification (Amicon®)

Fresh PCR product was transferred to a vial placed in a collection tube and centrifuged at 500 x g for 15 min. The vial was inverted, placed into a fresh collection tube and centrifuged at 1000 x g for 3 min. An aliquot of the purified product was then run on a 2.0 % (w/v) agarose gel to confirm purification of the product had been achieved and to determine the volume needed to use for further analysis.

Purification kit (GibcoBRL®)

Fresh PCR product was added to 400 µl of binding solution H1 (concentrated guanidine hydrochloride, EDTA, Tris-HCl, isopropanol). The solution was vortexed, transferred to a spin cartridge in a labelled wash tube, incubated at room temperature for 1 min and centrifuged at 12, 000 x g for 1 min. The outflow was discarded and 700 µl of wash buffer H2 (NaCl, EDTA, Tris-HCl) added to the cartridge; containing the bound product and centrifuged at 12, 000 x g for 1 min. Residual wash buffer was removed by centrifuging for 1 min and the outflow discarded. Thirty µl of pre-warmed TE was added to the cartridge and incubated for 5 min at room temperature. The eluted, purified product was centrifuged at 12, 000 x g for 1 min and 5.0 µl visualised on a 2.0 % (w/v) agarose gel.

Gel Extraction kit (GibcoBRL®)

The correct sized product band was excised from the agarose gel under a UV transilluminator using a sterile scalpel blade and placed into a microcentrifuge tube. The gel splice was weighed and the appropriate volume of gel dissolving buffer L1

(concentrated sodium perchlorate, sodium acetate, TBE solubiliser) added to it (30 µl of L1 for every 10 mg of gel). The tube containing the gel and buffer L1 was incubated at 50°C and occasionally mixed until the gel had totally dissolved. The dissolved gel was transferred to a binding column in a collecting tube and centrifuged at 12, 000 x g for 1 min. The outflow was discarded and 700 µl of buffer L2 (NaCl, EDTA, Tris-HCl) added to the column containing the bound sample. Following 5 min of incubation at room temperature, the sample was centrifuged twice for 1 min and the outflow discarded. The column was transferred to a microcentrifuge tube and 30 µl of pre-warmed TE added to elute the DNA. The sample was incubated for 5 min at room temperature, centrifuged at 12, 000 x g for 1 min and 5 µl of it was then visualised on a 2.0 % (w/v) agarose gel.

Purification of products extracted from agarose gels

After RT-PCR, the correct sized product band was excised from a 0.8 % (w/v) agarose gel and transferred to a nebuliser (Amicon®). The sample was centrifuged at 12, 000 x g for 5 min and 4 µl of the purified product was used in the TOPO® cloning reaction (section 2.2.6.4).

2.2.5.6. Restriction Digestion

The following restriction endonucleases and buffers were purchased from New England BioLabs® and stored at -20°C:

- *Bfa* I (buffer 4)
- *Eco*R I (buffer EcoRI)
- *Hpy*Ch4 V (buffer 4)
- *Xba* I (buffer 2)

Restriction enzyme buffer components were as follows:

Buffer EcoRI (50 mM NaCl, 100 mM Tris-HCl, 10 mM $MgCl_2$, 0.025 % Triton X-100 (pH 7.5).

Buffer 2 (50 mM NaCl, 10 mM Tris-HCl, 10 mM $MgCl_2$, 1 mM dithiothreitol (pH 7.9), BSA (100 µg/ml).

Buffer 4 (50 mM potassium acetate, 20 mM Tris-acetate, 10 mM magnesium acetate, 1 mM dithiothreitol (pH 7.9).

A 15 µl reaction mix containing the following components was made up in a sterile 1.5 ml microcentrifuge tube on ice:

- 5 µl of genomic DNA amplified product
- 10 X Buffer
- 10 units of restriction enzyme

made up to 15 µl with distilled water

The reaction mix was incubated at 37°C for at least 1 hour. One and a half µl of 10 X gel loading dye was added to the reaction mix and 5 µl of this was run on a 2.5 % (w/v) agarose gel for 30 min at 130 V, visualised on a UV-transilluminator and analysed by genescan (section 2.2.5.7).

2.2.5.7. Genescan analysis

The genescan plates (ABI®) were washed using Alconox® detergent and hot water, rinsed with distilled water and left to air dry. They were assembled with spacers and clamped on either side with bulldog clips.

The gel solution was made up in a 100 ml beaker and consisted of 32 ml of Sequagel-6 acrylamide solution, 8 ml of Sequagel-6 buffer (National Diagnostics®) and 300 µl of 10 % (w/v) APS. After mixing, the solution was taken up into a 25 ml syringe

(Terumo®) and poured between the two plates, which were tapped to ensure that the gel spread evenly and no air bubbles became trapped between them. Once the gel mixture had reached the bottom of the plates and no air bubbles were visible, a well-forming spacer was inserted between the plates and clamped with bulldog clips. The gel was left to set for two hours.

The clamps and well-forming spacer were removed and the plates cleaned with distilled water before being placed into the electrophoresis chamber. The plates were clamped in place before ABI instrumentation was set on plate check mode. Where the plate quality was sub-optimal, the laser-scanning region was repeatedly cleaned with distilled water until an optimal plate check was obtained. The buffer reservoir chamber and the bottom of the electrophoresis chamber were filled with 1 X TBE.

The following components were made up in a sterile 0.5 ml microcentrifuge tube on ice:

- 1.5 µl of sample
- 3.5 µl of blue dextran loading buffer
- 0.5 µl of TAMRA-500 size standard (ABI®)

The sample mix was denatured at 95°C for 3 min and 'snap chilled' on ice before being loaded and run on a 6.0 % (w/v) polyacrylamide gel for 5 hours. The traces were analysed using Genescan and Genotyper software.

2.2.6 RNA techniques

2.2.6.1. Total RNA extraction from zebrafish embryos

Two day old, dechorionated, zebrafish embryos were separated into mutant and sibling pools and transferred into separate labelled microcentrifuge tubes. Seven hundred and fifty µl of TRIzol®LS Reagent (mono-phasic solution of phenol and guanidine isothiocyanate; GibcoBRL®) was added per 25 embryos. The embryos were homogenised and incubated for 5 min at room temperature to allow the complete

dissociation of nucleoprotein complexes before the addition of 200 µl of chloroform. The tubes were shaken vigorously by hand for 15 s and incubated at room temperature for 15 min. The samples were centrifuged at 12, 000 x g for 15 min at 4°C. The aqueous phase, containing the RNA, was transferred to a clean tube. The RNA was precipitated from the aqueous phase by mixing with 500 µl of isopropyl alcohol. The samples were incubated at room temperature for 10 min and centrifuged at 12, 000 x g for 10 min at 4°C. The RNA precipitate formed a gel-like pellet on the side and bottom of the tube. The supernatant was removed; the RNA pellet was washed with 1000 µl of 75 % (v/v) ethanol and the sample vortexed and centrifuged at 7, 500 x g for 5 min at 4°C. The RNA pellet was air-dried for 10 min and dissolved in 20 µl of RNase-free water. The RNA concentration was measured as described in section 2.2.1.2.

The following components were added to a 0.5 ml microcentrifuge tube on ice:

- 1.0 µl of 10 X MOPS
- 1.6 µl formaldehyde
- 3.0 µl RNA sample
- 5.0 µl formamide

The RNA sample solution was denatured at 68°C for 10 min and then placed on ice. Ten % (v/v) RNA sample loading buffer was added to the RNA solution and the whole sample was loaded onto a 1.0 % (w/v) RNA gel. The samples were run at 70 V for 3 hours. The gel was washed in distilled water for 30 min to remove formaldehyde, stained in 0.5 µg/ml ethidium bromide for 15 min and de-stained in distilled water for 1-3 hours.

2.2.6.2. First Strand cDNA Synthesis (RT reaction)

The following components were added to a sterile 0.5 ml microcentrifuge tube:

- 7.0 µl total RNA
- 1.0 µl Oligo(dT) primer
- 4.0 µl DEPC-treated water

The RNA solution was incubated at 68°C for 10 min, placed on ice and the following components added to it:

- 4.0 µl buffer containing DTT (Promega®)
- 2.0 µl of dNTP mix (10mM)
- 1.0 µl RNAase inhibitor (Promega®)
- 1.0 µl Murine Leukaemia Virus reverse transcriptase (Promega®)

The RT reaction mix was incubated at 42°C for 1.5 hours and stored at -20°C.

2.2.6.3. RT-PCR

A 20 µl reaction mix was made using the following components:

- 1.0 µl RT product
- 13.0 µl distilled water
- 2.0 µl of PCR buffer (10 X) containing $MgCl_2$ (22.5 mM) and detergents (Roche®)
- 1.0 µl of sense primer (50 nmol)
- 1.0 µl of antisense primer (50 nmol)
- 1.0 µl of 10mM dNTP mix
- 0.75 µl *Taq* DNA polymerase (Roche®)

The RT reaction mix was vortexed and amplified using the following PCR program:

40 cycles of:

- denaturation at 94°C for 5 min 30 s
- annealing at 53-60°C for 30 s (this temperature was optimised for each primer pair)
- extension at 72°C for 1 min 30 s

1 cycle of:

- extension at 72°C for 7 min

The amplified products were stored at 4°C until use. Four µl of 10 X gel loading dye was added to the PCR product. The entire 20 µl was loaded on a 0.8 % (w/v) agarose gel. Five µl of 1 kb molecular weight ladder (Gibco BRL®) was loaded alongside the samples. The samples were run by agarose gel electrophoresis at 100 V for 45 min and visualised using a UV transilluminator (Model 750-M; International Biotechnologies Inc.). The expected product band was excised from the agarose gel, purified (section 2.2.5.5) and cloned into the pCR® 2.1-TOPO® vector (section 2.2.6.4).

2.2.6.4. Cloning of RT-PCR products into pCR® 2.1-TOPO® vector

The following components were added to a sterile 0.5 ml microcentrifuge tube:

- 4.0 µl fresh purified PCR product
- 1.0 µl Salt solution (supplied in TOPO® cloning kit; Invitrogen®)
- 1.0 µl TOPO® vector (Invitrogen®)

The TOPO® cloning reaction was gently mixed and incubated at room temperature for 15 min and placed on ice. Two µl of the reaction was added to a vial of One Shot® E. *coli*, mixed and incubated on ice for 30 min. The cells were heat-shocked at 42°C for 30 s. Two hundred and fifty µl of room temperature SOC medium was added to the cells. Fifty µl from each transformation was spread onto LB plates containing X-Gal

(20 mg/ml) IPTG (200 mg/ml) and ampicillin (100 ng/ml). The plates were incubated overnight at 37°C. Single white colonies were picked and incubated in LB broth containing ampicillin (100 ng/ml) at 37°C on a shaker for 12 hours and then stored at 4°C. The plasmids were purified using the Qiagen® Miniprep kit and analysed by *Eco*RI restriction digestion to check for the presence of the insert and sequenced (section 2.2.7).

2.2.7 Cycle Sequencing

The cycle sequencing reaction was carried out using the ABI PRISM™ Dye Terminator Cycle Sequencing Ready Reaction Kit with AmpliTaq® DNA Polymerase, FS (ABI®) on a Perkin Elmer Thermal Cycler. The following reagents were mixed in a 0.5 ml microcentrifuge tube:

- 4 µl of Taq FS Terminator Ready Reaction Mix
- 3.2 pmol of primer
- 50-100 ng of purified PCR product

The reaction volume was made up to 20 µl with sterile distilled water, mixed and overlaid with a drop of mineral oil.

The amplification conditions were 25 cycles of:

- denaturation at 96°C for 1 min
- annealing at 50°C for 15 s
- extension at 60°C for 4 min

The reaction was cooled to 4°C and stored on ice prior to ethanol precipitation of samples.

The entire 20 µl reaction mixture was transferred to a sterile 0.5 ml microcentrifuge tube that contained 50 µl of 95 % (v/v) ethanol and 2.0 µl of 3.0 M sodium acetate (pH

5.2). The sample was mixed and placed on ice for 10 min before being centrifuged at 14, 000 x g for 30 min at 4°C. The supernatant was carefully removed to avoid disturbing the pellet. The pellet was washed in 70 % (v/v) ethanol, dried at 85°C for 1 hour and stored at -20°C.

2.2.7.1. Sequencing gel and preparation of samples for loading

The glass sequencing plates (ABI®) were washed using Alconox® detergent and hot water, rinsed with distilled water and left to air dry.

Sequencing gels were made by mixing 30 g of urea, 9.0 ml of 40 % (v/v) acrylamide/bisacrylamide 19:1 (Bio-Rad®), 23 ml of distilled water and 0.5 g of Amberlite bed resin in a beaker with a magnetic stirrer for one hour.

The dried plates were assembled on top of an inverted tip box covered with tissue paper. The solid rectangle plate was first placed on the tip box stand and the relevant gel thickness spacers were placed on either of the long sides of the plate. The second plate, which had a well forming indentation at one end of its short side, was placed on top of the spacers and the two plates were clamped together with six bulldog clips evenly spaced on the opposite long sides of the plate.

Prior to adding the gel mixture to the vacuum suction filtration apparatus (NALGENE®), 6.0 ml of 10 X TBE was first passed through the filter. Before pouring, 300 µl of 10 % (w/v) APS and 30 µl of TEMED (BDH®) were added to the degassed gel mixture, which was then gently swirled and taken up into a 25 ml syringe (Terumo®).

The gel mixture was poured into the indented side between the two plates, which were tapped to ensure that the gel spread evenly and no air bubbles became trapped between them. Once the gel mixture had reached the bottom of the plates and no air bubbles

were visible, a well-forming spacer was inserted between the plates and clamped with three bulldog clips. The gel was left to set for a minimum of two hours.

The clamps and well-forming spacer were removed from the plates containing the set gel. The plates were cleaned thoroughly with distilled water before being placed into the electrophoresis chamber of the ABI 373A sequencer. The plates were clamped in place before ABI instrumentation was set on plate check mode. Where the plate quality was sub-optimal, the laser-scanning region was repeatedly cleaned with distilled water until an optimal plate check was obtained. A cooling plate and buffer reservoir chamber were attached to the assembled plates. The buffer reservoir chamber and the bottom of the electrophoresis chamber were filled with 1 X TBE and the gel was pre-run for one hour prior to the addition of the samples.

Purified sample pellets were suspended in an appropriate volume of dextran blue loading buffer and denatured at 95°C for 2 min on a PCR machine.

Number of wells	Blue dextran loading buffer per sample (μl)
24	4.0
36	3.0
48	2.0
64	1.0

They were immediately 'snap chilled' on ice prior to loading onto a 6.0 % (w/v) denaturing acrylamide gel. Vertical electrophoresis of the samples in the gel was performed on an ABI 373A sequencer at constant 30 Watts in 1 X TBE for 12 hours. The trace sequence was analysed using ABI PRISM software. The sequences were analysed using Sequence Navigator software.

2.2.8 Protein techniques

2.2.8.1. Protein extraction from zebrafish embryos

Two to three day old live dechorionated embryos were anaesthetised in 0.02 % (w/v) tricaine and pinned to small Petri dishes coated with Sylgard silicone elastomer (BDH®) with fine pins. Sharpened tungsten needles and fine forceps were used to dissect the yolk sac as it contains the protein vitellogenin that retards migration of proteins on an SDS gel. The de-yolked embryos were transferred to a 1.5 ml microcentrifuge tube and 15 µl of 2 X SDS sample buffer was added per 10 embryos. The sample was homogenised, using an autoclaved pellet homogeniser, until uniform in consistency and incubated at 95°C for 5 min. The sample was centrifuged at 14, 000 x g for 5 min and the supernatant removed and stored at -20°C or denatured and run on a gel (section 2.2.8.3).

2.2.8.2. Protein extraction from zebrafish liver

A sample of zebrafish liver was crudely chopped with a scalpel blade, 1.0 ml of protein extraction buffer added to it and homogenised using an autoclaved pellet homogeniser. The sample was sonicated 3 to 4 times for 5 seconds and the crude extract centrifuged (Sorvall JA-21 Centrifuge, Beckman®) at 33, 000 x g for 30 min at 4°C to remove the solid debris. The supernatant was then removed, made up in a 1:1 ratio with 2 X SDS sample buffer, stored at -20°C or denatured and run on a gel (section 2.2.8.3).

2.2.8.3. Preparation of SDS-PAGE gels

The glass plates and spacers of the minigel apparatus (Bio-Rad®) were washed with hot soapy water, 95 % (v/v) ethanol and distilled water and left to air dry. They were assembled and aligned in the clamp, which was then tightened on the casting stand.

The resolving gel mixture was poured into the glass plate sandwich up to about 6 cm from the bottom using a Pasteur pipette. The gel mixture was overlaid with water-

saturated isobutanol to exclude oxygen from the surface and left to polymerise for 45 min. The isobutanol was drained off and the gel surface rinsed with distilled water and dried using filter paper. The stacking gel mixture was poured onto the set resolving gel and a well-forming Teflon comb inserted, making sure that no air bubbles were trapped beneath it. The well positions were marked on the glass plate, and the gel left to polymerise for 45 min. After the stacking gel had polymerised, the comb was removed and the wells were rinsed with distilled water to remove any unpolymerised acrylamide.

Sample preparation, loading and SDS-PAGE electrophoresis

Ten µl of the protein samples (50-100 µg) from zebrafish embryos and liver, containing 2 X SDS sample buffer, were denatured at 98°C for 10 min to break the disulphide bonds, cooled to room temperature and centrifuged for 5 min to remove insoluble materials and avoid protein streaking during gel electrophoresis. A positive control (human hepatoblastoma cell lysate, HepG2; Santa Cruz®) sample containing SDS sample buffer was also denatured and loaded onto the gel. In order to determine the molecular weight of the samples, proteins of known molecular weight (low range prestained SDS page molecular weight standards; Bio-Rad®) containing SDS sample buffer were also denatured and loaded onto the gel. The remaining samples, positive control and molecular weight standards were stored at -20°C.

The gel electrophoresis apparatus (Bio-Rad®) was set up according to the manufacturer's instructions. Running buffer (1 X) was added to the lower and upper reservoirs of the electrophoresis apparatus and any air bubbles removed from the wells. The supernatants from the centrifuged samples, positive control and prestained SDS page standards were collected and loaded into the wells using a Hamilton microlitre syringe, which was rinsed in 1 X running buffer between each load. The electrophoresis

apparatus was connected to the power pack and the gel run at 100 V until the dye front reached about 1.0 cm from the bottom of the gel (2-3 hours).

Staining the polyacrylamide gel with Coomassie blue

Immediately after electrophoresis, the gel was stained in Coomassie blue staining solution at room temperature with gentle agitation overnight. After staining, the staining solution was poured off and destaining solution added. The gel was left in destaining solution at room temperature with gentle agitation for several hours. The destaining solution was replaced with fresh destaining solution hourly until the gel background was clear. The destaining solution was poured off and the gel was rinsed and stored in distilled water at room temperature.

Drying the polyacrylamide gel

A gel drying kit (Promega®) containing cellulose films and drying frames was used to dry the gel. The gel that had been destained and stored in distilled water was placed between two moistened sheets of clear cellulose film. Air bubbles were removed as they caused cracking of the gel during drying. The edges and sides of the cellulose films containing the gel were pulled over and clamped to the frames. The frame assembly was placed in a horizontal position and dried overnight at room temperature.

2.2.8.4. Western blotting (Towbin *et al.*, 1979)

Transfer of proteins from the gel to the nitrocellulose membrane

Six pieces of filter paper (Whatman®) and a piece of nitrocellulose membrane (Schleicher and Schuell®) were cut to the size of the gel and soaked in transfer buffer together with the gel for 5 min. A corner of the gel was cut off to mark its orientation. The membrane was placed on top of the gel and these were sandwiched between three pieces of filter paper on either side. Trapped air bubbles between the layers were removed by gently rolling a pipette over the surface of the top piece of filter paper. The

semi dry transfer apparatus was assembled according to the manufacturer's instructions and a current of 130 mA applied for 40 min. The membrane was placed in Ponceau S staining solution and the gel in Coomassie blue staining solution to ensure successful transfer of proteins.

Immunostaining

The membrane was rinsed in transfer buffer and incubated in excess blocking buffer for a minimum of 1 hour at room temperature to saturate non-specific protein binding sites. The membrane was rinsed in distilled water and incubated in primary antibody (HNF-3β; Santa Cruz®) diluted 1:500 in 5.0 % (w/v) non-fat dried milk in PBS-Tween overnight at 4°C with gentle agitation. The unreacted primary antibody was removed by 3 x 5 min washes in excess PBS-Tween. The membrane was incubated in secondary antibody (donkey anti-goat IgG-HRP; Santa Cruz®) diluted 1:500 in 5.0 % (w/v) non-fat dried milk in TBS-Tween for 1 hour at room temperature with gentle agitation. Excess antibody was removed by 3 x 5 min washes in excess TBS-Tween and the membrane rinsed in distilled water.

Detection

The bound secondary antibody was detected by incubating the membrane in pre-mixed ECL reagent (1 part solution A : 1 part solution B; Santa Cruz®) in the dark at room temperature for 1 min. Excess ECL reagent was blotted off the membrane, which was then placed face down on a piece of filter paper and wrapped in Saranwrap in an X-ray cassette (Sterling Diagnostics®) and exposed to X-ray film (Kodak®) for between 5 seconds and 5 min and developed.

3. The *monorail* mutant: Phenotypic characterisation and genetic mapping

3.1 Phenotypic characterisation of *monorail*

The *monorail*^{tv53a} mutant was isolated from the 1996 Tübingen mutagenesis screen and identified by its curled down tail (Fig. 3.1) and lethality by 5 days post-fertilisation (Brand *et al.*, 1996). *Monorail*^{tv53a} mutants have been analysed in a behavioural screen for optokinetic/optomotor responses and the phenotype observed judged to be due to the previous defects identified in brain development (Neuhauss *et al.*, 1999).

Morphologically, *monorail* embryos show an 'indistinct' floor plate with a reduced width along the body axis (Brand *et al.*, 1996). The midline defect in *monorail* has been further characterised by wholemount labelling of 48 hpf embryos with an antibody to acetylated α-tubulin to reveal early axon pathways in the brain (Piperno and Fuller, 1985). Axons of the medial longitudinal fascicles are disorganised and fused at the ventral hindbrain midline in *monorail* (Fig. 3.2A). The position and size of the eyes and eye projections were normal in *monorail* embryos (data not shown).

The axons of the fourth cranial nerve, the trochlear motor nucleus, normally grow dorsally and across the dorsal midline before exiting the brain to innervate the eye muscles. The trochlear motor nucleus is completely absent in *monorail* embryos (Fig. 3.4C), which consequently lack a trochlear decussation (Fig. 3.2B).

The segmental organisation of the zebrafish hindbrain, characterised by rows of radial glial fibers separating segment centres from their borders, is detected by using an antibody to zrf-1 (Trevarrow *et al.*, 1990; Fig. 3.3A). In *monorail* embryos, the number and pattern of dorso-ventrally orientated glial bundles that are normally organised into two transverse rows in each hindbrain segment is reduced and disrupted respectively (Figs.

3.3A and B). In addition, some of these glial bundles occupy the floor plate, an area that is normally devoid of cells and neurons. The elongate morphology of radial glial cells viewed along their long axis gives the labelling its 'speckled' appearance (Fig. 3.3B).

To study the patterning of neurons adjacent to the floor plate in *monorail*, a GFP transgene driven by *islet1* regulatory elements was crossed into the *monorail* line. This transgene labels cranial motor neurons soon after their birth (Higashijima *et al.* 2000). The cranial motor neuron phenotype in *monorail* embryos is that the facial (cranial motor nucleus VII) and oculomotor (cranial motor nucleus III) form a single nucleus at the midline rather than bilateral pairs of nuclei (Figs. 3.4A and B). There is also a reduction in the number of posterior trigeminal motor neurons (Vp) and the trochlear nucleus (IV) is absent in *monorail* embryos (Figs. 3.4B and C), which consequently lack a trochlear decussation (Fig. 3.2B). Further characterisation of the *monorail* mutant phenotype was carried out by Dr William Norton (See Table 3.1).

3.2 Genetic mapping in *monorail*

The mol^{tv53a} locus was mapped in F_2 offspring of a Tü x WIK reference cross (Rauch *et al.*, 1997) with the use of simple sequence length polymorphic markers (Knapik *et al.*, 1996) on pools of 48 mutants and 48 siblings and localised to linkage group 17 between flanking markers Z21703 and Z21194 (Table 3.2A and Figs. 3.5 and 3.7).

Linkages from the pools were confirmed and refined by genotyping single mutant and sibling embryos (Table 3.2B). Five recombinants in 240 meioses were identified with marker Z21703 (Fig. 3.6) and 8 recombinants in 68 meioses with marker Z21194. Hence the markers Z21703 and Z21194 are 2cM and 11cM away from *monorail* respectively (Fig. 3.7). Radiation hybrid mapping placed *foxA1* and *foxA2* (Strähle *et al.*, 1997) in the same mapping region as *monorail* and 0 recombination events were identified in 188 meioses with a marker in the *foxA2* gene (Fig. 3.7).

3.1 Identification of *monorail* mutants

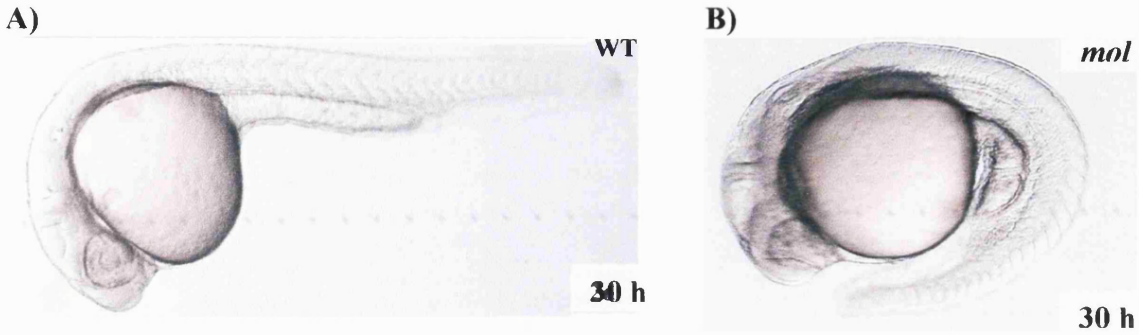

Fig. 3.1 Lateral views of 30 hpf wild-type **(A)** and *monorail* **(B)** embryos showing a curled down tail in *monorail*.

3.2 Floor plate and axonogenesis defects in *monorail*

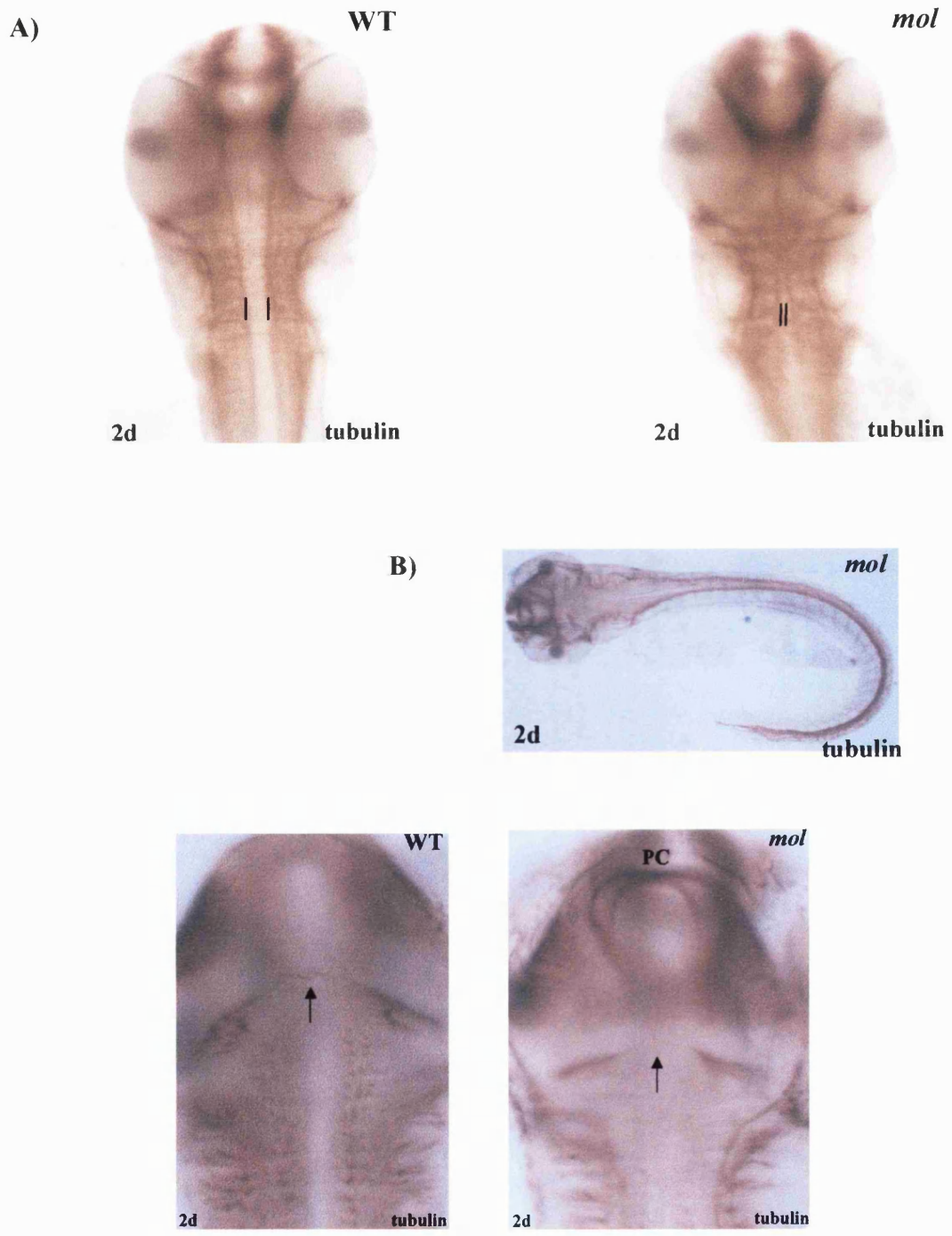

Fig. 3.2 A) Ventral views of 48 hpf wild-type (left panel) and *monorail* (right panel) embryos labelled with anti-acetylated tubulin. *Monorail* embryos show a variable reduction in the width of the floor plate along the body axis as indicated by disorganisation and fusion of axons of the medial longitudinal fascicles at the ventral hindbrain midline.
B) Dorsal view of a wholemount *monorail* embryo labelled with anti-acetylated tubulin (top panel). Ventral views of 48 hpf wild-type (bottom left panel) and *monorail* (bottom right panel) embryos labelled with anti-acetylated tubulin. Arrows show the trochlear decussation in wild-type and its absence in *monorail* embryos. PC; posterior commissure.

3.3 Glial patterning defects in *monorail*

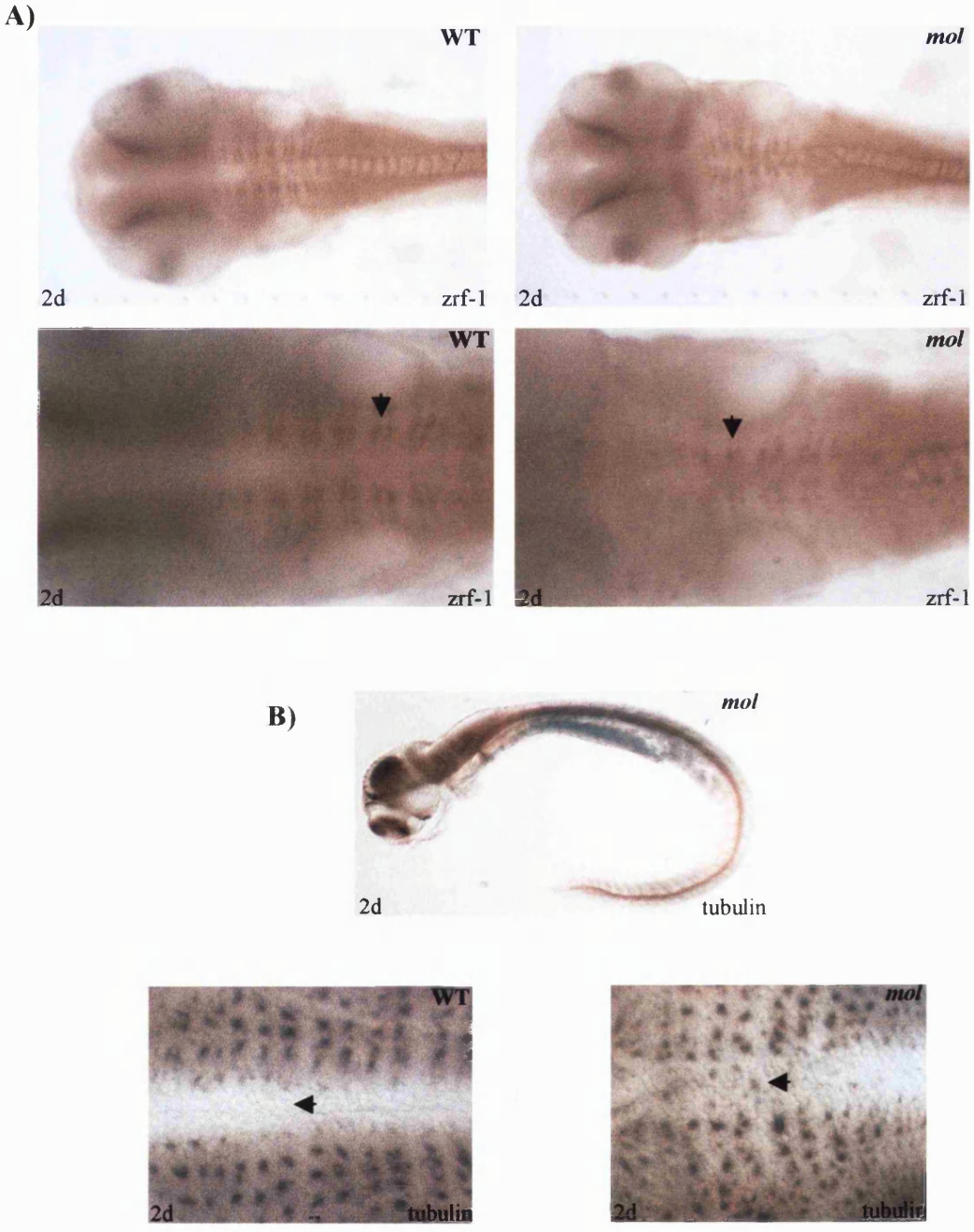

Fig. 3.3 A) Ventral views of 48 hpf wild-type (top and bottom left panels) and *monorail* (top and bottom right panels) embryos labelled with zrf-1. Anterior is to the left, bottom panel shows higher magnification views of the floor plate in the hindbrain region. The arrow in the bottom left panel shows the dorso-ventrally orientated glial bundles that are normally organised into two transverse rows in each hindbrain segment. The segmental pattern of glial bundles is disrupted in *monorail*.
B) Lateral view of a wholemount *monorail* embryo labelled with anti-acetylated tubulin (top panel). Ventral views of 48 hpf wild-type (bottom left panel) and *monorail* (bottom right panel) embryos labelled with anti-acetylated tubulin, anterior is to the left. Arrows indicate the presence of glial fibers in the floor plate in *monorail* and their absence in wild-type embryos.

3.4 *Monorail* embryos show a cranial motor neuron phenotype

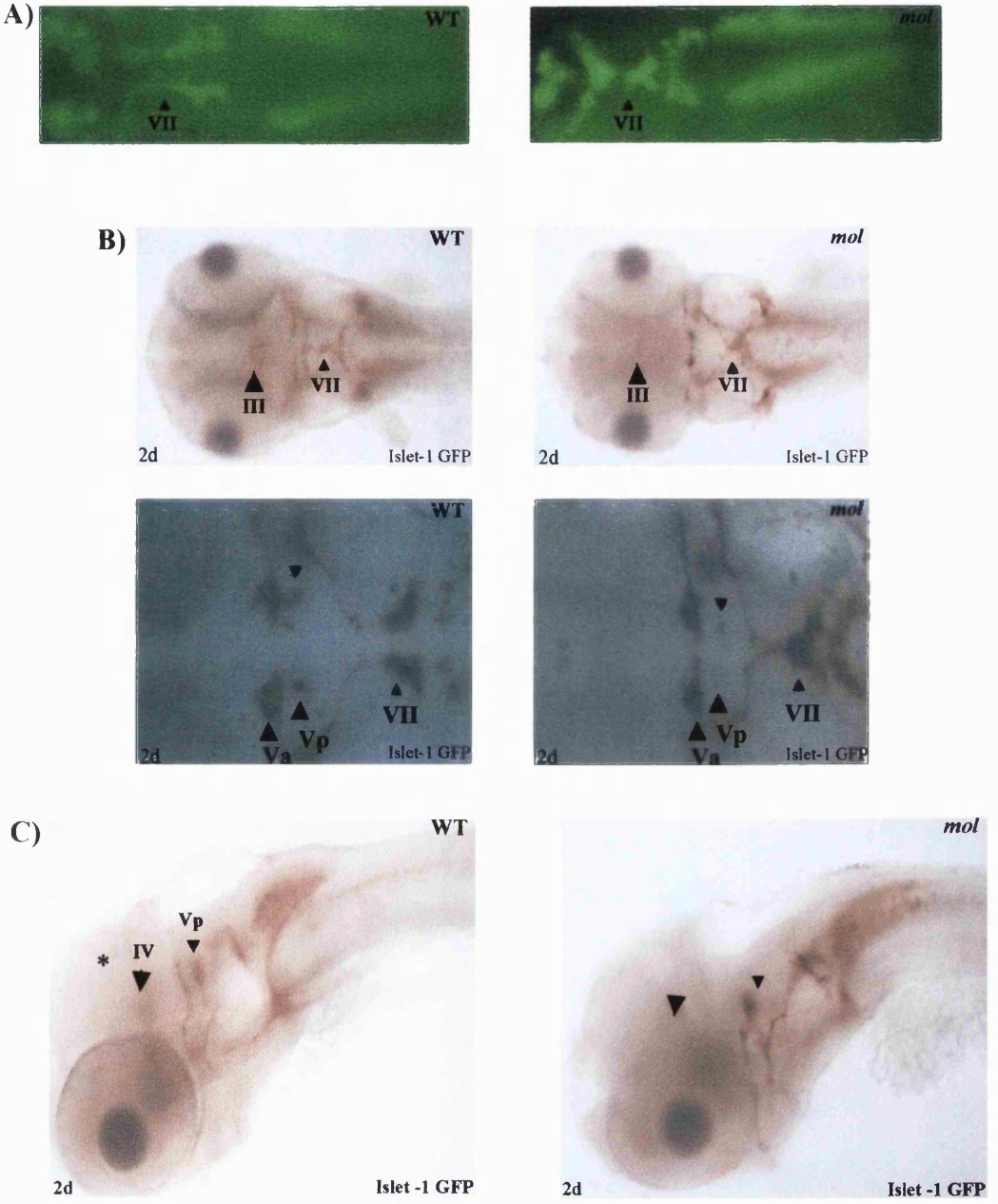

Fig. 3.4 A) Ventral views showing GFP expression in cranial motor neurons in 48 hpf wild-type (left panel) and *monorail* transgenic embryos (right panel). Cranial motor nerve VII, indicated by an arrowhead, forms a single nucleus at the midline in *monorail* rather than bilateral pairs of nuclei. Anterior is to the left. **B)** Ventral views of 48 hpf wild-type (left panel) and *monorail* embryos (right panel) labelled with anti-GFP. Anterior arrowheads show fusion of the oculomotor nucleus (III), posterior arrowheads show collapse of cranial nerve VII to the midline in *monorail*. Bottom panels show high magnification views of the trigeminal (Va, Vp) and facial (VII) motor neurons. The posterior trigeminal neuron (Vp) cluster is reduced in number and cranial nerve VII collapses to the midline in *monorail*. Anterior is to the left.
C) Lateral views of 48 hpf wild-type (left panel) and *monorail* embryos (right panel) labelled with anti-GFP. Anterior arrowheads show loss of trochlear nucleus (IV), posterior arrowheads show a reduction of posterior trigeminal neurons (Vp) in *monorail*.
*-location of oculomotor nucleus III (out of the plane of focus in this view).

Table 3.1 Summary of phenotypic characterisation results for the *monorail*^{tv53a} mutant

Phenotype	Developmental stage	Description
Abnormal body shape	30 hpf	Curled-down tail.
Reduced floor plate width	48 hpf	Axons of the MLF are disorganised and fused at the ventral hindbrain midline.
Disorgnised segmental pattern of hindbrain rhombomeres	48 hpf	The number and pattern of dorso-ventrally orientated glial bundles that are normally organised into two transverse rows in each hindbrain segment is reduced and disrupted Some glial fibers occupy the floor plate.
Floor plate cell morphology	36 hpf	Slightly enlarged floorplate cells with typical cuboidal morphology evident along the entire axis of the CNS.
LFP cells are absent	36-48 hpf	Expression of *foxA* and *foxA2* is reduced to a 1-3 cell wide row. Gaps of expression appear in the posterior midbrain and hindbrain and reduced levels of expression in the spinal cord.
Expression of MFP regulatory genes is not maintained	14 somites-48 hpf	Reduced and patchy expression of *shh*, *twhh* and *foxA1* in the hindbrain. Reduced or absent expression further caudally.
Failure of floor plate differentiation despite the presence of floor plate cells	36 hpf	Expression of *col2A1*, *mindin-1* and *mindin-2* is severely reduced or absent in the spinal cord and reduced or patchy further rostrally.
Midbrain and hindbrain defect in floor plate maturation	60 hpf	*Netrin-1* transcripts are absent from the most ventral CNS cells. Ectopic patches of expression are observed in ventricular zone cells positioned more dorsally. *nk2.2* ventricular zone expression in the hindbrain is more dorsally positioned.
Midbrain patterning defect of the serotonergic Raphe nucleus	72 hpf	Most *tryptophan hydroxylase* expressing cells are absent. The few remaining neurons are located caudally within the Raphe.
Midbrain commissural defect	48 hpf	Lack of trochlear decussation.
Midbrain and hindbrain cranial motor neuron induction and patterning defects	48 hpf	The oculomotor and facial motor nuclei form a single nucleus at the midline rather than bilateral pairs of nuclei, there is a reduction in the number of posterior trigeminal motor neurons and the trochlear nucleus is absent.

Results boxed in red were carried out by Dr William Norton.

Table 3.2 Genetic mapping of *monorail* (*mol*^{tv53a})

A) Rough mapping of *mol*^{tv53a}

Rough mapping localised *monorail* to linkage group (LG) 17
The following SSLPs were linked to *mol*^{tv53a}:

SSLP	Mapping panel positions from top of LG 17			
	MGH /cM**	T51/cR**	HS/cM**	LN54/cR**
Z9847	40.9	847.00	—	—
Z15738	34.2	582.00	—	—
Z22674	29.9	582.00	22.2	127.99

B) Fine mapping results from Tübingen

SSLP	Mapping panel positions from top of LG 17				
	MGH /cM**	T51/cR**	HS/cM**	LN54/cR**	MOP/cM**
Z9847	40.9	847.00	—	—	—
Z1490	15.1	476.00	7.4	95.33	15.1
Z3123	78.7	2170.00	—	—	212.10

KEY:
MGH, HS and MOP- Meiotic mapping panels
T51 and LN54- Radiation hybrid mapping panels
**- Position of markers on mapping panel source: http://zfin.org

3.5 Rough mapping of the *monorail* mutation

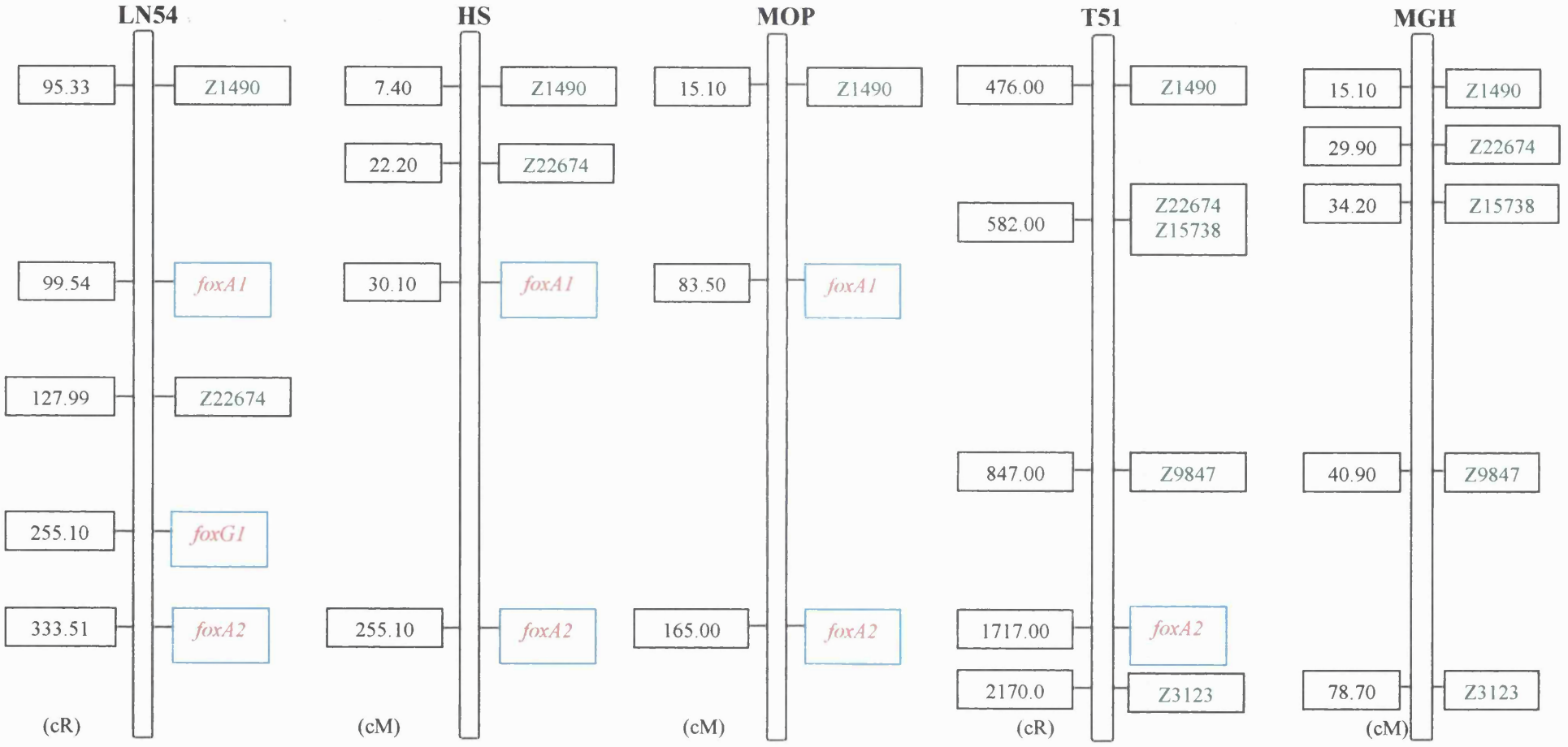

Fig. 3.5 Schematic diagram showing the position of SSLP markers used for rough mapping of the *monorail*^{tv53a} mutation and candidate *fork head* genes in these regions on LG 17. Numbers in boxes to the left of each panel indicate the position of SSLP markers on each mapping panel (Source: http://zfin.org). *Fork head* gene candidates are shown in red and boxed in blue. Linked SSLPs tested on pooled samples for rough mapping are shown in green.

3.6 Z21703 recombinants

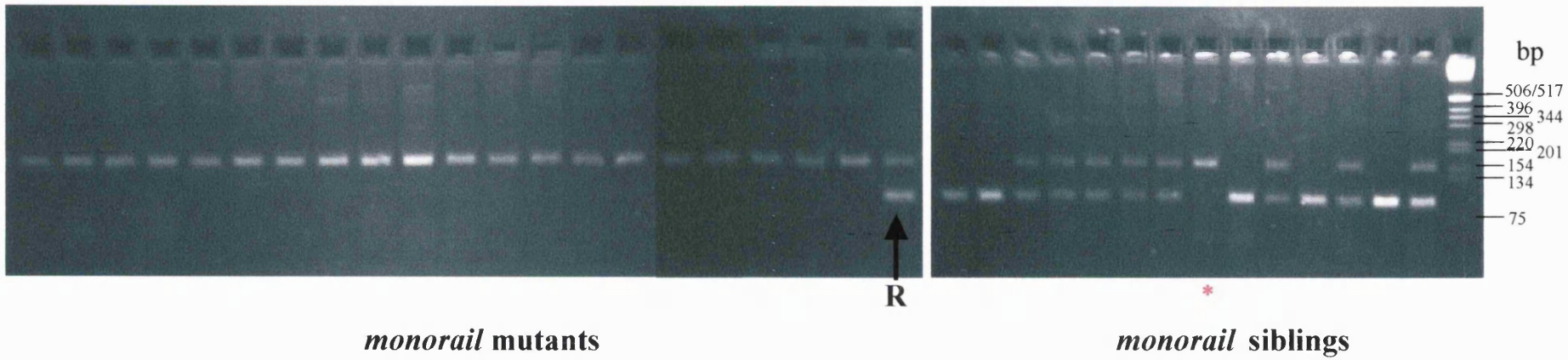

Fig. 3.6 Genotype analysis of single embryo *monorail* mutants and siblings using the SSLP marker Z21703.
The lower band is the WIK allele that segregates with *monorail*; the upper band is the Tü allele.
One recombination event (R) in 42 meioses is shown.
* double recombinant or missorted individual (most likely to be missorted as the number of individuals genotyped is relatively small).

Fig. 3.7 Schematic diagram showing fine mapping results for the *monorail*^{tv53a} mutation using SSLPs from the MGH panel. The corresponding position of these markers on the T51, HS, MOP and LN54 panels is shown in order to identify possible candidate genes in regions showing tight linkage on LG 17. Polymorphic (linked) SSLPs are shown in blue. Numbers in brackets indicate recombination frequencies. A non-informative marker tested is shown in orange. *Fork head* gene candidates are shown in red. A marker within the *foxA2* gene was tested and no recombinants were detected in 188 meioses (result from William Talbot).

3.7 Fine mapping of the *monorail* mutation

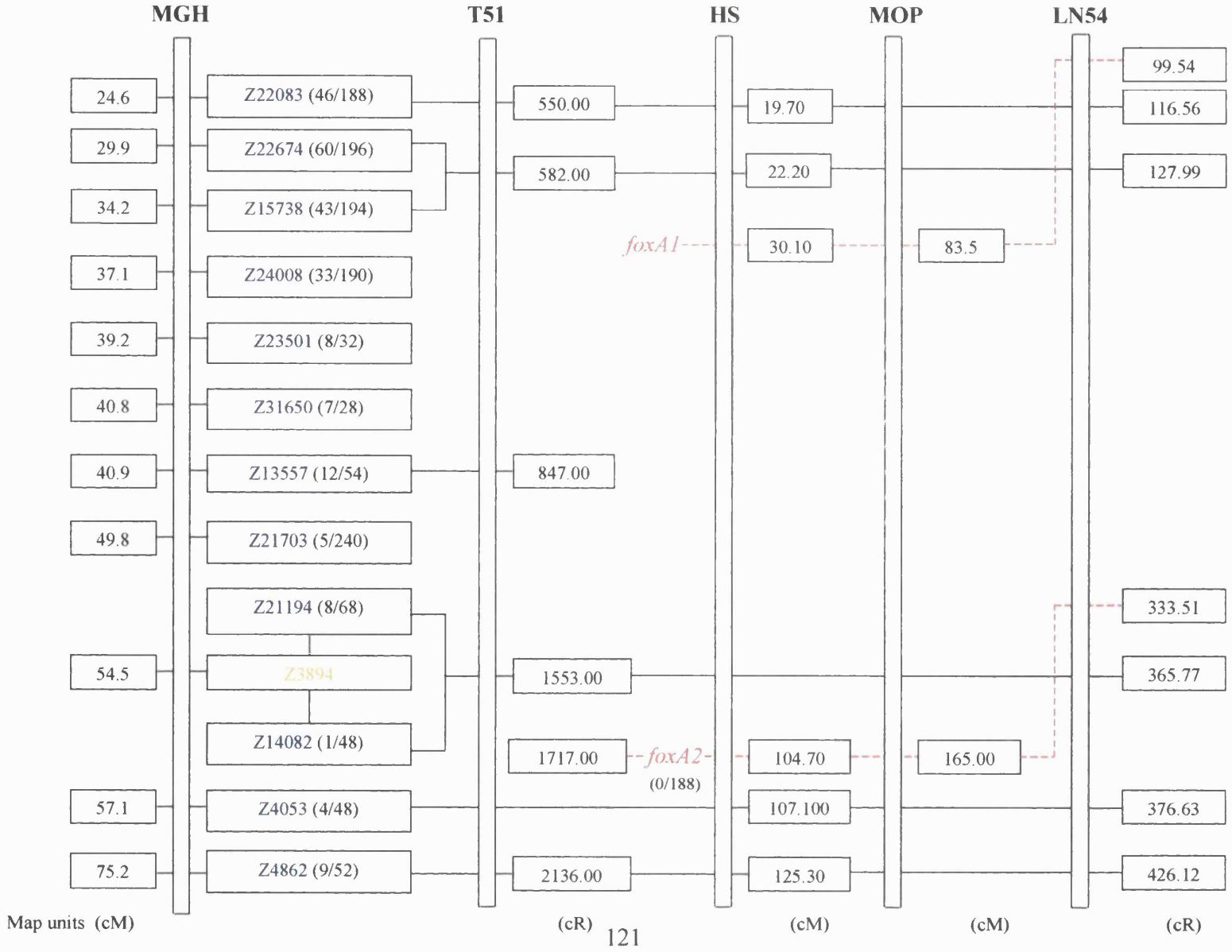

4. The *monorail* mutant: Gene identification

Analysis of candidate genes mapping to the same region on linkage group 17 as SSLPs showing strong linkage to *monorail* (Fig. 3.7; http://zfin.org/cgi-bin/mapper_select.cgi), revealed two *fork head* domain genes *foxA1* and *foxA2* (Odenthal and Nüsslein-Volhard, 1998), the expression patterns of which also correlate with the *monorail* phenotype (Brand *et al.*, 1996). *foxA1* is expressed in the medial floor plate and *foxA2* is expressed in both medial and lateral floor plate cells of the ventral neural tube (Odenthal and Nüsslein-Volhard, 1998).

4.1 Mutational analysis of *foxA1*

The entire coding sequence of the *foxA1* gene (1284 bp) was sequenced in both reverse and forward directions using internal primers (Table 9.2.1). The published *foxA1* sequence (Fig. 4.1A) was compared to *foxA1* sequences from pooled *monorail* and wild-type cDNA to determine any alterations, which might encode a functionally significant amino acid change. The base shown in red and indicated as region '*' is at the start of a codon (CAG; glutamine). The *monorail* sequence showed a T in place of the C at position 1032. This was observed in 8 out of 9 mutant pools tested. However, 1 out of 9 mutant pools showed a C at position 1032. The wild-type sequence showed a C at this position in 2 out of 8 pools tested but in 6 out of 8 pools, a T was observed. This base change in the *monorail* sequence would lead to a change from a glutamine344 to a stop codon.

However, on sequencing *foxA1* from pooled WT cDNA, differences were detected in this sequence compared with the published sequence. Among these differences were two single base insertions in the coding sequence before region '*' which, if correct, would put base C1032 out of frame and at the end of a codon rather

than the beginning as previously thought (Fig. 4.1B). This meant that the difference sometimes seen at base pair 1032 between mutants and WT and siblings no longer changed glutamine344 to a stop codon. Hence this C-T transition represented a polymorphism rather than a mutation and meant that instead this codon encoded proline343 and remained unchanged (CCC in WT and *monorail* siblings compared with CCT in mutants).

The revised *foxA1* coding sequence was deposited in GenBank; Accession number AY247950, Figs. 4.1B, C).

The gene *foxA1* is listed by ZFIN with reference to LocusLink entry 30541 (source: http://zfin.org/cgi-bin/webdriver?MIval=aa-markerview.apg&OID=ZDB-GENE-990415-78). The gene was found by the ensembl gene build (source: http://www.ensembl.org/Danio_rerio/geneview?gene=ENSDARG00000019150). The information is based on the genome assembly and the alignment of the original *foxA1* sequence to it. There is no way to compare it with the revised *foxA1* sequence as it does not turn up in the supporting evidence for the ensembl gene (source: http://www.ensembl.org/Danio_rerio/exonview?transcript=ENSDART00000022920 &db=core&showall=1). Current sequence information for both the original and revised sequence can be retrieved from the following webpage http://pre.ensembl.org/Danio_rerio/contigview?chr=17&vc_start=8588993&vc_end= 8688993&highlight=BLAST_NEW:BLA_7hrEioW4b!!20040112.

Further experimentation and analysis is needed before the revised sequence of *foxA1* can be confirmed and completely compared to the original *foxA1* sequence. Initially, a BAC clone containing this region can be identified and sequenced (see http://pre.ensembl.org/Danio_rerio/cytoview?highlight=&chr=17&vc_start=8300000 &vc_end=9000000&x=45&y=13).

4.2 Mutational analysis of *foxA2*

The second candidate gene, *foxA2*, was then investigated by sequence analysis. In order to identify possible mutations in *foxA2*, RNA from pools of twenty 24 hpf *monorail* and 20 wild-type embryos was reverse transcribed. The entire coding sequence of the *foxA2* gene (1229 bp) was amplified by PCR using the following forward and reverse primer respectively:

5'-TTCCAGGATGCTCGGTGCTGTCAAAATGG-3'

5'-GTCACAAGGTCCAAGAGAGTTTAGGAAG-3'

The PCR product was cloned into the TOPO® TA vector (Invitrogen®) for sequence analysis. Automated fluorescent sequencing was carried out on an ABI 373A sequencer. Internal *foxA2* sequencing primers were designed (Table 9.2.2) and 17 *monorail* and 7 wild-type samples analysed. Sequence analysis was also carried out on PCR products from single embryo genomic DNA from 5 *monorail*, 3 wild-type and 9 *monorail* siblings.

A single base change was identified at position 676. This C676T transition represents a Q166X mutation in the conserved *fork head* domain i.e. a nonsense mutation that changes a glutamine codon to a stop codon (Figs. 4.2A, B). It was confirmed that this was the only consistent difference between the published *foxA2*, wild-type and mutant sequences (Fig. 4.3) and the only change that would alter an amino acid. FoxA2 encoded by *monorail* displays a premature stop codon in the *fork head* DNA binding domain (84 % of this domain is lost) resulting in complete absence of transactivating domains II and III and a carboxy terminally truncated FoxA2 protein (Fig. 4.4).

The mutation was present in all *monorail* individuals tested in both the forward and reverse direction. None of the 10 wild-type individuals analysed showed

the mutation. The 9 *monorail* siblings tested were either wild-type or heterozygotes (Fig. 4.2C). Hence it was concluded that *foxA2* is the *monorail* gene.

To further confirm the presence of this change a PCR based test was devised. The amplification created restriction site (ACRS) method (Halliosis *et al.*, 1989) is based on the introduction of an artificial restriction site, using a modified primer during the PCR, which creates a RFLP indicative of the studied mutation. This RFLP is detected by a radiolabeled oligonucleotide probe, which is not related to the mutation. One *monorail*, three *monorail* siblings, and one WT individual were analysed with the restriction enzyme *Hpy*CH4 V (Fig. 4.5).

The ACRS method was also tested on three *monorail* and two heterozygous *monorail* sibling individuals and the resulting PCR product sizes were shown quantitatively by the Genescan approach (Fig. 4.6). These results provide further evidence that *monorail* encodes a mutation in *foxA2*.

According to cDNA sequence analysis, FoxA2 protein in *monorail* terminates just after the start of the *fork head* DNA binding domain, situated at the carboxy terminus. FoxA2 is the HNF-3β homologue in human and mouse. An HNF-3β antibody (Santa Cruz Biotechnology®) binding to a peptide at the carboxy terminus of HNF-3β protein was tested to show that in *monorail* mutants, HNF-3β protein should not be detected. An HepG2 (human hepatoblastoma whole cell lysate) positive control was tested and as expected, gave an HNF-3β-positive band (47 kDa), which was also present in the wild-type extract lane but at a lower intensity. However, the *monorail* protein extract gave an HNF-3β-positive band of the same size. This result is possibly due to the antibody recognising a related Fork head protein in fish given the large number of members in this transcription factor family (Fig. 4.7).

4.1 Screening of the candidate gene *foxA1*

A) Published *foxA1* mRNA sequence (GenBank Accession Number AF052250):

```
903   gga aaa agg tca gag gga aag aga gag cag tcc agc gct cgg gct ctc cgg cca gcg
        G   K   R   S   E   G   K   R   E   Q   S   S   A   R   A   L   R   P   A
960   aca gac cag agg caa acc cgt gca cat gga ctc cag ctc cat cac ctc ctc aaa cca gtc
        T   D   Q   R   Q   T   R   A   H   G   L   Q   L   H   H   L   L   K   P   V
1020  gtc cag tcc gcc cag ttt gga cca cag gag cgg gag ccc ccc aaa ctc gga act gaa gag c
        V   Q   S   A   Q   F   G   P   Q   E   R   E   P   P   K   L   G   T   E   E
                        ▲
                       '*'
```

B) Revised wild-type *foxA1* mRNA sequence:

```
                                                    ▼
903   gga aaa agg tca gag gga aag aga gag cag tcc agc ggc tcg ggc tct ccg gcc agc gac
        G   K   R   S   E   G   K   R   E   Q   S   S   G   S   G   S   P   A   S   D
        ▼
963   agc acc agc agc aaa ccc gtg cac atg gac tcc agc tcc atc acc tcc tca aac cag tcg
        S   T   S   S   K   P   V   H   M   D   S   S   S   I   T   S   S   N   Q   S
1023  tcc agt ccg ccc agt ttg gac cac agg agc ggg agc tcc gcc aac tcg gaa ctg aag agc
        S   S   P   P   S   L   D   H   R   S   G   S   S   A   N   S   E   L   K   S
                    ▲
                   '*'
```

Fig. 4.1 Comparison of the published **(A)** and revised wild-type **(B)** sequence of *foxA1* nucleotides.
The numbers indicate the position of the base at the beginning of the line in relation to the original published and revised coding sequence region respectively.
The changes indicated in the coding sequence above are in a region between the *fork head* domain and transactivating domain II.
The amino acid code is also shown. Region '*' indicates the polymorphism site.
Blue arrows indicate two of the single base insertion sites in the revised *foxA1* sequence. Base changes are shown in green.

C)

```
   1 atgttgggcg cagtgaaaat ggaaggacac gaaactccag actggagcag ctactataat
  61 gatgcacaag aggtctattc tcccatgacg aacagcagca tgaaccctgg gctgagctcc
 121 atgaataata tgaacagtta catgggcatg tccaccagtg ggaatatgac ttccagttct
 181 ttcaacatgt cctatgcgaa cccagcgctc ggcgccgggc tgagcccggg caccatggcc
 241 gggatgccca ccggtggcgc catgaacggg atgggcggcg gagtgtcgag catgggcact
 301 gcgctcagcc cgtccaacct gaacgccatg acggctcagc acagctccat gaacgcgctg
 361 aacccctaca ccagcatgag ccccaccatg agctccatga cctacgcgca gcccaacctg
 421 aaccgggcca gagacaacaa gactttcagg aggagttacc cgcacgcgaa gccccctat
 481 tcctacatct ccctcatcac aatggctatc cagcaggcac ccagcaaaat gcttaccttg
 541 agtgagattt accagtggat aatggacttg ttcccctact accgtcagaa ccagcaaagg
 601 tggcagaact ccatcaggca ctcgttgtcg ttcaacgact gcttcgtcaa agtgtccagg
 661 tcacccgaca agccgggaaa aggctcctac tggaccctgc accctgattc tgggaatatg
 721 tttgagaatg gctgttacct gcgaagacag aagcgcttta aatgcgacaa aaagttgccc
 781 gacggaaaaa ggtcagaggg aaagagagag cagtccagcg gctcgggctc tccggccagc
 841 gacagcacca gcagcaaacc cgtgcacatg gactccagct ccatcacctc ctcaaaccag
 901 tcgtccagtc cgcccagttt ggaccacagg agcgggagct ccgccaactc ggaactgaag
 961 agcggtggcc cgcaggtgca cccggtctct acgtccctgt cctcgctgca ctctatggcc
1021 cacgaatccc tgctgcacct caaaggagac ccccattact ccttcaacca cccgttttcc
1081 atcaataatt taatgtcttc ttcagagcaa cagcataaac tggaattgaa agcctacgaa
1141 caagcgttgc aatattcctc ctacggctca gggatgtctt ccaatttgcc catggccggg
1201 agagccagca tggacccttc ggcggcttta gaggcctctt actaccaagg tgtgtattcc
1261 aggcctgttc tcaatacatc gtag
```

Fig. 4.1C *Danio rerio foxA1* revised mRNA coding sequence (Genbank Accession number AY247950). The coding sequence is 1284 bp in length.
Source:
http://www.ncbi.nlm.nih.gov/entrez/viewer.fcgi?db=nucleotide&val=29170618

4.2 Screening of the candidate gene *foxA2*

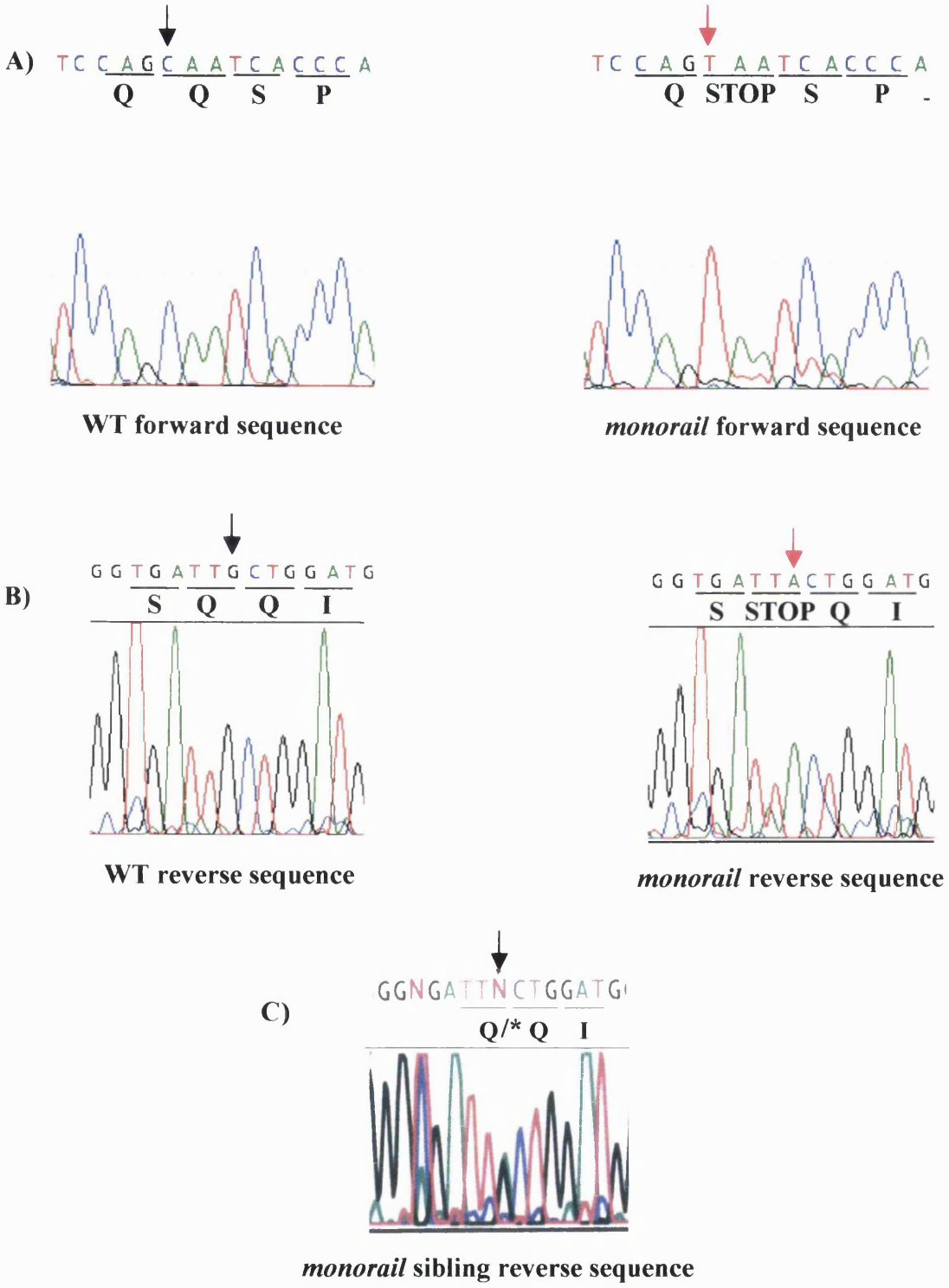

Fig. 4.2 Electropherograms comparing the forward **(A)** and reverse **(B** and **C)** sequence of *foxA2* nucleotides 671-685 from wild-type, heterozygote *monorail* sibling and *monorail*^{tv53a} cDNA. The mutation Q166X in the *monorail* sequence is indicated by a red arrow. *, STOP codon.

4.3 *foxA2* sequence comparison

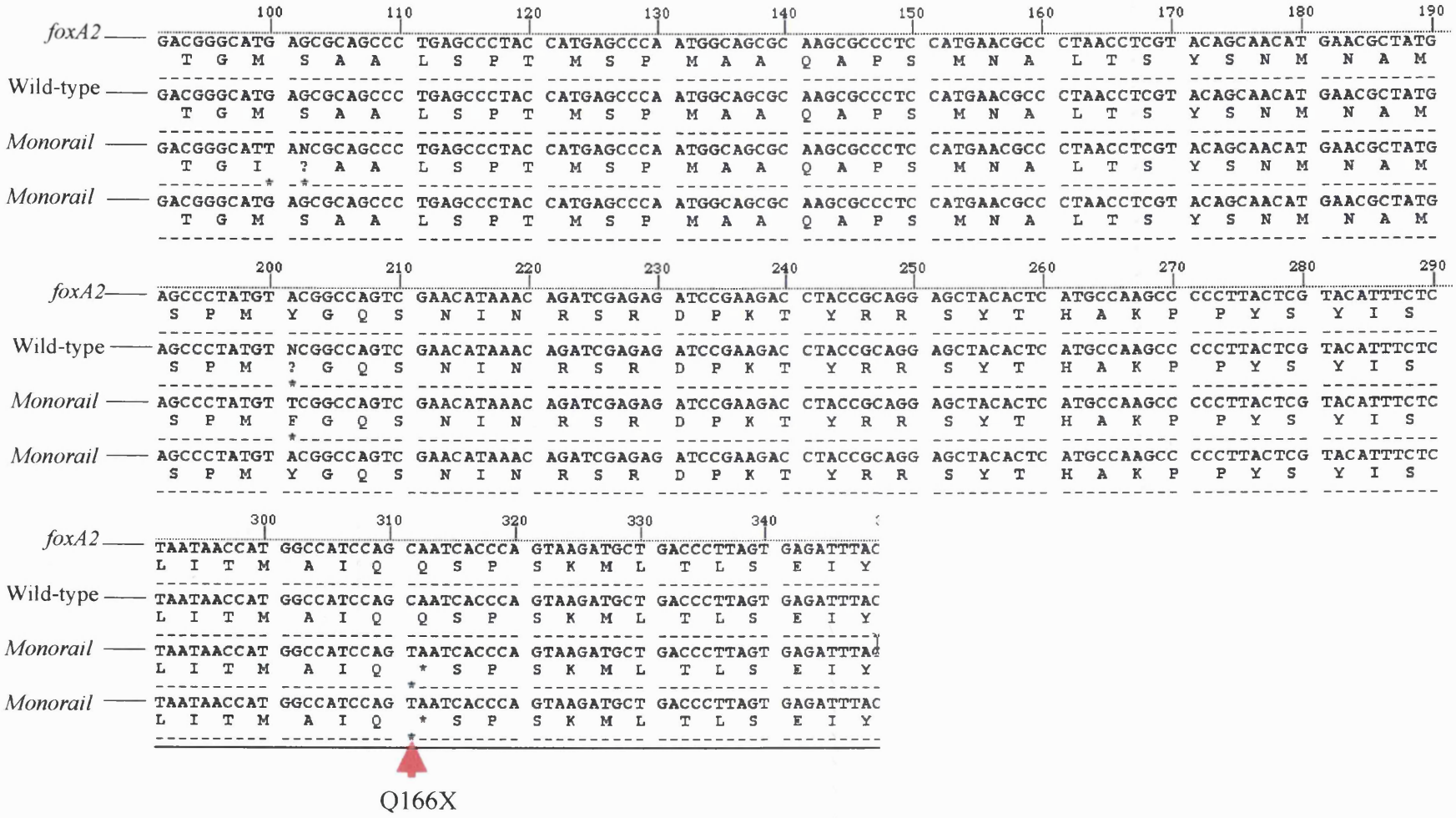

Fig. 4.3 Alignment of *foxA2* mRNA coding sequence region 456-714 bp in one wild-type and two *monorail* individuals.
This region surrounds the mutation site and is compared to the published *foxA2* sequence, GenBank Accession Number NM_130949.
The nucleotide sequence and one letter amino acid code are shown above. ------ shows regions of identical sequence; * indicates a difference in sequence.

4.4 Domain structure of FoxA2 in *monorail*

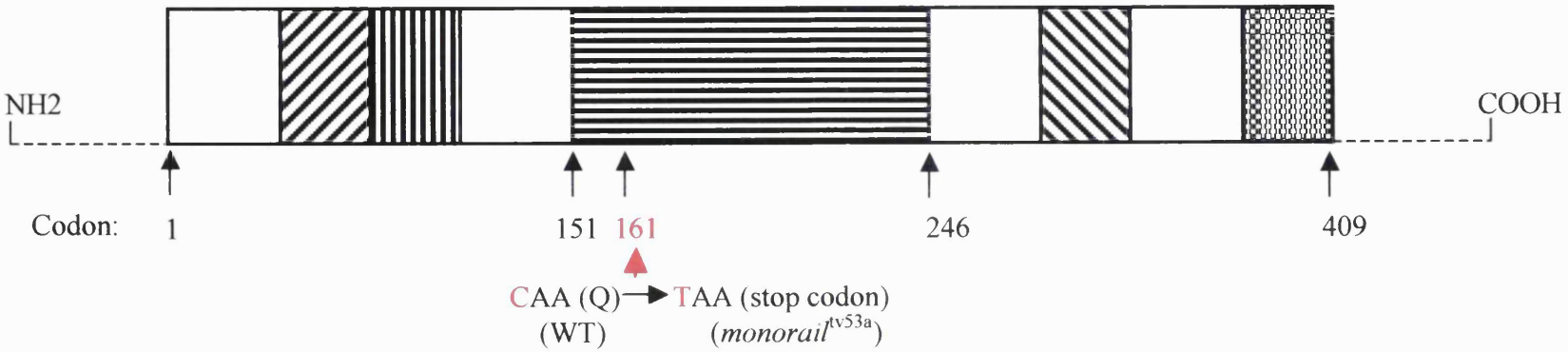

Fig. 4.4 Schematic illustration of the domain structure of FoxA2 protein. As indicated in red, FoxA2 encoded by *monorail*^{tv53a} displays a premature stop codon in the *fork head* DNA binding domain (84 % of this domain is lost) resulting in complete absence of transactivating domains II and III and a carboxy terminally truncated FoxA2 protein.

Key:

- Transactivating domain IV
- *fork head* DNA binding domain
- Transactivating domain V
- Transactivating domain II
- Transactivating domain III

Source: Domain structure of FoxA2 protein from Odenthal *et al.*, 1998 and NCBI; protein Accession number Q07342.

4.5 *foxA2* mutation confirmation

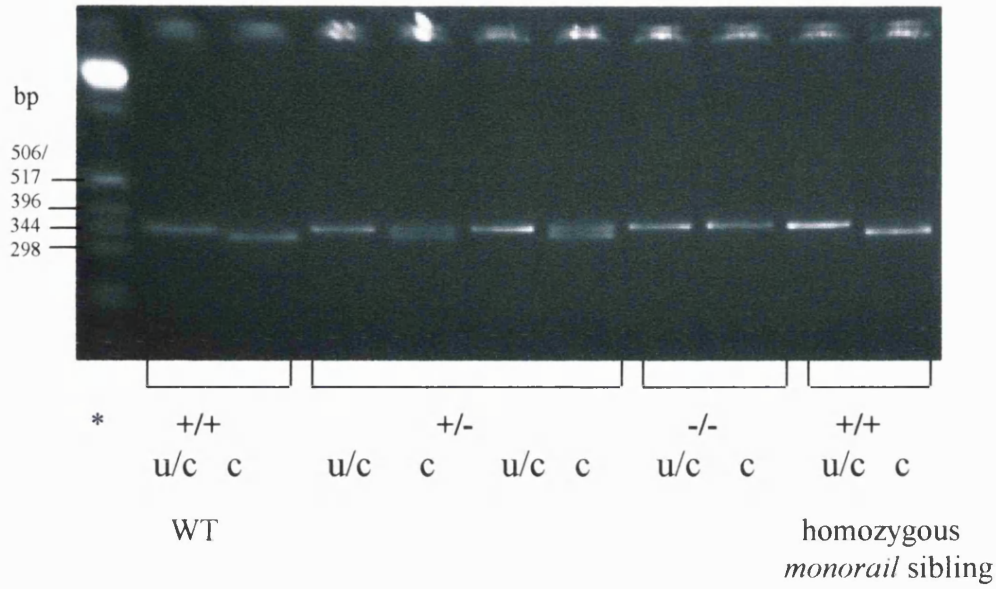

Fig. 4.5 *Hpy*CH4 V restriction enzyme digest of wild-type (WT), *monorail* and *monorail* sibling single embryo genomic DNA samples.

Genotypes are indicated by '+' (wild-type), '+/-' (heterozygote *monorail* sibling) and '-/-' (mutant).
*; 1 kb DNA ladder
u/c; undigested PCR product; 339 bp
c; digested PCR product, 319 bp

4.6 Genescan analysis

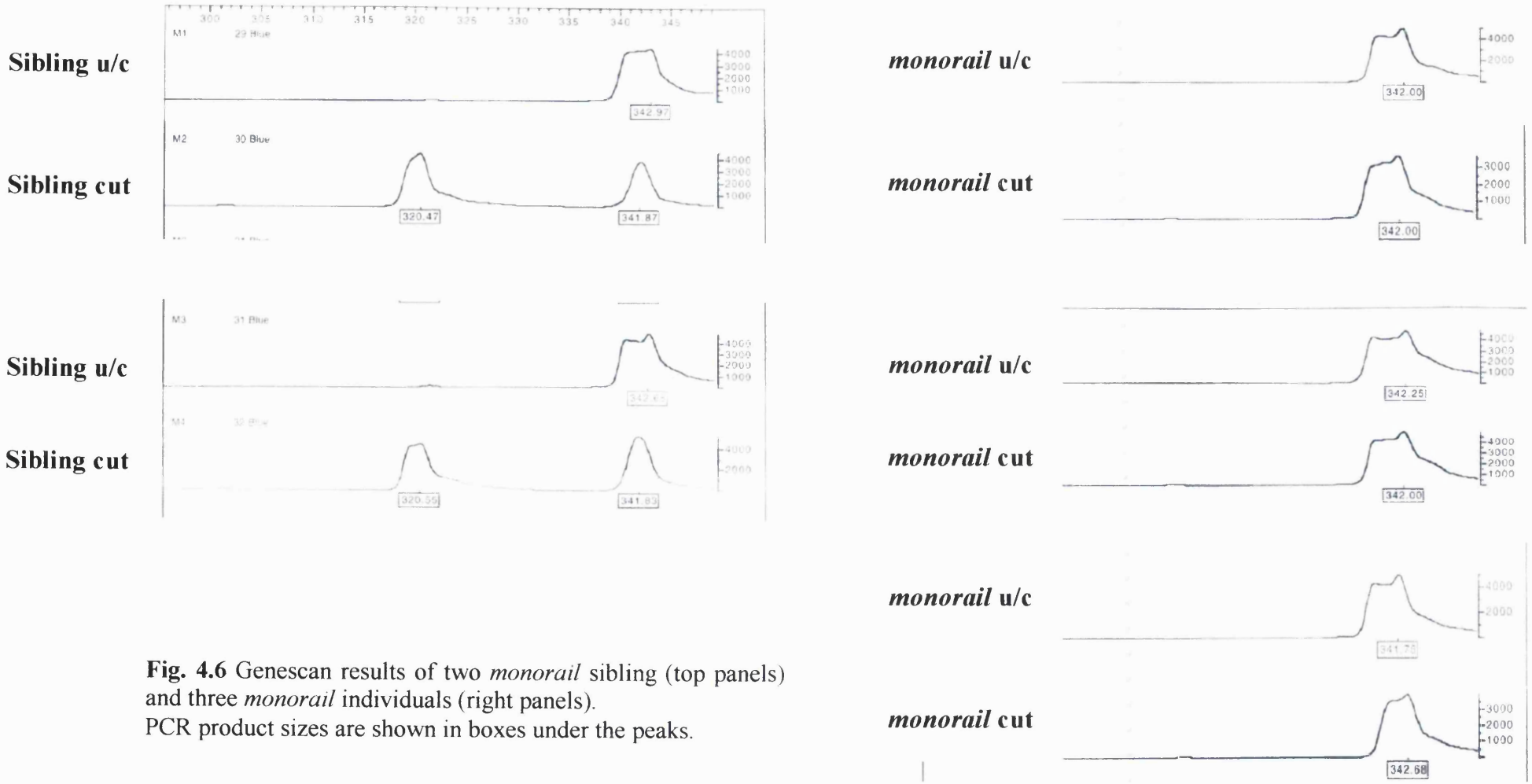

Fig. 4.6 Genescan results of two *monorail* sibling (top panels) and three *monorail* individuals (right panels).
PCR product sizes are shown in boxes under the peaks.

4.7 FoxA2 protein analysis

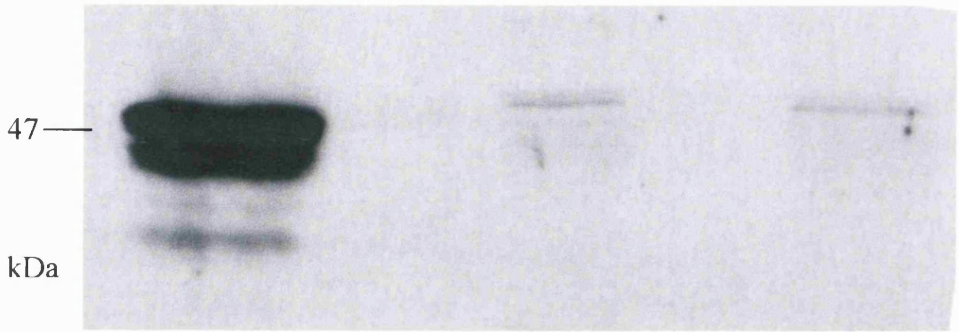

Fig. 4.7 Western blot analysis of protein extracts from a *monorail* and wild-type embryo with a polyclonal antibody against the carboxy terminus of HNF-3β of mouse origin. HepG2; human hepatoblastoma whole cell lysate positive control.

5. The *shrink* mutant: Phenotypic characterisation and genetic mapping

5.1 Phenotypic characterisation

The mutant *shrink*^{U41} was isolated from the 1998 King's College mutagenesis screen (Corinne Houart, personal communication). *Shrink* embryos can be identified by their curled up tail, relatively smaller eyes and head and thinner yolk tube extension compared to their wild-type siblings. They also show substantial areas of cell death in the head region by day 2 of development (Figs. 5.1 and 5.3A).

In wild-type embryos, commissures form a tightly fasciculated bundle of axons due to the balance of attractive signals to the midline and inhibitory signals preventing them from decussating at incorrect locations. Labelling of *shrink* embryos with anti-tubulin antibody showed that post-optic commissural axon pathfinding errors occur in *shrink* embryos; the post-optic commissure is less fasciculated and axons extend rostrally from the chiasm toward the anterior commissure (Fig. 5.2A).

In wild-type zebrafish, retinal ganglion cell axons form a crossed projection with axons from one eye passing adjacent to axons from the other eye within the optic chiasm and projecting to their target, the contralateral optic tectum in the dorsal midbrain (Burrill and Easter, 1995). Retinal nerve projections were visualised using dil and diO dissolved in dimethylformamide and pressure injected into the eyes of fixed larvae and analysed with a confocal microscope. In *shrink* embryos, retinal axons either project into the opposite eye or anteriorly (Fig. 5.2B).

In situ terminal deoxynucleotidyl transferase (TdT)- mediated dUTP nick-end labelling (TUNEL) is used to reveal the fragmented DNA of apoptotic cells during development. The process of apoptotic cell death is essential to remove excess cells

produced during normal development. However *shrink* embryos display a significant increase in the number of apoptotic cells, beginning in the head region and spreading all over the body by day 3 of development (Fig. 5.3).

The escape response of wild-type and *shrink* embryos to an external stimulus was also analysed. An Axioplan 2 microscope (Zeiss) with DIC optics was used and images were taken using the Open Lab program (Improvision®). A needle was used to carefully poke embryos at the tail and observe their behaviour. Wild-type embryos showed a rapid escape response, swimming relatively large distances away from the source of the external stimulus. However *shrink* embryos were less motile than their wild-type siblings and showed a delayed response to the external stimulus, swimming relatively short distances, often in abnormal circular movements (data not shown).

5.2 Genetic Mapping

The *shrink*^{U41} locus was mapped in F_2 offspring of a Tü x WIK reference cross (Rauch *et al.*, 1997) using simple sequence length polymorphic markers (Knapik *et al.*, 1996; Table 9.1.2) on pools of 48 mutants and 48 siblings to identify linkage. The mutation was rough mapped by William Talbot and localised to LG 6, 6 cM from SSLP marker Z6767 and 3 cM from Z12094 (Table 5.1). Fine mapping was carried out at UCL by genotyping single mutant and sibling embryos with further SSLP markers (Fig. 5.4). Four recombinants were identified in 52 meioses with marker Z14826. This result places marker Z14826 a distance of 8cM away from *shrink* (Fig. 5.5A). A schematic representation of Fig. 5.5A is shown as Z14826 was not used at its optimal PCR reaction conditions and the product bands are difficult to interpret (Fig. 5.5B). The gene *jak1 kinase* (Conway *et al.*, 1997) involved in early brain development, maps to the same region on LG 6 as *shrink* and is therefore a candidate (Fig. 5.4).

5.1 Identification of *shrink* mutants

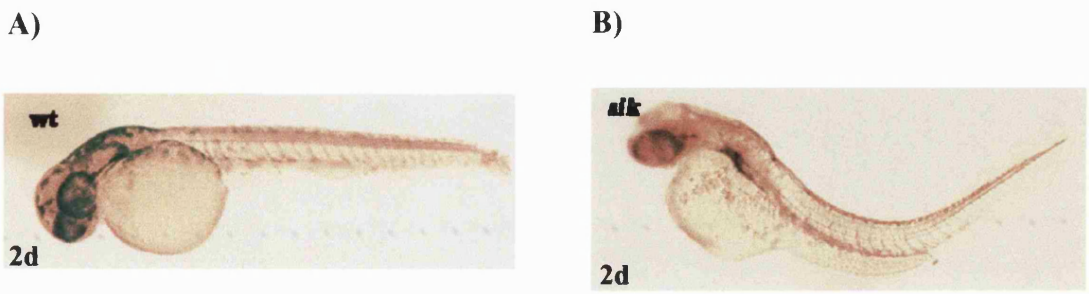

Fig. 5.1 Lateral views of 48 hpf wild-type **(A)** and *shrink* **(B)** embryos showing a curled up tail in *shrink*.

5.2 Axonogenesis phenotype in *shrink*

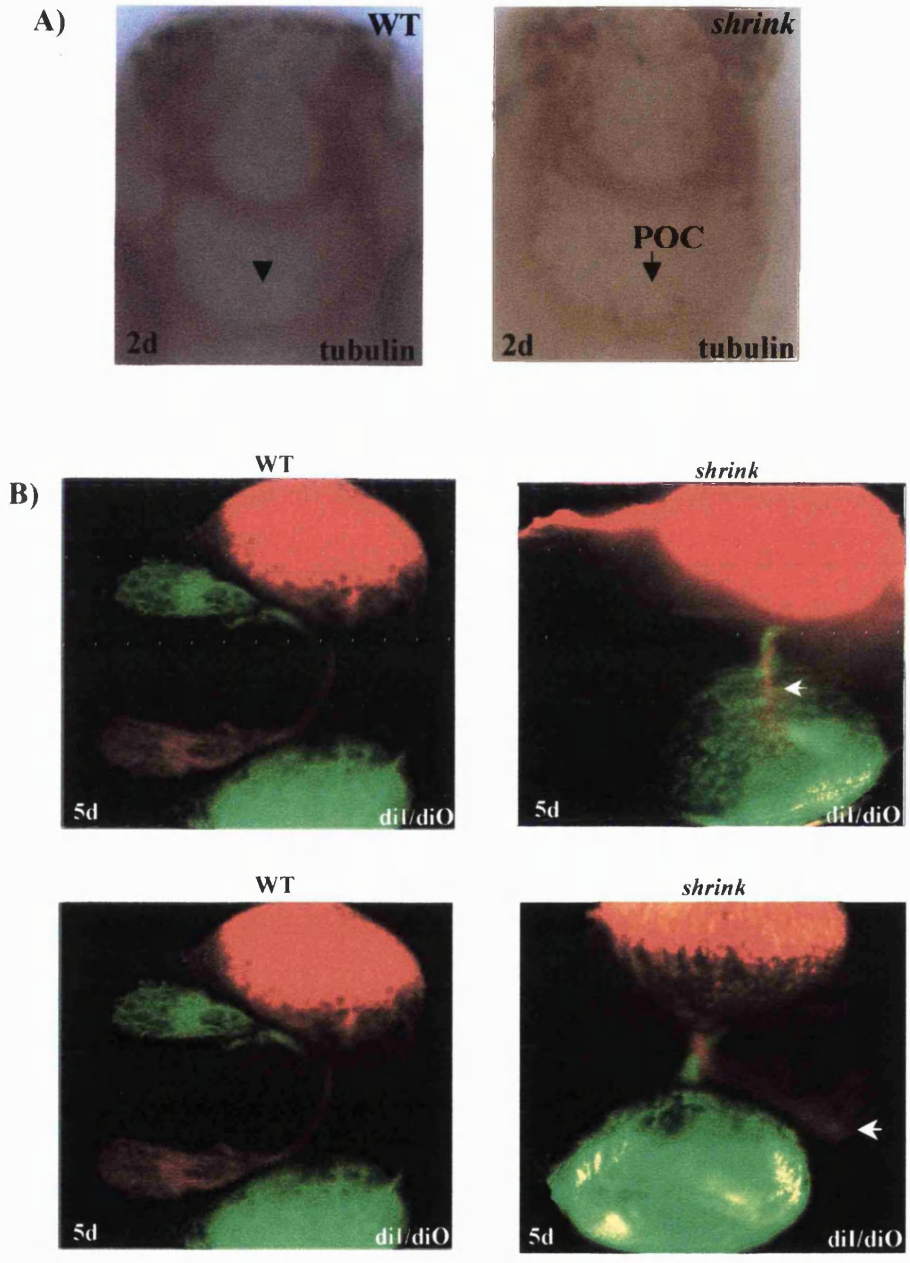

Fig. 5.2 A) Ventral views of 48 hpf wild-type (left panel) and *shrink* (right panel) embryos labelled with anti-acetylated tubulin showing defasciculation of the post-optic commissure (POC) in *shrink* embryos. Anterior is to the top.
B) Ventral views of 5 day old wild-type (left panels) and *shrink* (right panels) embryos labelled with dil (red) and diO (green) to reveal retinotectal projections. The retinal ganglion cell axons in *shrink* embryos project to the opposite eye (white arrow, top right panel) or anteriorly (white arrow, bottom right panel) rather than posteriorly to the contralateral optic tectum (left panels). Anterior is to the right.

5.3 *Shrink* embryos exhibit increased cell death

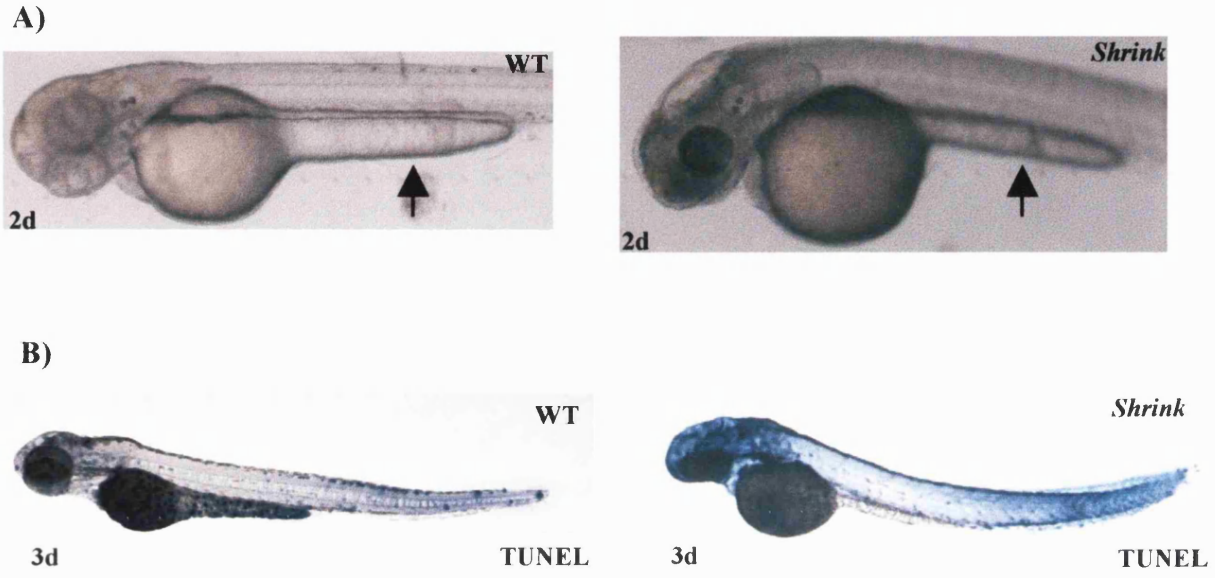

Fig. 5.3 A) Lateral views of 48 hpf wild-type (left panel) and *shrink* (right panel) embryos. *Shrink* embryos exhibit cell death in the head, smaller eyes and head and a thinner yolk tube extension (indicated by arrows) compared to wild-type embryos. Anterior is to the left.
B) Lateral views of 72 hpf wild-type (left panel) and *shrink* (right panel) embryos. Cell death is visible all over the embryonic body at this stage in *shrink* and is confirmed by TUNEL labelling (blue staining).

Table 5.1 Genetic mapping of *shrink* (*sik*^{U41})

Rough mapping localised *shrink* to linkage group (LG) 6
The following SSLPs were linked to *sik*^{U41} :

SSLP	Mapping panel positions from top of LG 6		
	MGH /cM**	T51/cR**	HS/cM**
Z6767	47.80	—	64.50
Z12094	49.00	1090.00	72.10

KEY:
MGH, HS and MOP- Meiotic mapping panels
T51- Radiation hybrid mapping panel
**- Position of markers on mapping panel source: http://zfin.org

5.4 Genetic mapping of the *shrink* mutation

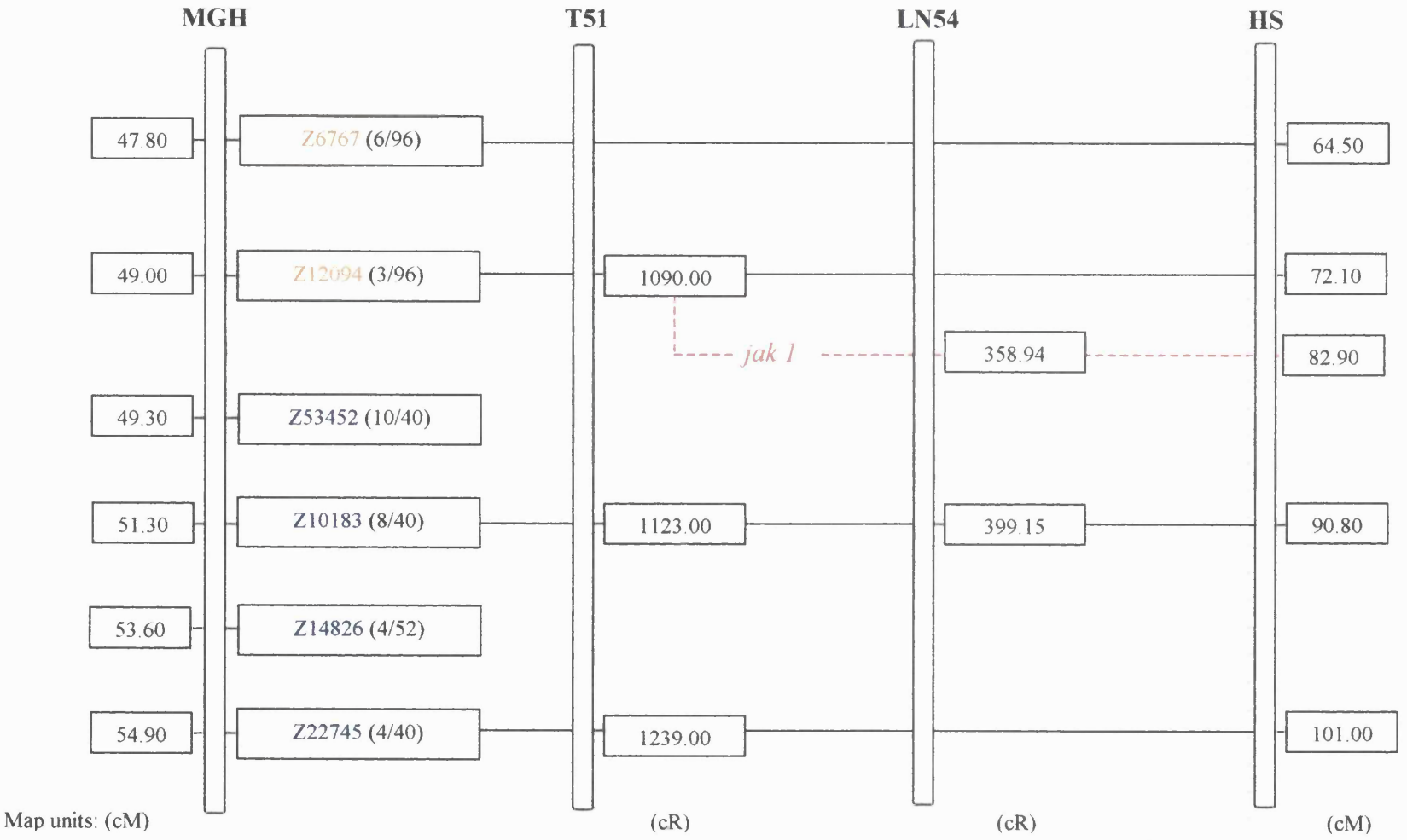

Fig. 5.4 Schematic diagram showing the position of SSLP markers used for fine mapping of the *shrink*^{U41} mutation and a candidate gene in the region (shown in red). The corresponding position of these markers on the T51, LN54 and HS panels is shown in order to identify possible candidate genes in regions showing tight linkage on LG 6. Polymorphic (linked) SSLPs are shown in blue. Numbers in brackets indicate recombination frequencies. The results for markers shown in orange are from Dr William Talbot.

5.5 Z14826 recombinants

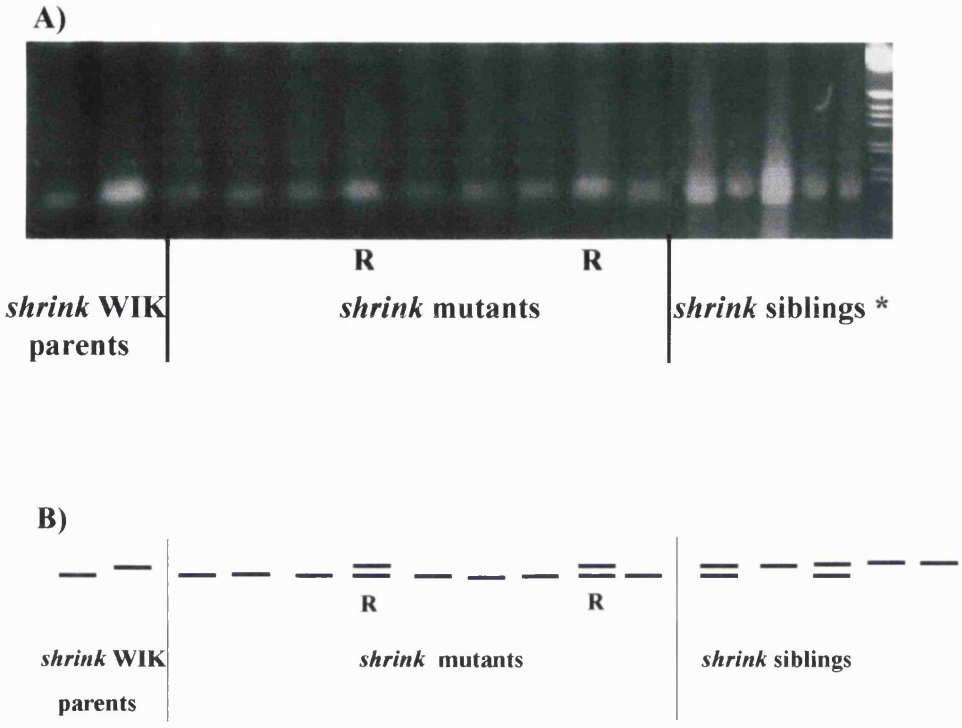

Fig. 5.5 A) Genotype analysis of single embryo *shrink* mutants and siblings using the SSLP marker Z14826.
The upper band is the WIK allele that segregates with *shrink*; the lower band is the Tü allele. Two recombination events (R) in 18 meioses are shown.
*, 1 kb DNA ladder
B) A schematic representation of Fig. 5.5A.

6. *Otter* and *eisspalte*: Phenotypic characterisation and genetic mapping

The mutants *otter*^{ta76b} and *eisspalte*^{ty77e} were isolated from the 1996 Tübingen mutagenesis screen and grouped into a class of mutations affecting neurogenesis and early brain morphology (Jiang *et al.*, 1996). *Otter*^{ta76b} mutants have been analysed in a behavioural screen for optokinetic/optomotor responses and the phenotype observed judged to be due to the previous defects identified in brain development, degeneration and retardation (Neuhauss *et al.*, 1999). *Eisspalte*^{ty77e} mutants were also identified in a screen to isolate mutations disrupting the ordering and topographic mapping of axons in the retinotectal projection of zebrafish (Trowe *et al.*, 1996). The projection of retinal axons onto the tectum in *eisspalte* was not affected but the size of the tecta were siginificantly reduced (Trowe *et al.*, 1996).

6.1 *Otter*

Further phenotypic characterisation of the *otter* mutant has revealed disrupted development of the midbrain hindbrain boundary, cerebellum and brain ventricle formation (Dr Jacqueline Hoyle, personal communication). Other defects in *otter* embryos include defects in ear, jaw and heart development (Jiang *et al.*, 1996).

Labelling of *otter* embryos with acetylated tubulin antibody has shown commissural axon pathfinding defects within the forebrain. The anterior and post-optic commissures form thicker bundles compared to their wild-type siblings, axons cross between the anterior and post-optic commissure and the optic nerve splits on exiting the eye (Fig. 6.1).

The *otter*^{ta76b} locus was mapped in F_2 offspring of a Tü x WIK reference cross (Rauch *et al.*, 1997) using simple sequence length polymorphic markers (Knapik *et al.*,

1996; Table 9.1.3) on pools of 48 mutants and 48 siblings to identify linkage to the mutation. *Otter* was localised to LG 14 and mapped to a region between SSLP markers Z7043 and Z5435 (Robert Geisler, personal communication; Table 6.1, Fig. 6.2). Linkage was confirmed by genotyping single mutant and sibling embryos with further SSLP markers in the region. Fifteen recombinants in 124 meioses were identified with marker Z7030 and 3 recombinants in 28 meioses with marker Z5435. Hence markers Z7030 and Z5435 are 12cM and 11cM away from *otter* respectively (Figs. 6.3 and 6.4). Complementation studies have revealed that *otter* is allelic to *motionless*, a mutant isolated from a screen for mutations affecting development of catecholaminergic neurons in zebrafish (Guo *et al.*, 1999b). *Motionless* maps between SSLP markers Z3868 and Z22094 on LG 14 and identification of candidates in this region is underway (Su Guo, personal communication). The mapping results from the Guo lab place markers Z3868 and Z22094 at distances of 1.8cM and 0.3cM away from *motionless* respectively (Fig. 6.3).

6.2 *Eisspalte*

The *eisspalte* mutant is identified by its curled down tail phenotype which is visible from day 1 of development and although less severe at day 2, a significant difference from the wild-type sibling is still observed (Fig. 6.5). Labelling with acetylated tubulin antibody revealed commissural axon pathfinding defects in the forebrain of *eisspalte* embryos. Specifically, the anterior commissure is less fasciculated than normal and the optic nerve projects in different directions on exiting the eye (Fig. 6.6).

The *eisspalte*^{ty77e} locus was mapped in F_2 offspring of a Tü x WIK reference cross (Rauch *et al.*, 1997) using simple sequence length polymorphic markers (Knapik *et al.*, 1996) on pools of 48 mutants and 48 siblings. *Eisspalte* was rough mapped to a region between SSLP markers Z1226 and Z1801 on LG 14 (Robert Geisler, personal

communication; Tables 6.2 and 9.1.4; Fig. 6.7). Linkage was confirmed by genotyping single mutant and sibling embryos with further SSLP markers in the region. Seven recombinants in 84 meioses were identified with marker Z9057 and 18 recombinants in 72 meioses with marker Z1226. Hence markers Z9057 and Z1226 are 8cM and 25cM away from *eisspalte* respectively (Figs. 6.8 and 6.9).

6.1 Axonogenesis phenotype in *otter*

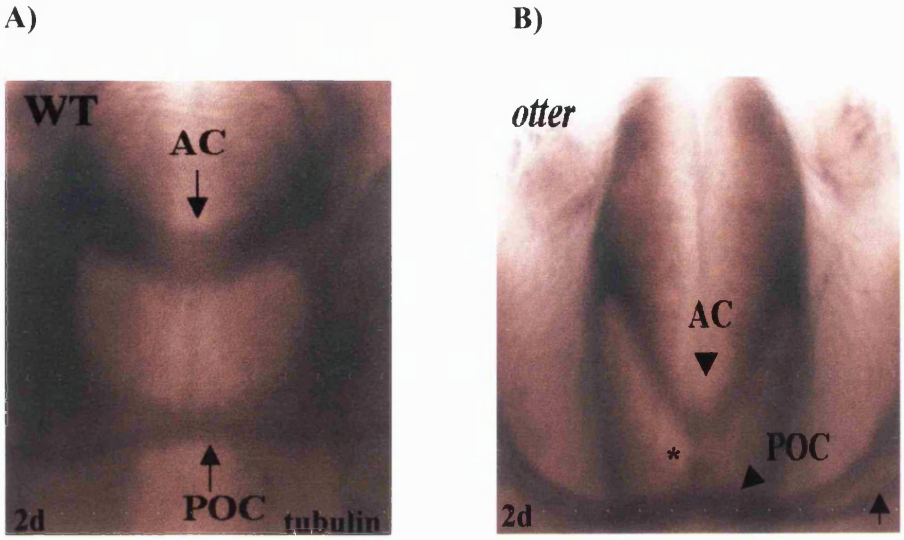

Fig. 6.1 Ventral views of 48 hpf wild-type **(A)** and *otter* **(B)** embryos labelled with anti-acetylated tubulin. Commissural axons cross between anterior and post-optic commissure in *otter* embryos, as indicated by *. The optic nerve defasiculates as it leaves the eye in *otter*, as indicated by the arrow.
AC; anterior commissure, POC; post-optic commissure
Anterior is to the top.

Table 6.1 Genetic mapping of *otter* (*ott* ^{ta76b})

Rough mapping localised *otter* to linkage group (LG) 14
The following SSLPs were linked to *ott*^{ta76b}:

SSLP	Mapping panel positions from top of LG 14				
	MGH /cM**	T51/cR**	HS/cM**	LN54/cR**	MOP/cM**
Z7043	10.50	117.00	7.30	—	—
Z5435	34.60	336.00	30.90	258.54	36.60
Z1226	60.60	2667.00	102.20	—	175.60

KEY:

MGH, HS and MOP- Meiotic mapping panels
T51 and LN54- Radiation hybrid mapping panels
**- Position of markers on mapping panel source: http://zfin.org
Muts; mutants in tup longfin background, sibs; siblings, WIK; wild-type strain.

6.2 Rough mapping of the *otter* mutation

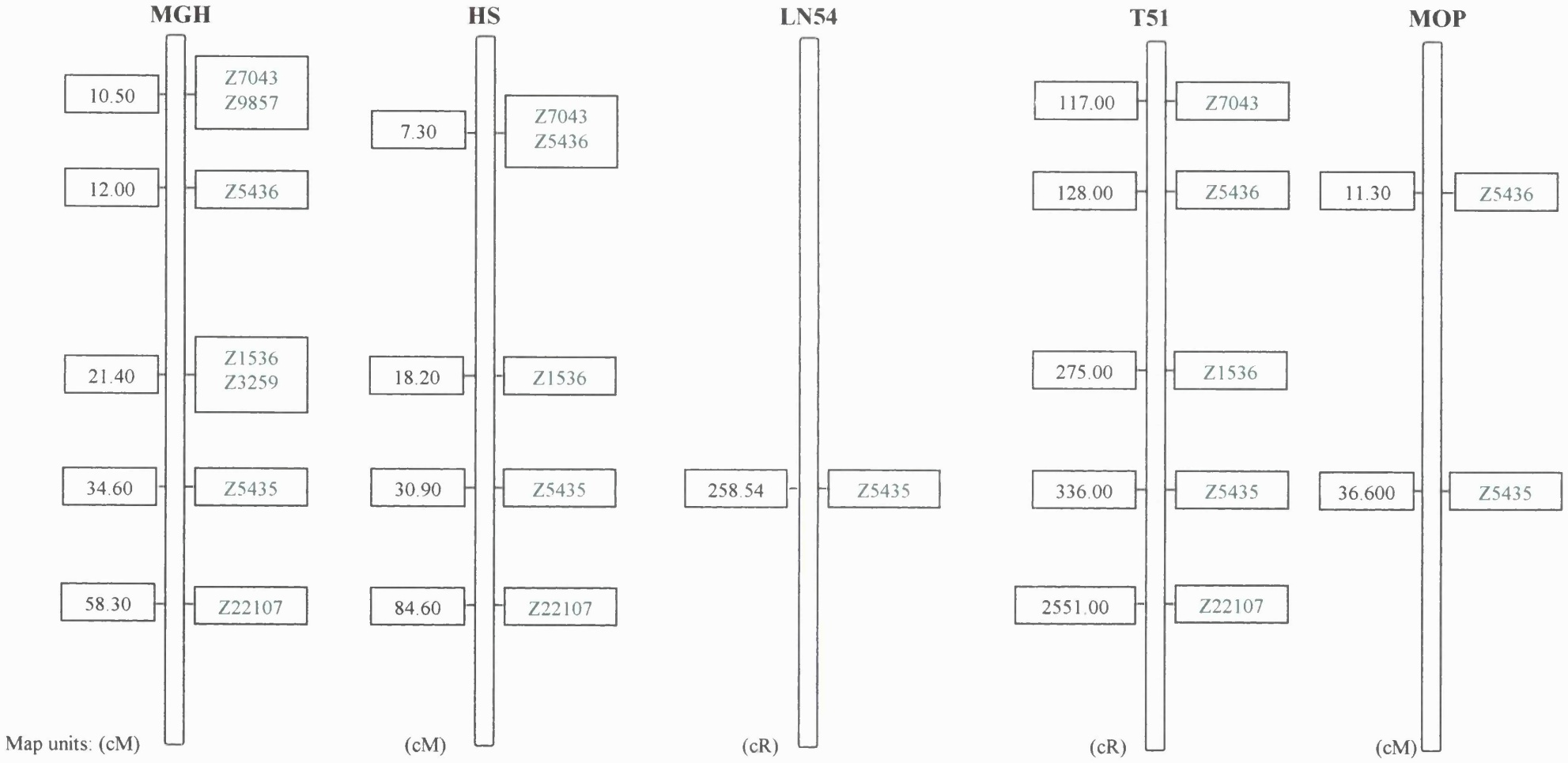

Fig. 6.2 Schematic diagram showing the position of SSLP markers used for rough mapping of the *otter*^{ta76b} mutation on LG 14. Numbers in boxes to the left of each panel indicate the position of SSLP markers on each mapping panel (Source: http://zfin.org). Linked SSLPs tested on pooled samples for rough mapping are shown in green.

6.3 Fine mapping of the *otter* mutation

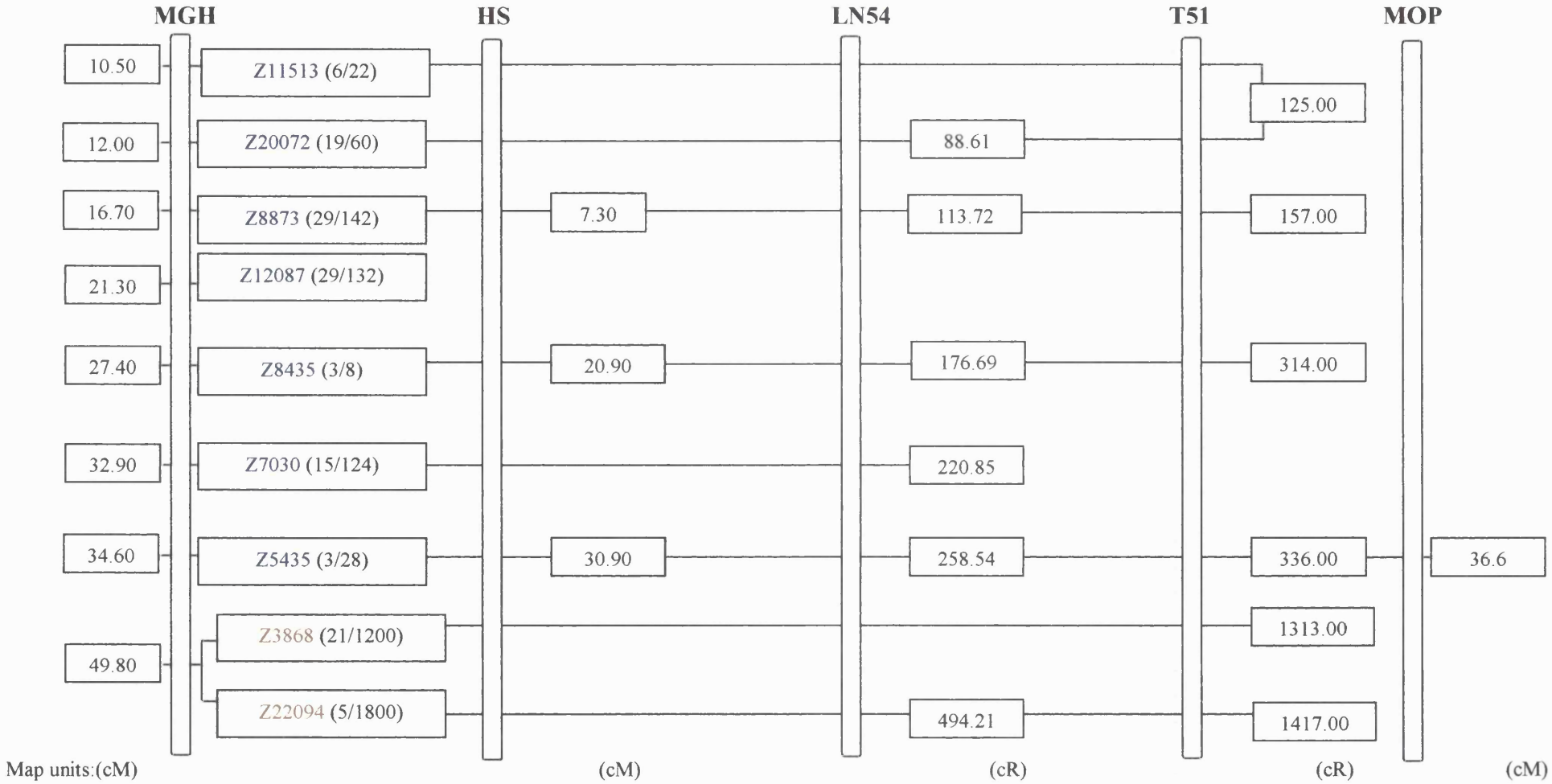

Fig. 6.3 Schematic diagram showing fine mapping results for the *otter*^{ta76b} mutation using SSLPs from the MGH panel. The corresponding position of these markers on the HS, LN54, T51 and MOP panels is shown in order to identify possible candidate genes in regions showing tight linkage on LG 14. Polymorphic (linked) SSLPs are shown in blue. Numbers in brackets indicate recombination frequencies.
Results obtained from linkage with markers shown in brown are from Su Guo and mapping of the *motionless* mutant, which is allelic with *otter*.

6.4 Z5435 recombinants

Fig. 6.4 Genotype analysis of single embryo *otter* mutants and siblings using the SSLP marker Z5435.
The upper band is the WIK allele that segregates with *otter*; the lower band is the Tü allele. Three recombination events (R) in 24 meioses are shown.
*, 1 kb DNA ladder

6.5 Identification of *eisspalte* mutants

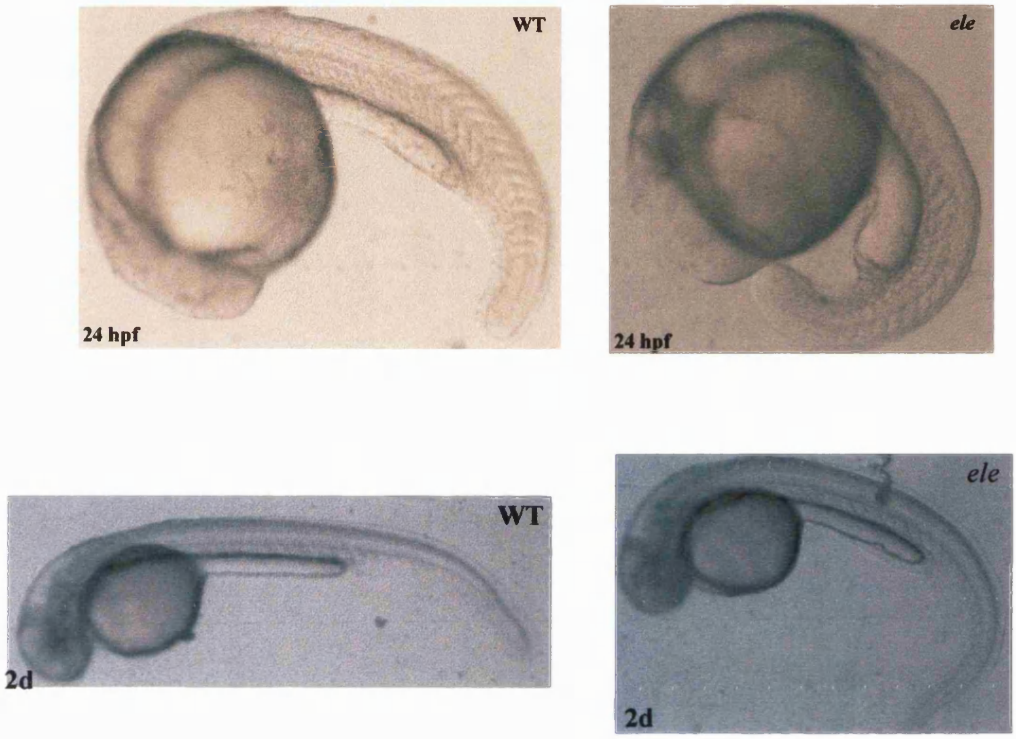

Fig. 6.5 Lateral views of 24 hpf and 48 hpf wild-type and *eisspalte* embryos showing a curled down tail in *eisspalte*.

6.6 Axonogenesis phenotype in *eisspalte*

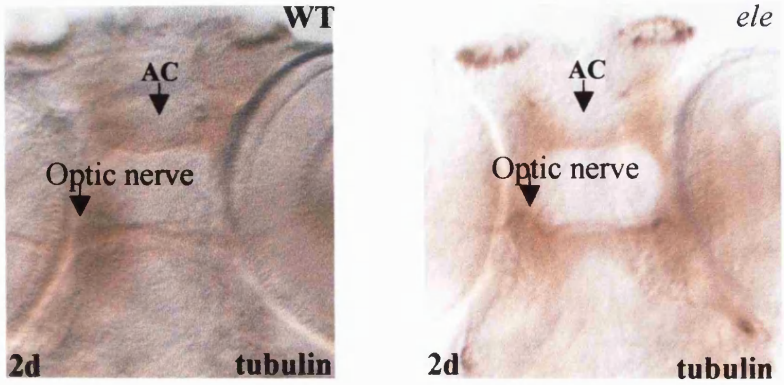

Fig. 6.6 Ventral views of 48 hpf wild-type (left panel) and *eisspalte* (right panel) embryos labelled with anti-acetylated tubulin showing defasciculation of the anterior commissure (AC) and disorganised projection of the optic nerve in *eisspalte* embryos. Anterior is to the top.

Table 6.2 Genetic mapping of *eisspalte* (*ele* ^{ty77e})

Rough mapping localised *eisspalte* to linkage group (LG) 14
The following SSLPs were linked to *ele*^{ty77e}:

SSLP	Mapping panel positions from top of LG 14			
	MGH /cM**	T51/cR**	HS/cM**	MOP/cM**
Z4203	38.10	493.00	38.20	—
Z22107	58.30	2551.00	84.60	—
Z1226	60.60	2667.00	102.20	175.60

KEY:

MGH, HS and MOP- Meiotic mapping panels
T51- Radiation hybrid mapping panel
**- Position of markers on mapping panel source: http://zfin.org

6.7 Rough mapping of the *eisspalte* mutation

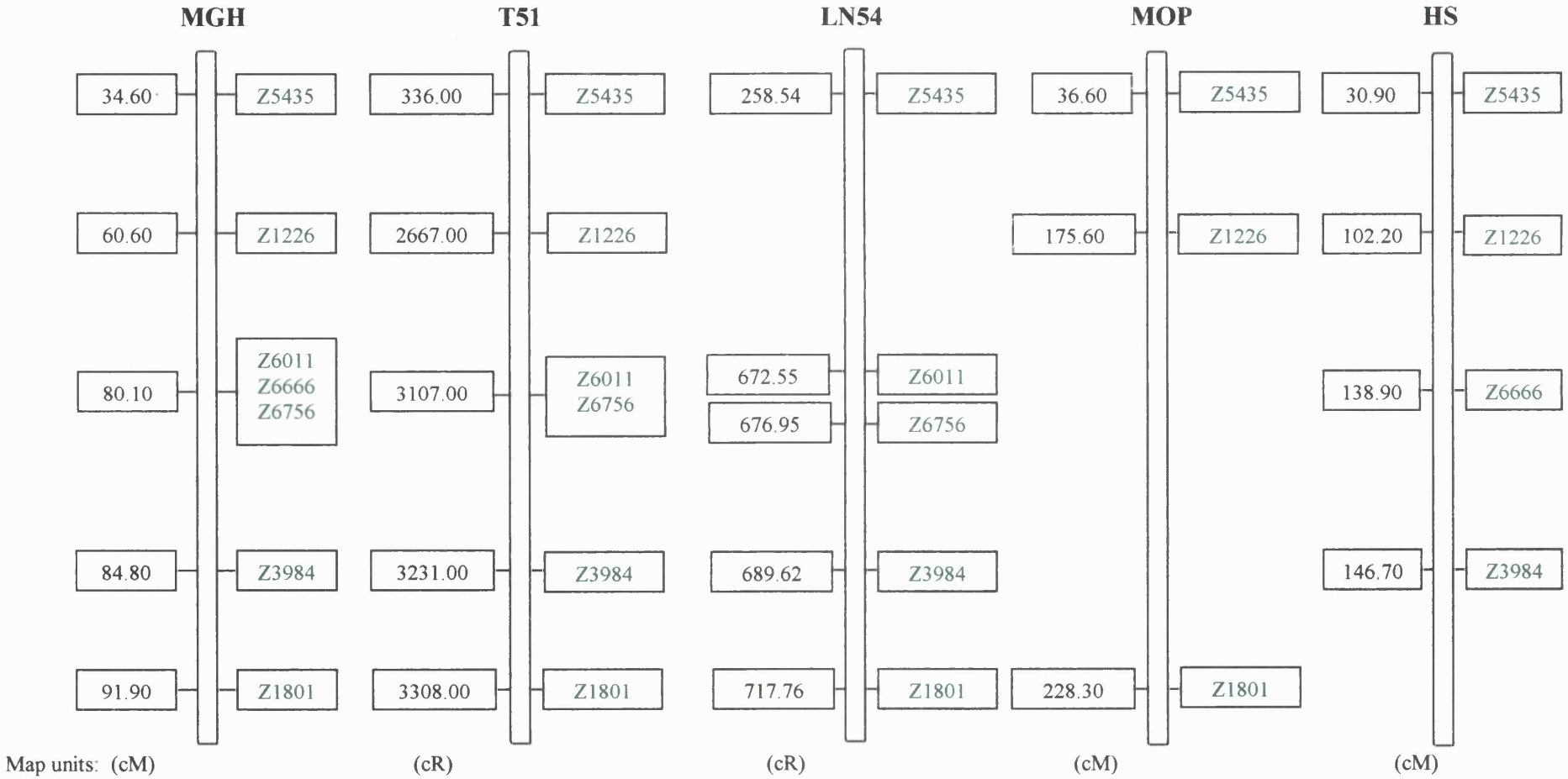

Fig. 6.7 Schematic diagram showing the position of SSLP markers used for rough mapping of the *eisspalte*^{ty77e} mutation on LG 14. Numbers in boxes to the left of each panel indicate the position of SSLP markers on each mapping panel (Source: http://zfin.org). Linked SSLPs tested on pooled samples for rough mapping are shown in green.

6.8 Fine mapping of the *eisspalte* mutation

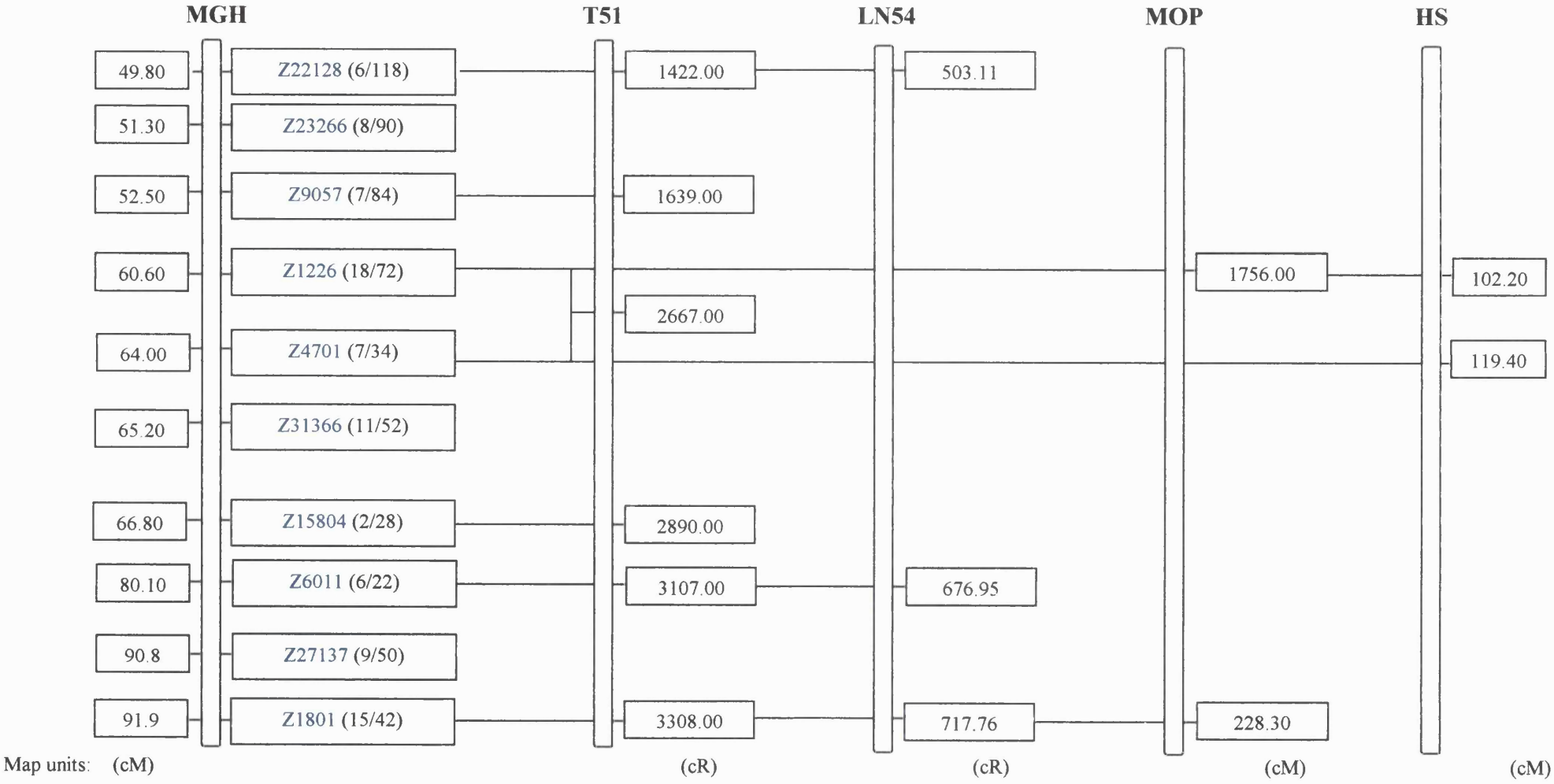

Fig. 6.8 Schematic diagram showing fine mapping results for the *eisspalte*^{ty77e} mutation using SSLPs from the MGH panel. The corresponding position of these markers on the T51, LN54, MOP and HS panels is shown in order to identify possible candidate genes in regions showing tight linkage on LG 14. Polymorphic (linked) SSLPs are shown in blue. Numbers in brackets indicate recombination frequencies.

6.9 Z1226 recombinants

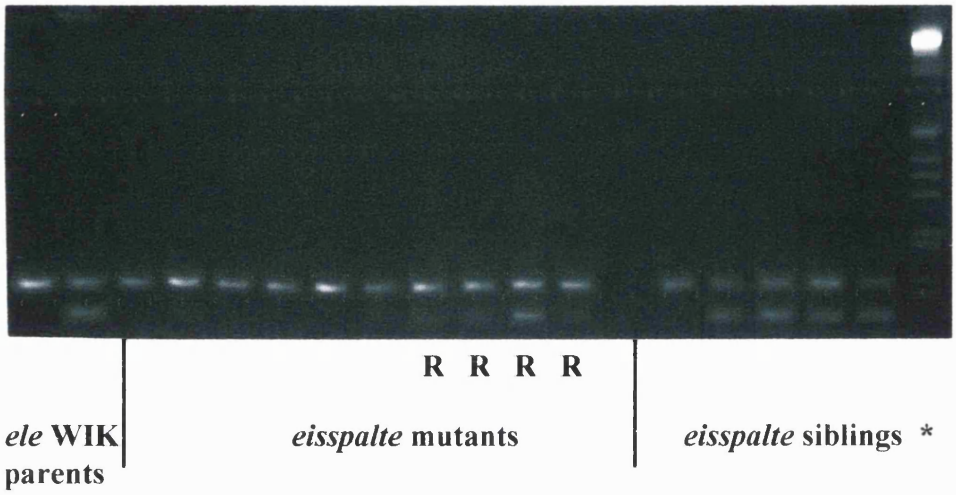

Fig. 6.9 Genotype analysis of single embryo *eisspalte* mutants and siblings using the SSLP marker Z1226.
The lower band is the WIK allele that segregates with *eisspalte*; the upper band is the Tü allele. Four recombination events (R) in 20 meioses are shown.
*, 1 kb DNA ladder

7. Discussion

The work presented in this thesis has focussed on phenotypic characterisation and genetic mapping of *monorail*^{tv53a}, *shrink*^{U41}, *otter*^{ta76b} and *eisspalte*^{ty77e}, zebrafish mutants isolated from ENU mutagenesis screens (Brand *et al.*, 1996; Jiang *et al.*, 1996; Corinne Houart, personal communication). These mutations affect various aspects of brain development including neural tube specification, neurogenesis and axon pathfinding in the embryonic zebrafish. It was envisaged that re-screening of these mutant lines together with genetic mapping and identification of the affected genes would provide new insights into early development of the vertebrate brain. The findings from each mutant have increased our knowledge of neuronal patterning and axon pathway development in the central nervous system and will be discussed below.

7.1 The *monorail* mutant

7.1.1 Midline defects in *monorail*

The *monorail* mutant is morphologically identified by its ventrally curled body axis, which forms as a result of defects in midline signalling. Other mutants in the same class include *one-eyed pinhead*, *cyclops* and *schmalspur* and all display ventral midline defects leading to a curly tail phenotype (Brand *et al.*, 1996; Karlstrom *et al.*, 1996). The reason for the downward curved body axis in mutants with defects in floor plate formation may be due to the absence or reduction of Reissner's fiber (Higashijima *et al.*, 1997), a thread-like elastic structure located in the central canal of the spinal cord in the vertebrate phylum (Reissner, 1860). Components of Reissner's fiber are secreted from the floor plate cells at early stages of development and later from the subcommissural organ (SCO) located at the dorsal midline of the diencephalon (for review see Meiniel *et al.*, 1996). F-spondins are a class of secreted proteins expressed

by the floor plate cells and a subtype of these molecules, F-spondin2, is localised to regions corresponding to Reissner's fiber (Higashijima *et al.*, 1997). In *one-eyed pinhead* mutants, formation of the floor plate is severely affected (Schier *et al.*, 1996) and *F-spondin2* mRNA expression is significantly reduced in this region (Higashijima *et al.*, 1997). *Drosophila* M-spondin shares two conserved domains with the NH_2-terminal half of F-spondin. The zebrafish genes *mindin-1* and *mindin-2* are more closely related to *Drosophila* M-spondin than to F-spondin and are expressed in floor plate cells. In *monorail* embryos, the expression of *mindin-1* and *mindin-2* is absent in the floor plate (Dr William Norton, personal communication). Hence the Mindin/F-spondin family, which are expressed in the embryonic axis in the region corresponding to the location of Reissner's fiber, are important in development of the midline and body shape (Higashijima *et al.*, 1997).

Monorail embryos show a variable reduction in the width of the floor plate, as shown by fusion and disorganisation of axons of the medial longitudinal fascicles at various locations along the entire body axis. The phenotype of other zebrafish mutants with absence of, or partial defects in, floor plate development also involves fusion and disorientated growth of axons close to the midline. These mutants include *cyclops* (Hatta, 1992), *schmalspur*, *detour* and *monorail* (Brand *et al.*, 1996). The reason that only a subset of axons is affected in these 'midline' mutants is that axon growth depends on multiple guidance cues from the midline (Colamarino and Tessier-Lavigne, 1995).

Monorail embryos display defects in maintenance of segmental organisation of cells in the hindbrain, glial bundle organisation and axonal pathfinding across the midline. The number and pattern of dorso-ventrally orientated glial bundles that are normally organised into two transverse rows in each hindbrain segment are reduced and

disrupted. Glial bundles also occupy the floor plate in *monorail*, an area that is normally devoid of cells and neurons.

Glial cells are the major non-neuronal components in the nervous system and play a role in early pattern formation and establishment of neural pathways. During the formation of axon scaffolds, glia support their outgrowth, form boundaries around tracts and between neuromeres and facilitate axonal fasciculation and defasciculation of later developing axons (Marcus and Easter, 1995; Freeman *et al.*, 2003). In *Drosophila*, the path of axonal growth cones is in part determined by glia, which act as 'guideposts' at choice points along their route (Hidalgo, 2003). In the mouse, ablation of midline glia after the initial establishment of commissures causes defasciculation of axons across the midline (Zhou *et al.*, 1997). In the zebrafish, lateral line glia are guided by growing axons and laser ablation of the nerve results in glial stalling (Gilmour *et al.*, 2002; for review see Chien and Piotrowski, 2002). The role of glial cells during axon outgrowth in zebrafish has been shown by expression analysis of the glial-specific intermediate filament, glial fibrillary acidic protein (GFAP; Marcus and Easter, 1995). Glial cells are first evident at 15 hpf just before the first axon outgrowth in the brain. At 24 hpf glial processes border axons in the medial longitudinal fasciculus in the hindbrain and by 48 hpf associate with axon tracts and commissures and define boundaries between rhombomeres (Marcus and Easter, 1995). Glial cells are present in the floor plate of *monorail* embryos. Their precise location has yet to be determined, however it may correspond to regions where fusion and disorganisation of axons of the medial longitudinal fascicles have occurred.

The patterning of cranial motor neurons adjacent to the floor plate is also disrupted in *monorail* embryos. A GFP transgene driven by *islet1* regulatory elements was crossed into the *monorail* line in order to label cranial motor neurons (Higashijima

et al. 2000). The oculomotor and facial motor nuclei form a single cluster of neurons at the midline rather than bilateral pairs of nuclei. There is also a reduction in the number of posterior trigeminal motor neurons (Vp) and the trochlear nucleus (IV) is absent in *monorail* embryos, which consequently lack a trochlear decussation. Cranial motor neurons are generally induced by Hedgehog proteins and the lack of maintenance of floor plate expression of *hedgehog* genes results in production of less Hedgehog protein to induce these neurons (Table 3.1; Chandrasekhar *et al.*, 1999; Lewis and Eisen, 2001).

The trochlear motor nucleus develops in the first hindbrain rhombomere, which is patterned through graded signals from the isthmic 'organiser' at the midbrain hindbrain boundary (MHB) by Fgf8 activity (Irving and Mason, 1999; for review see Rhinn and Brand, 2001). The trochlear nerve axons extend from cell bodies in rhombomere 1 and fasciculate, growing along a dorsal trajectory to innervate the contralateral superior oblique muscle of the eye (Colamarino and Tessier-Lavigne, 1995). The dorsal projection of the trochlear (IV) as well as the lateral trajectories of the trigeminal (V), facial (VII) and glossopharyngeal (IX) cranial nerves is due in part to chemorepulsive signals from the floor plate. These signals include members of the Netrin and Semaphorin families. At 24 hpf *sema4E* is expressed in the dorsal hindbrain, in dorsal and ventral cells of the spinal cord, in the dorsal tectum and in the pharyngeal arches of the zebrafish embryo. Sema4E is a repulsive guidance signal for facial cranial motor axons and acts as a barrier for branchiomotor axons at the boundaries of the pharyngeal arches (Xiao *et al.*, 2003).

Evidence for the role of signalling molecules from floor plate cells in guidance of branchiomotor axons has been shown in other species. In rat, both *Netrin-1*, expressed by the floor plate and *Sema3A*, expressed by ventral tissues, repel growing trochlear axons *in vitro* (Varela-Echavarria *et al.*, 1997). The projection of trochlear

nerve axons in rat has recently been shown to be due to a combination of factors. These involve repulsive cues (including Netrin signalling) from the floor plate, Sema3F repulsion from posterior rhombomere 1 and an attractive signal from Fgf8 at the isthmic organiser (Irving *et al.*, 2002). In mouse, *Sema3F*, which is expressed in the posterior midbrain and anterior hindbrain, repels trochlear axons and mice lacking the Sema3F receptor, Neuropilin2, exhibit defects in the axon migration from the neuroepithelium (Chen *et al.*, 2000). Chick branchiomotor axons are repelled by ectopic floor plate cells, which indicates a role for floor plate derived repulsive cues in normal axonogenesis of these neurons (Guthrie and Pini, 1995).

The zebrafish *cyclops* mutant shows absence of ventral midline cells in the neural tube and leads to disruption of branchiomotor nuclei and axon pathway formation (Hatta *et al.*, 1991). The branchiomotor phenotype in *cyclops* embryos indicates that ventral midline cells of the neural tube, most likely floor plate cells, are important in specification of branchiomotor neurons and in preventing their axons from crossing the ventral midline. The facial (nVII) axons cross the ventral midline in *cyclops* embryos; this is consistent with a role for floor plate cells in their guidance (Chandrasekhar *et al.*1997; Colamarino and Tessier-Lavigne, 1995). Some cranial motor neurons fail to differentiate in the Hh pathway mutant *detour* (Chandrasekhar *et al.*, 1999). Disorganisation of axons near the floor plate, abnormal trajectories of commissural interneurons and cyclopia are likely to be the consequences of the observed midline defect in *cyclops* mutants (Hatta, 1992; Bernhardt *et al.*, 1992).

Axons of the medial longitudinal fasciculus (MLF) grow along lateral floor plate cells (Kuwada and Bernhardt, 1990; Hatta *et al.*, 1991). Since the nVII axons fasciculate with the MLF, the fusion of the MLF in *cyclops* embryos (Hatta, 1992) could be the cause of the midline crossing phenotype of nVII axons in mutant embryos.

Uncle freddy (*unf*^{368}) mutants display partial fusion of the MLFs at the midline (Schier *et al.*, 1996). In *monorail* embryos, axons of the medial longitudinal fasciculi are closer together or occasionally fused in the midline and the facial motor nucleus forms a single cluster of neurons at the midline rather than a bilateral pair of nuclei.

It was anticipated that identification of the gene underlying the *monorail* phenotype and investigation of its function would enhance our present knowledge of the role of the floor plate in D-V patterning and axon guidance across the midline.

7.1.2 The *monorail* gene encodes a truncated FoxA2 protein

The *monorail*^{tv53a} mutation was localised to linkage group (LG) 17 between flanking markers Z21703 and Z21194. Radiation hybrid mapping placed the genes *foxA1* and *foxA2* (Strähle *et al.*, 1997) in the same mapping interval region as *monorail.* These genes were therefore considered as candidates not only on the basis of their genetic map location but also because of their known expression in the floor plate of the developing embryo (Odenthal and Nüsslein-Volhard, 1998), which correlates with the *monorail* phenotype.

Screening of the entire coding sequence of the *foxA1* gene (1284 bp) was undertaken. Sequencing *foxA1* from pooled WT cDNA revealed differences in this sequence compared with the published sequence. The nucleotide changes observed between the original and revised *foxA1* sequence would result in a protein differing from the original over a contiguous stretch of over 100 amino acids. The nucleotide changes observed between the original and revised *foxA1* sequence are described in Chapter 4, Fig. 4.1A, B and C. The total changed amino acid sequence encompasses transactivating domain II completely (amino acids 273-383 with respect to the original reported position of transactivating domain II at amino acids 350-366). It is important to determine whether this FoxA protein does contain transactivating domain II or

whether it could be a variant without transactivating domain II. Further experimentation and analysis is needed before the revised sequence of *foxA1* can be confirmed.

DNA sequence analysis of the second candidate gene, *foxA2*, revealed a C to T transition at position 676 of the *foxA2* coding sequence in all *monorail* individuals tested in both the forward and reverse direction and changes a glutamine codon (CAA) to a stop codon (TAA). None of the ten wild-type individuals tested showed the mutation. The nine *monorail* siblings tested were either wild-type or heterozygotes. Hence it was concluded that *foxA2* is the *monorail* gene. This nonsense mutation results in a premature stop codon in the *fork head* DNA binding domain (84 % of this domain is lost). Hence transactivating domains II and III are completely absent and this creates a carboxy (COOH) terminally truncated FoxA2 protein. The COOH-terminal transcriptional activation domains of FoxA proteins contain functionally important region II and III sequences that are conserved in this family of transcription factors (Costa *et al.*, 2001).

Further approaches were undertaken to confirm the mutation. Firstly no recombination events were identified in 188 meioses with a marker in the *foxA2* gene. In addition, the amplification created restriction site method (Halliosis *et al.*, 1989), based on introduction of an artificial restriction site using a modified primer in the PCR reaction was used. This creates a RFLP for the presence of the mutation, which is detected by a radiolabeled oligonucleotide probe. One *monorail* homozygote, three *monorail* siblings, and one WT individual were analysed with the restriction enzyme *Hpy*CH4 V and the results further confirmed that *monorail* encodes a mutation in *foxA2*.

7.1.3 Zebrafish *fork head* domain genes and floor plate development

The vertebrate HNF-3/fork head box (Fox) gene family encodes transcription factors

originally identified as regulators of liver-specific gene expression (Lai *et al.*, 1991). Members of the fork head family play important roles in regulating cellular proliferation, differentiation and metabolic homeostasis (for review see Kaufmann and Knöchel, 1996). They have also been implicated in early embryonic patterning of the CNS ventral midline (Ruiz i Altaba *et al.*, 1993; Sasaki and Hogan, 1994; Odenthal and Nüsslein-Volhard, 1998).

The HNF-3 protein family consists of more than fifty mammalian proteins (Kaestner *et al.*, 2000) that are defined by a 110 amino acid residues region, which encompasses a DNA binding domain of winged helix structure. This region is common to a number of developmental regulatory proteins including the *Drosophila* homeotic protein fork head (Weigel *et al.*, 1989). The DNA binding domain is involved in specific DNA recognition, is widely conserved among species and has been described in organisms as diverse as yeast and human (Kaestner *et al.*, 1993; for review see Kaufmann and Knöchel, 1996). The FoxA1 (HNF-3α) and FoxA2 (HNF-3β) proteins share 93 % homology in the winged-helix motif and bind to similar target DNA sequences (Lai *et al.*, 1991).

The FoxA proteins also show homology in the NH_2- and COOH-terminal transcriptional activation domains (Pani *et al.*, 1992). Transcriptional activation domains are amino acid motifs that initiate transcription. They function at various positions with respect to the DNA binding domain within the protein and activate other transcription factors via their DNA binding domain. They also function by interaction with basal transcription factors either directly or through co-activator proteins (Pani *et al.*, 1992). The transcription factor HNF-6 has recently been shown to function as a coactivator protein to potentiate the transcriptional activity of FoxA2. At a FoxA-specific site, HNF-6 acts as a coactivator protein to enhance FoxA2-dependent

transcription, whereas at an HNF-6-specific site, FoxA2 represses HNF-6-dependent transcription by inhibiting HNF-6 DNA binding activity (Rausa *et al.*, 2003).

In zebrafish, nine members of the *fork head* (*fkd*) domain gene family (*fkd1* to *fkd9*) have been identified and grouped into three classes based on sequence similarities within the DNA binding and transcription activation domains; as well as similarities in expression patterns (Odenthal and Nüsslein-Volhard, 1998). The *foxA2* gene (also known as *fkd1*, *axial* and *hnf3β*) falls into Class I, which also includes zebrafish *foxA1* (also known as *fkd7*, *hnf3α*) and *foxA* (also known as *fkd4*, *pintallavis*). *foxA2* RNA is detected in the embryonic shield at the start of gastrulation and its expression continues in the axial mesendoderm, the prechordal plate, notochord and endoderm until somitogenesis. The Class I genes *foxA2*, *foxA* and *foxA1* are expressed in the floor plate of the ventral neural tube (Strähle *et al.*, 1993; Odenthal and Nüsslein-Volhard, 1998).

The zebrafish FoxA2 protein belongs to the fork head or HNF-3β family of winged-helix transcription factors (Strähle *et al.*, 1993), so called because they contain two flexible loops or 'wings' in the COOH-terminal region (Clark *et al.*, 1993). It shows high levels of sequence identity to its homologues in other species; 65 % to human, mouse and rat HNF-3β; 41 % to *Drosophila* fkh and 39 % to *C. elegans* fork head domain transcription factor (http://www.ncbi.nlm.nih.gov/UniGene). Zebrafish FoxA2 can activate the zebrafish *shh* gene promoter (Chang *et al.*, 1997). Rat HNF-3β can also activate this promoter; therefore as well as a structural similarity between these transcription factors, a functional homology also exists.

The mouse *Hnf-3β* gene is expressed in the node at the anterior end of the primitive streak in all three germ layers and then localised in the floor plate and ventral midline cells of the CNS (McMahon, 1994). The *Hnf-3β* mouse knockout phenotype shows absence of all node and midline structures, including the notochord, floor plate

and gut (Ang *et al.*, 1993; Kaestner *et al.*, 1994). Mouse embryos heterozygous for both *Hnf-3β* and the TGFβ-related gene *Nodal*, exhibit cyclopia and midline patterning defects (Varlet *et al.*, 1997). Like mouse *Hnf-3β*, *foxA2* is expressed in the fish organiser, the shield, but there is no gastrula phenotype in fish, most likely due to redundancy of function between Class I Fox transcription factors.

The expression of HNF-3β/FoxA2 is important for floor plate development as shown by misexpression of *foxA2* leading to ectopic activation of floor plate marker genes (Sasaki and Hogan, 1994; Ruiz i Altaba *et al.*, 1995). FoxA2 can also be induced by the Nodal signal Cyclops and its intracellular transducer Smad2, has been shown to up-regulate *foxA2* expression (Müller *et al.*, 2000). Exogenous FoxA2 can rescue floor plate gene expression in Nodal pathway mutants (Rastegar *et al.*, 2002).

Several studies have focussed on identification of gene enhancer elements necessary for floor plate expression. The findings include a Gli binding site in the enhancer of mouse *FoxA2*, which is essential for induction of *FoxA2* expression in the floor plate (Sasaki *et al.*, 1997). In addition, FoxA2 binding sites have been identified within the enhancers of mouse and zebrafish *shh* genes (Epstein *et al.*, 1999; Müller *et al.*, 2002). A *Shh* floor plate enhancer showing highly conserved binding sites to FoxA transcription factors has been isolated and mutational analysis has revealed that the FoxA binding site is required for activation of the *Shh* floor plate enhancer (Jeong and Epstein, 2003).

7.1.4 Distribution of *fox* genes in the zebrafish genome

Monorail/foxA2 maps to linkage group 17 of the zebrafish genome. Radiation hybrid mapping has localised two other *fox* genes, *foxA1* and *foxG1* to linkage group 17; whereas the other ten mapped *fox* genes to date are dispersed throughout the zebrafish genome (source: www.zfin.org/mapping panels). This clustering of *FOX* genes is also

seen in the human genome, *FOXF1*, *FOXL1* and *FOXC2* all map to chromosome 16q24.3 (Kaestner *et al.*, 1996), whereas the other *FOX* genes mapped to date are spread out throughout the genome. The zebrafish orthologues of the three *FOX* genes on human chromosome 16q24.3 have not yet been identified.

The zebrafish genome shares large regions of conserved synteny with mammalian genomes (Postlethwait *et al.*, 1998). There is strong conserved synteny between zebrafish linkage group 17 and human chromosomes 14 and 20 (Woods *et al.*, 2000). The three zebrafish *fox* genes, *foxA1*, *foxA2* and *foxG1* and their human orthologues, *FOXA1*, *FOXA2* and *FOXG1A* respectively map to a strongly conserved region. *FOXA1*, *FOXA2* and *FOXG1A* map to human chromosomes 14q12-q13, 20p11 and 14q13 respectively. The reason that the human orthologues of these zebrafish genes on linkage group 17 are distributed on human chromosomes 14 and 20 may be because human chromosomes 14 and 20 were ancient duplicates before the divergence of human and zebrafish lineages. Another explanation might be that the last common ancestor of zebrafish and human had a single chromosome that was a mixture of the present human chromosomes 14 and 20. This single chromosome might have become separated by translocation events in the human but not zebrafish lineage (Postlethwait *et al.*, 2000).

7.1.5 *FOX* genes and disease

Mutations in *FOX* genes have been shown to underlie specific human disorders. These include mutations in the *FOXC1* gene identified in families with congenital glaucoma phenotypes, including Axenfeld Reiger anomaly (Mears *et al.*, 1998); mutations in *FOXE1* lead to thyroid agenesis (Clifton-Bligh *et al.*, 1998) and those in *FOXP2* cause language disorder (Lai *et al.*, 2001) and have also been identified in individuals diagnosed with autism (Gauthier *et al.*, 2003).

The gross morphological defect in the zebrafish midline mutants including *monorail, schmalspur* and *uncle freddy* is a downward-curved body axis, or 'curly-tail'. *Schmalspur* and *uncle freddy* mutants are allelic and exhibit loss-of-function mutations in the fork head domain of the *foxH1/fast1* gene (Pogoda *et al.*, 2000; Sirotkin *et al.*, 2000). Several mouse mutants with abnormal neural tube development also have altered body shape. In *curly-tail* mouse embryos, closure of the neural folds is altered, leading to spina bifida or exencephaly (Copp *et al.*, 1990). Despite the great deal of phenotypic analysis on *curly tail* embryos, the gene product still remains unidentified. However candidates are in the process of being screened and it remains to be seen if the gene product turns out to be a transcription factor (for review see van Straaten and Copp, 2001; van Straaten, personal communication).

7.1.6 *Monorail* conclusions and future work

Analysis of gene expression patterns and antibody labelling in *monorail* mutants has revealed a role for FoxA2 in induction of lateral floor plate cells, maintenance of expression of regulatory genes expressed in the medial floor plate and differentiation of these cell types, formation of the serotonergic Raphe nucleus, induction of specific cranial motor nuclei and midline crossing of axons of the trochlear nucleus and segmental organisation of glial bundles in the hindbrain (Chapter 3 of this thesis and Dr William Norton, personal communication). A summary of the results from phenotypic analysis of the *monorail* mutant is shown in Table 3.1.

Future work should include injection of a mutated *foxA2* mRNA containing the C to T transition identified in *monorail* cDNA to determine whether the mutant protein retains any residual activity. Further investigation of FoxA2 protein expression in *monorail* is also required. The expression of the zebrafish FoxA2 protein was investigated using a polyclonal antipeptide antibody made to mouse HNF-3β (Santa

Cruz Biotechnology®). This antibody recognises the carboxy (COOH) terminus of the HNF-3β protein. The *monorail* mutation is predicted to lead to truncation of the protein product. Therefore it was anticipated that the normal HNF-3β 47 kDa positive band, as seen in the HepG2 (human hepatoblastoma whole cell lysate) positive control, would be absent on western blots probed with the antibody. However, the *monorail* protein extract gave an HNF-3β-positive band of the same size. This result is possibly due to other homologous members of the *fork head* genes having partially overlapping or redundant expression patterns and functions. Hence there may be cross hybridisation between HNF-3β and other members of this gene family.

An antibody binding to the NH_2-terminal of FoxA2 should be tested to detect a shorter product in *monorail* and prove truncation of the protein at the start of the fork head domain due to presence of the mutation. An explanation for the result obtained above is that the antibody tested was not raised against a peptide of zebrafish FoxA2 protein. Although HNF-3β and FoxA2 are similar (65 % identical in their sequence), structural differences do exist between species. Mouse *Hnf-3β* gives rise to multiple mRNAs due to variations within the transcription start site or to different splicing of primary transcripts (Lai *et al.*, 1993).

Future work should also include optimisation of the protein extraction and western blot experiments. Technical problems were encountered with the protein extraction technique; incomplete removal of the yolk sac from embryos resulted in retardation of actual protein sample migration on the SDS gel due to the presence of the yolk sac protein vitellogenin. In order to remove the yolk sac completely, dechorionated embryos should be anaesthetised in tricaine and pinned to Petri dishes coated with Sylgard silicone elastomer. Sharpened tungsten needles and fine forceps should be used to dissect the yolk sac.

7.2 *Shrink*, *otter* and *eisspalte*

The mutants *shrink* (Corinne Houart, personal communication); *otter* and *eisspalte* (Yiang *et al.*, 1996) commonly exhibit defects in pathfinding and fasciculation of axons in the forebrain as well as curvature of the body axis and a range of other developmental defects (Dr Jacqueline Hoyle, personal communication). There follows a discussion of each mutant in turn.

7.2.1 The *shrink* mutant

The *shrink* mutant is characterised by defasciculation of the post-optic commissure and extension of these axons rostrally from the chiasm towards the anterior commissure together with mis-projection of retinal ganglion cell axons. The phenotype also includes a significant increase in the number of apoptotic cells in the head region and relatively smaller size of the eyes and head and a thinner yolk tube extension compared to wild-type siblings as well as dorsal curvature of the body axis.

Other zebrafish mutants including *cyclops*, *no isthmus*, *acerebellar*, *astray*, *chameleon*, *detour*, *iguana*, *umleitung* and *you-too* (Brand *et al.*, 1996; for review see Culverwell and Karlstrom, 2002) also show a retinotectal pathfinding phenotype, as well as abnormal differentiation of midline structures due to defects in Hh signalling.

The midline secretes signalling molecules involved in retinal axon guidance. The chemorepellent signalling proteins Slit1 and Slit2 and their receptor Robo2 have been shown to control midline crossing of axons at the optic chiasm in zebrafish (for review see Hutson and Chien, 2002). Retinal ganglion cell axon pathfinding defects are observed in Netrin-1/DCC or EphB ligand deficient mouse embryos (Jin *et al.*, 2003). Mice deficient in both Slit1 and Slit2 show a significant number of axon guidance errors in major axonal pathways in the mammalian forebrain, including the corticofugal, callosal and thalamocortical tracts (Bagri *et al.*, 2002).

Investigation of the *no isthmus* (*noi*) mutant has revealed that gene expression domain boundaries correlate with sites of commissural growth. Defasciculation of the anterior and post-optic commissures in *noi* results from defects in expression of the Netrin family of guidance molecules and the signalling protein Shh in forebrain patterning (Macdonald *et al.* 1997).

The *shrink*^{U41} mutation was rough mapped to LG 6, 6 cM from SSLP marker Z6767 and 3 cM from Z12094. Fine mapping was carried out at UCL by genotyping single mutant and sibling embryos with further SSLP markers. Four recombinants were identified in 52 meioses with marker Z14826, however this marker requires further optimisation.

The gene *jak1 kinase* (Conway *et al.*, 1997) maps to the same interval as *shrink*, is involved in early brain development and is a possible candidate. Jak1 is a member of the tyrosine kinase family, ubiquitously expressed in adult mouse tissues and has been shown to transduce signals by phosphorylation of STAT (signal transducers and activators of transcription) proteins (Ihle, 1996). STAT proteins are located in the cytoplasm until they are tyrosine phosphorylated, which leads to dimerisation and nuclear translocation to bind targets and activate transcription. During early development, Jak1 kinase is exclusively maternally expressed. Overexpression studies have identified that this kinase plays a role in cell migration, *goosecoid* expression and formation of the anterior shield (Conway *et al.*, 1997).

The *shrink* phenotype is not restricted to a specific region of the embryo. Further detailed gene expression analysis needs to be performed before it is possible to define a particular pathway in which *shrink* might be involved. Further phenotypic characterisation of the *shrink* mutant should test whether *jak1 kinase* is able to rescue the *shrink* phenotype to show if *shrink* encodes Jak1 kinase. The onset of cell death and

defasciculation of the post-optic commissure also need to be determined by analysing embryos at a range of developmental stages from the start of axonogenesis. Cell autonomy experiments similar to those carried out on the *acerebellar* (*ace*) mutant would determine whether *shrink* is required in the eye or brain (Shanmugalingam *et al.*, 2000).

7.2.2 The *otter* mutant

The *otter* mutant was isolated in a screen for mutations affecting neurogenesis and brain morphology in the zebrafish (Jiang *et al.*, 1996). In the pharyngula period, the brain region is significantly reduced in size and the brain ventricles are collapsed. *Otter* mutants have a curled down head, show failure of midbrain-hindbrain boundary and cerebellum formation, have an enlarged heart cavity, ear and jaw formation defects, a reduced touch response, general retardation and cell death; they subsequently die in the early larval period (Jiang *et al.*, 1996; Dr Jacqueline Hoyle, personal communication). Zebrafish mutants with a defective cardiovascular system show a reduction or absence of cerebrospinal fluid pressure, which leads to an incomplete inflation of brain ventricles, failure of brain enlargement and subsequent degeneration (Schier *et al.*, 1996). Further screening of *otter* mutants with anti-acetylated alpha tubulin antibody revealed that the anterior and post-optic commissures form thicker bundles compared to their wild-type siblings, axons cross between the anterior and post-optic commissure and the optic nerve splits on exiting the eye.

Subsequent complementation studies have revealed that *otter* is allelic to *motionless*, a mutant isolated from a screen for mutations affecting development of catecholaminergic neurons in zebrafish (Guo *et al.*, 1999b). In *motionless* mutants, there is a reduction of hypothalamic dopaminergic (DA) neurons at 30 hpf and a reduction of telencephalic and diencephalic DA and locus coeruleus sympathetic

neurons at 48 hpf. In addition to a catecholaminergic neuron phenotype, *motionless* mutants also have defects similar to those of *otter* mutant embryos. These include a slightly cyclopic brain and failure of the brain ventricles to inflate properly. Blood circulation is also disrupted in *motionless* mutants and at 48 hpf, bradycardia is evident with accumulation of blood near the heart. *Motionless* mutants also show high levels of apoptosis in the lens and telencephalon at 52 hpf, do not respond to external stimuli and die at 4 days post fertilisation (Guo *et al.*, 1999b).

Future work including characterisation of *otter* by gene expression analysis is needed to reveal specific patterning defects and identify whether this is the primary cause of the ventricle collapse phenotype. Analysis of neuronal differentiation in *otter* mutants using the anti-HuC antibody and a more detailed investigation of axon tract development by screening mutants with anti-acetylated alpha tubulin antibody needs to be undertaken to reveal further defects in neurogenesis and axon pathfinding respectively.

The *otter*^{ta76b} mutation was rough mapped to LG 14 to a region between SSLP markers Z7043 and Z5435. Fifteen recombinants in 124 meioses were identified with marker Z7030 and 3 recombinants in 28 meioses with marker Z5435. The *motionless* mutation has also been mapped to LG 14 and is the subject of a positional cloning project (Su Guo, personal communication). There are several interesting candidate genes in this region that are currently being screened for mutations by the Guo lab. They include a kinesin molecule that is similar to KIF3A (kinesin-like protein3A) and a heat shock protein 110 (HSP110) family member that is homologous to APG-2 (ATP and peptide-binding protein in germ cells-2). These have been chosen as candidates due to the pleiotropic phenotype of *otter/motionless*. KIF3A is a member of the kinesin microtubule-associated motor protein family involved in anterograde transport. It is one

of the two motor subunits of kinesin-II that is essential for cilia formation. KIF3A is expressed in the inner segment and connecting cilium of fish photoreceptors (Whitehead *et al.*, 1999) as well as in the kidney, where its inactivation leads to polycystic kidney disease (Lin *et al.*, 2003). Knockout mice that completely lack KIF3A fail to synthesise cilia in the embryonic node and show randomisation of left-right asymmetry and structural abnormalities of the neural tube, pericardium, branchial arches and somites (Takeda *et al.*, 1999; Marszalek *et al.*, 2000). APG-2 is expressed at high levels in the testis and ovary and lower levels of expression have been detected in various other tissues including brain, heart, liver, lung, spleen and kidney (Kaneko *et al.*, 1997). Both KIF3A and APG-2 have been mapped to human chromosome 5 which shares high regions of conserved synteny with zebrafish LG 14, where *otter* and *motionless* have been mapped.

7.2.3 The *eisspalte* mutant

The *eisspalte* mutant was isolated in a screen for mutations affecting neurogenesis and brain morphology in the zebrafish (Jiang *et al.*, 1996). During the pharyngula stage of development, *eisspalte* embryos show a dent after the midbrain-hindbrain boundary and general retardation (Jiang *et al.*, 1996; Dr Jacqueline Hoyle, personal communication). The *eisspalte* mutant is identified by its curled down tail phenotype. Further screening of *eisspalte* mutants with anti-acetylated alpha tubulin antibody revealed that the anterior commissure is less fasciculated than normal and the optic nerve projects in different directions on exiting the eye.

The *eisspalte*^{ty77e} mutation was localised to LG 14 between SSLP markers Z1226 and Z1801. Seven recombinants in 84 meioses were identified with marker Z9057 and 18 recombinants in 72 meioses with marker Z1226. Fine mapping of this mutation is now underway (Dr Jacqueline Hoyle, personal communication). Likely

candidates will be genes with predicted roles in formation of the cytoskeleton, such as cell adhesion molecules, actin-related genes and those involved with the extracellular matrix and in cell movement processes. These molecules have been associated with a wide variety of processes including neuronal migration, survival, axonal growth and guidance.

Future phenotypic characterisation of *eisspalte* mutants should involve gene expression analysis to reveal specific defects in neuronal patterning and axon tract development. This should initially involve wholemount labelling of *eisspalte* embryos with antibodies to HuC to label neuronal cell bodies, zrf-1 to reveal patterning and glial cell organisation in the hindbrain and examination of retinotectal axon pathfinding by dil/diO eye injections and screening mutants with anti-acetylated alpha tubulin antibody.

7.3 Conclusions

The aim of this project was to characterise zebrafish mutants with defects in commissural axonal development and guidance and using a positional/candidate cloning approach, identify the affected genes. The results demonstrate commissural axon pathfinding defects in the mutants *monorail*^{tv53a}, *shrink*^{U41}, *otter*^{ta76b} and *eisspalte*^{ty77e} (Brand *et al.*, 1996; Jiang *et al.*, 1996; Corinne Houart, personal communication) in addition to abnormalities in neuronal patterning in the midbrain and hindbrain (*monorail*). The *monorail* mutation primarily affects patterning of neurons in the midbrain and hindbrain. The mutants *otter*^{ta76b} and *eisspalte*^{ty77e} and *shrink*^{U41} show more widespread abnormalities including defects in various aspects of brain development, circulation, body shape and swimming behaviour respectively.

FoxA2 is the HNF-3β homologue in human and mouse and has been shown to have important roles in early developmental processes in a variety of organisms. The

importance and function of FoxA2 in patterning of the ventral CNS in zebrafish has been possible through phenotypic characterisation of *monorail* embryos that show a mutation in the *foxA2* gene.

Hundreds of genes of unknown biochemical function essential for vertebrate development have yet to be identified. The work from this thesis has contributed to this task through identification of the *monorail* gene. The findings from *shrink*^{U41}, *otter*^{ta76b} and *eisspalte*^{ty77e} have provided a basis for further characterisation and genetic mapping in order to identify and/or validate candidates, decipher the affected gene and increase our knowledge of the processes and components involved in neuronal patterning and axon pathfinding in the central nervous system (CNS).

8. References

1. Agius,E., Oelgeschlager,M., Wessely,O., Kemp,C., and De Robertis,E.M. (2000). Endodermal Nodal-related signals and mesoderm induction in *Xenopus*. Development *127*, 1173-1183.

2. Albert,S., Müller,F., Fischer,N., Biellmann,D., Neumann,C., Blader,P., and Strähle,U. (2003). Cyclops-independent floor plate differentiation in zebrafish embryos. Dev. Dyn. *226*, 59-66.

3. Altaba,A. and Jessell,T.M. (1993). Midline cells and the organization of the vertebrate neuraxis. Curr. Opin. Genet. Dev. *3*, 633-640.

4. Altaba,A., Placzek,M., Baldassare,M., Dodd,J., and Jessell,T.M. (1995). Early stages of notochord and floor plate development in the chick embryo defined by normal and induced expression of HNF-3β. Dev. Biol. *170*, 299-313.

5. Amacher,S.L., Draper,B.W., Summers,B.R., and Kimmel,C.B. (2002). The zebrafish T-box genes *no tail* and *spadetail* are required for development of trunk and tail mesoderm and medial floor plate. Development *129*, 3311-3323.

6. Amemiya,C.T., Zhong,T.P., Silverman,G.A., Fishman,M.C., and Zon,L.I. (1999). Zebrafish YAC, BAC, and PAC genomic libraries. Methods Cell Biol. *60*, 235-258.

7. Amores,A., Force,A., Yan,Y.L., Joly,L., Amemiya,C., Fritz,A., Ho,R.K., Langeland,J., Prince,V., Wang,Y.L., Westerfield,M., Ekker,M., and Postlethwait,J.H. (1998). Zebrafish *hox* clusters and vertebrate genome evolution. Science *282*, 1711-1714.

8. Ando,H., Furuta,T., Tsien,R.Y., and Okamoto,H. (2001). Photo-mediated gene activation using caged RNA/DNA in zebrafish embryos. Nat. Genet. *28*, 317-325.

9. Ang,S.L., Wierda,A., Wong,D., Stevens,K.A., Cascio,S., Rossant,J., and Zaret,K.S. (1993). The formation and maintenance of the definitive endoderm lineage in the mouse: involvement of HNF3/fork head proteins. Development *119*, 1301-1315.

10. Bagri,A., Marin,O., Plump,A.S., Mak,J., Pleasure,S.J., Rubenstein,J.L., and Tessier-Lavigne,M. (2002). Slit proteins prevent midline crossing and determine the dorsoventral position of major axonal pathways in the mammalian forebrain. Neuron *33*, 233-248.

11. Baier,H. and Bonhoeffer,F. (1992). Axon guidance by gradients of a target-derived component. Science *255*, 472-475.

12. Baier,H., Klostermann,S., Trowe,T., Karlstrom,R.O., Nüsslein-Volhard,C., and Bonhoeffer,F. (1996). Genetic dissection of the retinotectal projection. Development *123*, 415-425.

13. Barresi,M.J., Stickney,H.L., and Devoto,S.H. (2000). The zebrafish *slow-muscle-omitted* gene product is required for Hedgehog signal transduction and the development of slow muscle identity. Development *127*, 2189-2199.

14. Barth,K.A. and Wilson,S.W. (1995). Expression of zebrafish nk2.2 is influenced by sonic hedgehog/vertebrate hedgehog-1 and demarcates a zone of neuronal differentiation in the embryonic forebrain. Development *121*, 1755-1768.

15. Bashaw,G.J. and Goodman,C.S. (1999). Chimeric axon guidance receptors: the cytoplasmic domains of slit and netrin receptors specify attraction versus repulsion. Cell *97*, 917-926.

16. Bashaw,G.J., Kidd,T., Murray,D., Pawson,T., and Goodman,C.S. (2000). Repulsive axon guidance: Abelson and Enabled play opposing roles downstream of the roundabout receptor. Cell *101*, 703-715.

17. Beattie,C.E., Melancon,E., and Eisen,J.S. (2000). Mutations in the stumpy gene reveal intermediate targets for zebrafish motor axons. Development *127*, 2653-2662.

18. Behar,O., Golden,J.A., Mashimo,H., Schoen,F.J., and Fishman,M.C. (1996). Semaphorin III is needed for normal patterning and growth of nerves, bones and heart. Nature *383*, 525-528.

19. Belloni,E., Muenke,M., Roessler,E., Traverso,G., Siegel-Bartelt,J., Frumkin,A., Mitchell,H.F., Donis-Keller,H., Helms,C., Hing,A.V., Heng,H.H., Koop,B., Martindale,D., Rommens,J.M., Tsui,L.C., and Scherer,S.W. (1996). Identification of *Sonic hedgehog* as a candidate gene responsible for holoprosencephaly. Nat. Genet. *14*, 353-356.

20. Bernhardt,R.R., Patel,C.K., Wilson,S.W., and Kuwada,J.Y. (1992). Axonal trajectories and distribution of GABAergic spinal neurons in wild-type and mutant zebrafish lacking floor plate cells. J. Comp Neurol. *326*, 263-272.

21. Bonkowsky,J.L. and Thomas,J.B. (1999). Cell-type specific modular regulation of *derailed* in the *Drosophila* nervous system. Mech. Dev. *82*, 181-184.

22. Brand,M., Heisenberg,C.P., Warga,R.M., Pelegri,F., Karlstrom,R.O., Beuchle,D., Picker,A., Jiang,Y.J., Furutani-Seiki,M., van Eeden,F.J., Granato,M., Haffter,P., Hammerschmidt,M., Kane,D.A., Kelsh,R.N., Mullins,M.C., Odenthal,J., and Nüsslein-Volhard,C. (1996). Mutations affecting development of the midline and general body shape during zebrafish embryogenesis. Development *123*, 129-142.

23. Briscoe,J., Chen,Y., Jessell,T.M., and Struhl,G. (2001). A hedgehog-insensitive form of patched provides evidence for direct long-range morphogen activity of *sonic hedgehog* in the neural tube. Mol. Cell *7*, 1279-1291.

24. Brose,K., Bland,K.S., Wang,K.H., Arnott,D., Henzel,W., Goodman,C.S., Tessier-Lavigne,M., and Kidd,T. (1999). Slit proteins bind Robo receptors and have an evolutionarily conserved role in repulsive axon guidance. Cell *96*, 795-806.

25. Brownlie,A., Donovan,A., Pratt,S.J., Paw,B.H., Oates,A.C., Brugnara,C., Witkowska,H.E., Sassa,S., and Zon,L.I. (1998). Positional cloning of the zebrafish *sauternes* gene: a model for congenital sideroblastic anaemia. Nat. Genet. *20*, 244-250.

26. Bruckner,K. and Klein,R. (1998). Signaling by Eph receptors and their Ephrin ligands. Curr. Opin. Neurobiol. *8*, 375-382.

27. Burrill,J.D. and Easter,S.S., Jr. (1994). Development of the retinofugal projections in the embryonic and larval zebrafish (Brachydanio rerio). J. Comp Neurol. *346*, 583-600.

28. Burrill,J.D. and Easter,S.S., Jr. (1995). The first retinal axons and their microenvironment in zebrafish: cryptic pioneers and the pretract. J. Neurosci. *15*, 2935-2947.

29. Butler,S.J. and Dodd,J. (2003). A role for BMP heterodimers in roof plate-mediated repulsion of commissural axons. Neuron *38*, 389-401.

30. Callahan,C.A., Muralidhar,M.G., Lundgren,S.E., Scully,A.L., and Thomas,J.B. (1995). Control of neuronal pathway selection by a *Drosophila* receptor protein-tyrosine kinase family member. Nature *376*, 171-174.

31. Caras,I.W. (1997). A link between axon guidance and axon fasciculation suggested by studies of the tyrosine kinase receptor EphA5/REK7 and its ligand ephrin-A5/AL-1. Cell Tissue Res. *290*, 261-264.

32. Castellani,V. and Rougon,G. (2002). Control of semaphorin signaling. Curr. Opin. Neurobiol. *12*, 532.

33. Cavarec,L., Jensen,S., Casella,J.F., Cristescu,S.A., and Heidmann,T. (1997). Molecular cloning and characterization of a transcription factor for the copia retrotransposon with homology to the BTB-containing lola neurogenic factor. Mol. Cell Biol. *17*, 482-494.

34. Chakrabarti,S., Streisinger,G.,Singer,F., and Walker,C. (1983). Frequency of gamma-ray induced specific locus and recessive lethal mutations in mature germ cells of the zebrafish, *Brachydanio rerio*. Genetics *103*, 109-124.

35. Challa,A.K., Beattie,C.E., and Seeger,M.A. (2001). Identification and characterization of roundabout orthologs in zebrafish. Mech. Dev. *101*, 249-253.

36. Chandrasekhar,A., Moens,C.B., Warren,J.T., Jr., Kimmel,C.B., and Kuwada,J.Y. (1997). Development of branchiomotor neurons in zebrafish. Development *124*, 2633-2644.

37. Chandrasekhar,A., Schauerte,H.E., Haffter,P., and Kuwada,J.Y. (1999). The zebrafish detour gene is essential for cranial but not spinal motor neuron induction. Development *126*, 2727-2737.

38. Chang,B.E., Blader,P., Fischer,N., Ingham,P.W., and Strähle,U. (1997). Axial (HNF-3β) and retinoic acid receptors are regulators of the zebrafish *sonic hedgehog* promoter. EMBO J. *16*, 3955-3964.

39. Charron,F., Stein,E., Jeong,J., McMahon,A.P., and Tessier-Lavigne,M. (2003). The Morphogen Sonic Hedgehog Is an Axonal Chemoattractant that Collaborates with Netrin-1 in Midline Axon Guidance. Cell *113*, 11-23.

40. Chen,H., Chedotal,A., He,Z., Goodman,C.S., and Tessier-Lavigne,M. (1997). Neuropilin-2, a novel member of the neuropilin family is a high affinity receptor for the semaphorins Sema E and Sema IV but not Sema III. Neuron *19*, 547-559.

41. Chen,H., Bagri,A., Zupicich,J.A., Zou,Y., Stoeckli,E., Pleasure,S.J., Lowenstein,D.H., Skarnes,W.C., Chedotal,A., and Tessier-Lavigne,M. (2000). Neuropilin-2 regulates the development of selective cranial and sensory nerves and hippocampal mossy fiber projections. Neuron *25*, 43-56.

42. Chen,W., Burgess,S., and Hopkins,N. (2001). Analysis of the zebrafish *smoothened* mutant reveals conserved and divergent functions of Hedgehog activity. Development *128*, 2385-2396.

43. Cheng,A.M., Thisse,B., Thisse,C., and Wright,C.V. (2000). The lefty-related factor Xatv acts as a feedback inhibitor of nodal signaling in mesoderm induction and L-R axis development in *Xenopus*. Development *127*, 1049-1061.

44. Chiang,C., Litingtung,Y., Lee,E., Young,K.E., Corden,J.L., Westphal,H., and Beachy,P.A. (1996). Cyclopia and defective axial patterning in mice lacking *sonic hedgehog* gene function. Nature *383*, 407-413.

45. Chisholm,A. and Tessier-Lavigne,M. (1999). Conservation and divergence of axon guidance mechanisms. Curr. Opin. Neurobiol. *9* , 603-615.

46. Chitnis,A.B. and Kuwada,J.Y. (1990). Axonogenesis in the brain of zebrafish embryos. J. Neurosci. *10*, 1892-1905.

47. Clark,K.L., Halay,E.D., Lai,E., and Burley,S.K. (1993). Co-crystal structure of the HNF-3/fork head DNA-recognition motif resembles histone H5. Nature *364*, 412-420.

48. Clifton-Bligh,R.J., Wentworth,J.M., Heinz,P., Crisp,M.S., John,R., Lazarus,J.H., Ludgate,M., and Chatterjee,V.K. (1998). Mutation of the gene encoding human TTF-2 associated with thyroid agenesis, cleft palate and choanal atresia. Nat. Genet. *19*, 399-401.

49. Cohen,N.R., Taylor,J.S., Scott,L.B., Guillery,R.W., Soriano,P., and Furley,A.J. (1998). Errors in corticospinal axon guidance in mice lacking the neural cell adhesion molecule L1. Curr. Biol. *8*, 26-33.

50. Colamarino,S.A. and Tessier-Lavigne,M. (1995). The role of the floor plate in axon guidance. Annu. Rev. Neurosci. *18*, 497-529.

51. Cole,L.K. and Ross,L.S. (2001). Apoptosis in the developing zebrafish embryo. Dev. Biol. *240*, 123-142.

52. Conway,G., Margoliath,A., Wong-Madden,S., Roberts,R.J., and Gilbert,W. (1997). Jak1 kinase is required for cell migrations and anterior specification in zebrafish embryos. Proc. Natl. Acad. Sci. U. S. A *94*, 3082-3087.

53. Copp,A.J., Brook,F.A., Estibeiro,J.P., Shum,A.S., and Cockroft,D.L. (1990). The embryonic development of mammalian neural tube defects. Prog. Neurobiol. *35*, 363-403.

54. Costa,R.H., Kalinichenko,V.V., and Lim,L. (2001). Transcription factors in mouse lung development and function. Am. J. Physiol Lung Cell Mol. Physiol *280*, L823-L838.

55. Crowner,D., Madden,K., Goeke,S., and Giniger,E. (2002). Lola regulates midline crossing of CNS axons in *Drosophila*. Development *129*, 1317-1325.

56. Culotti,J.G. and Kolodkin,A.L. (1996). Functions of netrins and semaphorins in axon guidance. Curr. Opin. Neurobiol. *6*, 81-88.

57. Culverwell,J. and Karlstrom,R.O. (2002). Making the connection: retinal axon guidance in the zebrafish. Semin. Cell Dev. Biol. *13*, 497-506.

58. Currie,P.D. and Ingham,P.W. (1996). Induction of a specific muscle cell type by a Hedgehog-like protein in zebrafish. Nature *382*, 452-455.

59. Daga,R.R., Thode,G., and Amores,A. (1996). Chromosome complement, C-banding, Ag-NOR and replication banding in the zebrafish, *Danio rerio*. Chromosome. Res. *4*, 29-32.

60. Davidson,B.P. and Tam,P.P. (2000). The node of the mouse embryo. Curr. Biol. *10*, R617-R619.

61. De Robertis,E.M., Larrain,J., Oelgeschlager,M., and Wessely,O. (2000). The establishment of Spemann's organizer and patterning of the vertebrate embryo. Nat. Rev. Genet. *1*, 171-181.

62. Dearborn,R., Jr., He,Q., Kunes,S., and Dai,Y. (2002). Eph receptor tyrosine kinase-mediated formation of a topographic map in the *Drosophila* visual system. J. Neurosci. *22*, 1338-1349.

63. Ding,J., Yang,L., Yan,Y.T., Chen,A., Desai,N., Wynshaw-Boris,A., and Shen,M.M. (1998). Cripto is required for correct orientation of the anterior-posterior axis in the mouse embryo. Nature *395*, 702-707.

64. Dooley,K. and Zon,L.I. (2000). Zebrafish: a model system for the study of human disease. Curr. Opin. Genet. Dev. *10*, 252-256.

65. Drescher,U. (1997). The Eph family in the patterning of neural development. Curr. Biol. *7*, R799-R807.

66. Drescher,U., Bonhoeffer,F., and Muller,B.K. (1997). The Eph family in retinal axon guidance. Curr. Opin. Neurobiol. *7*, 75-80.

67. Driever,W., Stemple,D., Schier,A., and Solnica-Krezel,L. (1994). Zebrafish: genetic tools for studying vertebrate development. Trends Genet. *10*, 152-159.

68. Driever,W., Solnica-Krezel,L., Schier,A.F., Neuhauss,S.C., Malicki,J., Stemple,D.L., Stainier,D.Y., Zwartkruis,F., Abdelilah,S., Rangini,Z., Belak,J.,

and Boggs,C. (1996). A genetic screen for mutations affecting embryogenesis in zebrafish. Development *123*, 37-46.

69. Dutton,K.A., Pauliny,A., Lopes,S.S., Elworthy,S., Carney,T.J., Rauch,J., Geisler,R., Haffter,P., and Kelsh,R.N. (2001). Zebrafish *colourless* encodes *sox10* and specifies non-ectomesenchymal neural crest fates. Development *128*, 4113-4125.

70. Ekker,S.C., Ungar,A.R., Greenstein,P., von Kessler,D.P., Porter,J.A., Moon,R.T., and Beachy,P.A. (1995). Patterning activities of vertebrate Hedgehog proteins in the developing eye and brain. Curr. Biol. *5*, 944-955.

71. Ekker,M., Ye,F., Joly,L., Tellis,P., and Chevrette,M. (1999). Zebrafish/mouse somatic cell hybrids for the characterization of the zebrafish genome. Methods Cell Biol. *60*, 303-321.

72. Epstein,D.J., McMahon,A.P., and Joyner,A.L. (1999). Regionalization of Sonic hedgehog transcription along the anteroposterior axis of the mouse central nervous system is regulated by Hnf3-dependent and -independent mechanisms. Development *126*, 281-292.

73. Etheridge,L.A., Wu,T., Liang,J.O., Ekker,S.C., and Halpern,M.E. (2001). Floor plate develops upon depletion of tiggy-winkle and sonic hedgehog. Genesis. *30*, 164-169.

74. Feldman,B., Gates,M.A., Egan,E.S., Dougan,S.T., Rennebeck,G., Sirotkin,H.I., Schier,A.F., and Talbot,W.S. (1998). Zebrafish organizer development and germ-layer formation require nodal-related signals. Nature *395*, 181-185.

75. Feldman,B., Dougan,S.T., Schier,A.F., and Talbot,W.S. (2000). Nodal-related signals establish mesendodermal fate and trunk neural identity in zebrafish. Curr. Biol. *10*, 531-534.

76. Flanagan,J.G. and Vanderhaeghen,P. (1998). The ephrins and Eph receptors in neural development. Annu. Rev. Neurosci. *21*, 309-345.

77. Forcet,C., Stein,E., Pays,L., Corset,V., Llambi,F., Tessier-Lavigne,M., and Mehlen,P. (2002). Netrin-1-mediated axon outgrowth requires deleted in colorectal cancer-dependent MAPK activation. Nature *417*, 443-447.

78. Fournier,A.E., Nakamura,F., Kawamoto,S., Goshima,Y., Kalb,R.G., and Strittmatter,S.M. (2000). Semaphorin3A enhances endocytosis at sites of receptor-F-actin colocalization during growth cone collapse. J. Cell Biol. *149*, 411-422.

79. Freeman,M.R., Delrow,J., Kim,J., Johnson,E., and Doe,C.Q. (2003). Unwrapping glial biology. Gcm target genes regulating glial development, diversification, and function. Neuron *38*, 567-580.

80. Fricke,C., Lee,J.S., Geiger-Rudolph,S., Bonhoeffer,F., and Chien,C.B. (2001). *Astray*, a zebrafish roundabout homolog required for retinal axon guidance. Science *292*, 507-510.

81. Furuyama,T., Inagaki,S., Kosugi,A., Noda,S., Saitoh,S., Ogata,M., Iwahashi,Y., Miyazaki,N., Hamaoka,T., and Tohyama,M. (1996). Identification of a novel transmembrane semaphorin expressed on lymphocytes. J. Biol. Chem. *271*, 33376-33381.

82. Gale,N.W. and Yancopoulos,G.D. (1997). Ephrins and their receptors: a repulsive topic? Cell Tissue Res. *290*, 227-241.

83. Gates,M.A., Kim,L., Egan,E.S., Cardozo,T., Sirotkin,H.I., Dougan,S.T., Lashkari,D., Abagyan,R., Schier,A.F., and Talbot,W.S. (1999). A genetic linkage map for zebrafish: comparative analysis and localization of genes and expressed sequences. Genome Res. *9*, 334-347.

84. Gauthier,J., Joober,R., Mottron,L., Laurent,S., Fuchs,M., De,K., V, and Rouleau,G.A. (2003). Mutation screening of FOXP2 in individuals diagnosed with autistic disorder. Am. J. Med. Genet. *118A*, 172-175.

85. Geisler,R., Rauch,G.J., Baier,H., van Bebber,F., Brobeta,L., Dekens,M.P., Finger,K., Fricke,C., Gates,M.A., Geiger,H., Geiger-Rudolph,S., Gilmour,D., Glaser,S., Gnugge,L., Habeck,H., Hingst,K., Holley,S., Keenan,J., Kirn,A., Knaut,H., Lashkari,D., Maderspacher,F., Martyn,U., Neuhauss,S., Haffter,P. (1999). A radiation hybrid map of the zebrafish genome. Nat. Genet. *23*, 86-89.

86. Georgiou,M. and Tear,G. (2002). Commissureless is required both in commissural neurons and midline cells for axon guidance across the midline. Development *129*, 2947-2956.

87. Gilmour,D.T., Maischein,H.M., and Nüsslein-Volhard,C. (2002). Migration and function of a glial subtype in the vertebrate peripheral nervous system. Neuron *34*, 577-588.

88. Giniger,E., Tietje,K., Jan,L.Y., and Jan,Y.N. (1994). Lola encodes a putative transcription factor required for axon growth and guidance in *Drosophila*. Development *120*, 1385-1398.

89. Giordano,S., Corso,S., Conrotto,P., Artigiani,S., Gilestro,G., Barberis,D., Tamagnone,L., and Comoglio,P.M. (2002). The semaphorin 4D receptor controls invasive growth by coupling with Met. Nat. Cell Biol. *4*, 720-724.

90. Godement,P., Vanselow,J., Thanos,S., and Bonhoeffer,F. (1987). A study in developing visual systems with a new method of staining neurons and their processes in fixed tissue. Development *101*, 697-713.

91. Goff,D.J., Galvin,K., Katz,H., Westerfield,M., Lander,E.S., and Tabin,C.J. (1992). Identification of polymorphic simple sequence repeats in the genome of the zebrafish. Genomics *14*, 200-202.

92. Golling,G., Amsterdam,A., Sun,Z., Antonelli,M., Maldonado,E., Chen,W., Burgess,S., Haldi,M., Artzt,K., Farrington,S., Lin,S.Y., Nissen,R.M., and Hopkins,N. (2002). Insertional mutagenesis in zebrafish rapidly identifies genes essential for early vertebrate development. Nat. Genet. *31*, 135-140.

93. Gritsman,K., Zhang,J., Cheng,S., Heckscher,E., Talbot,W.S., and Schier,A.F. (1999). The EGF-CFC protein one-eyed pinhead is essential for nodal signaling. Cell *97*, 121-132.

94. Grunwald,I.C., Korte,M., Wolfer,D., Wilkinson,G.A., Unsicker,K., Lipp,H.P., Bonhoeffer,T., and Klein,R. (2001). Kinase-independent requirement of EphB2 receptors in hippocampal synaptic plasticity. Neuron *32*, 1027-1040.

95. Grunwald,I.C. and Klein,R. (2002). Axon guidance: receptor complexes and signaling mechanisms. Curr. Opin. Neurobiol. *12*, 250-259.

96. Guo,S., Brush,J., Teraoka,H., Goddard,A., Wilson,S.W., Mullins,M.C., and Rosenthal,A. (1999a). Development of noradrenergic neurons in the zebrafish

hindbrain requires BMP, FGF8, and the homeodomain protein Soulless/Phox2a. Neuron *24*, 555-566.

97. Guo,S., Wilson,S.W., Cooke,S., Chitnis,A.B., Driever,W., and Rosenthal,A. (1999b). Mutations in the zebrafish unmask shared regulatory pathways controlling the development of catecholaminergic neurons. Dev. Biol. *208*, 473-487.

98. Guthrie,S. and Pini,A. (1995). Chemorepulsion of developing motor axons by the floor plate. Neuron *14*, 1117-1130.

99. Haffter,P. and Nüsslein-Volhard,C. (1996). Large scale genetics in a small vertebrate, the zebrafish. Int. J. Dev. Biol. *40*, 221-227.

100. Haffter,P., Granato,M., Brand,M., Mullins,M.C., Hammerschmidt,M., Kane,D.A., Odenthal,J., van Eeden,F.J., Jiang,Y.J., Heisenberg,C.P., Kelsh,R.N., Furutani-Seiki,M., Vogelsang,E., Beuchle,D., Schach,U., Fabian,C., and Nüsslein-Volhard,C. (1996). The identification of genes with unique and essential functions in the development of the zebrafish, *Danio rerio*. Development *123*, 1-36.

101. Haliassos,A, Chomel,JC, Grandjouan,S, Kruh,J, Kaplan,JC and Kitzis,A (1989). PCR technique: a new approach for a sensitive diagnosis of tumor-progression markers. Nucleic Acids Research *17* (20), 8093-8099.

102. Hall,A. (1998). Rho-GTPases and the actin cytoskeleton. Science *279*, 509-514.

103. Hall,K.T., Boumsell,L., Schultze,J.L., Boussiotis,V.A., Dorfman,D.M., Cardoso,A.A., Bensussan,A., Nadler,L.M., and Freeman,G.J. (1996). Human

CD100, a novel leukocyte semaphorin that promotes B-cell aggregation and differentiation. Proc. Natl. Acad. Sci. U. S. A *93*, 11780-11785.

104. Halloran,M.C., Severance,S.M., Yee,C.S., Gemza,D.L., and Kuwada,J.Y. (1998). Molecular cloning and expression of two novel zebrafish semaphorins. Mech. Dev. *76*, 165-168.

105. Halloran,M.C., Severance,S.M., Yee,C.S., Gemza,D.L., Raper,J.A., and Kuwada,J.Y. (1999). Analysis of a zebrafish semaphorin reveals potential functions *in vivo*. Dev. Dyn. *214*, 13-25.

106. Halpern,M.E., Thisse,C., Ho,R.K., Thisse,B., Riggleman,B., Trevarrow,B., Weinberg,E.S., Postlethwait,J.H., and Kimmel,C.B. (1995). Cell-autonomous shift from axial to paraxial mesodermal development in zebrafish *floating head* mutants. Development *121*, 4257-4264.

107. Hao,J.C., Yu,T.W., Fujisawa,K., Culotti,J.G., Gengyo-Ando,K., Mitani,S., Moulder,G., Barstead,R., Tessier-Lavigne,M., and Bargmann,C.I. (2001). *C. elegans* slit acts in midline, dorsal-ventral, and anterior-posterior guidance via the SAX-3/Robo receptor. Neuron *32*, 25-38.

108. Harris,R., Sabatelli,L.M., and Seeger,M.A. (1996). Guidance cues at the *Drosophila* CNS midline: identification and characterization of two *Drosophila* Netrin/UNC-6 homologs. Neuron *17*, 217-228.

109. Hatta,K., Kimmel,C.B., Ho,R.K., and Walker,C. (1991). The *cyclops* mutation blocks specification of the floor plate of the zebrafish central nervous system. Nature *350*, 339-341.

110. Hatta,K. (1992). Role of the floor plate in axonal patterning in the zebrafish CNS. Neuron *9*, 629-642.

111. Hedgecock,EM., Culotti,JG., Hall, DH. (1990). The *unc-5*, *unc-6* and *unc-40* genes guide circumferential migrations of pioneer axons and mesodermal cells on the epidermis in *C. elegans*. Neuron *4* (1), 61-85.

112. Henderson,J.T., Georgiou,J., Jia,Z., Robertson,J., Elowe,S., Roder,J.C., and Pawson,T. (2001). The receptor tyrosine kinase EphB2 regulates NMDA-dependent synaptic function. Neuron *32*, 1041-1056.

113. Henkemeyer,M., Orioli,D., Henderson,J.T., Saxton,T.M., Roder,J., Pawson,T., and Klein,R. (1996). Nuk controls pathfinding of commissural axons in the mammalian central nervous system. Cell *86*, 35-46.

114. Hidalgo,A. (2003). Neuron-glia interactions during axon guidance in *Drosophila*. Biochem. Soc. Trans. *31*, 50-55.

115. Higashijima,S., Nose,A., Eguchi,G., Hotta,Y., and Okamoto,H. (1997). Mindin/F-spondin family: novel ECM proteins expressed in the zebrafish embryonic axis. Dev. Biol. *192*, 211-227.

116. Higashijima,S., Hotta,Y., and Okamoto,H. (2000). Visualization of cranial motor neurons in live transgenic zebrafish expressing green fluorescent protein under the control of the *islet-1* promoter/enhancer. J. Neurosci. *20*, 206-218.

117. Hindges,R., McLaughlin,T., Genoud,N., Henkemeyer,M., and O'Leary,D.D. (2002). EphB forward signaling controls directional branch

extension and arborization required for dorsal-ventral retinotopic mapping. Neuron *35*, 475-487.

118. Hinegardner,R., and Rosen,D.E. (1972). Cellular DNA content and the evolution of teleostean fishes. Am. Nat. *166*, 621-644.

119. His,W. (1889). Die Formentwicklung des menschlichen Vorderhirns vom Ende des ersten bis zum Beginne des dritten Monates. Abhandl. D. Math. Phy. Kl. Kon Sachs. Akad. Wissench. Bd. *15*, 675-735.

120. Hjorth,J.T., Gad,J., Cooper,H., and Key,B. (2001). A zebrafish homologue of deleted in colorectal cancer (zdcc) is expressed in the first neuronal clusters of the developing brain. Mech. Dev. *109*, 105-109.

121. Holland,S.J., Gale,N.W., Mbamalu,G., Yancopoulos,G.D., Henkemeyer,M., and Pawson,T. (1996). Bidirectional signalling through the EPH-family receptor Nuk and its transmembrane ligands. Nature *383*, 722-725.

122. Hong,K., Hinck,L., Nishiyama,M., Poo,M.M., Tessier-Lavigne,M., and Stein,E. (1999). A ligand-gated association between cytoplasmic domains of UNC5 and DCC family receptors converts netrin-induced growth cone attraction to repulsion. Cell *97*, 927-941.

123. Hovens,C.M., Stacker,S.A., Andres,A.C., Harpur,A.G., Ziemiecki,A., and Wilks,A.F. (1992). RYK, a receptor tyrosine kinase-related molecule with unusual kinase domain motifs. Proc. Natl. Acad. Sci. U.S.A. *89*, 11818-11822.

124. Hu,H., Marton,T.F., and Goodman,C.S. (2001). Plexin B mediates axon guidance in *Drosophila* by simultaneously inhibiting active Rac and enhancing RhoA signaling. Neuron *32*, 39-51.

125. Hutson,L.D. and Chien,C.B. (2002). Wiring the zebrafish: axon guidance and synaptogenesis. Curr. Opin. Neurobiol. *12*, 87-92.

126. Ihle,J.N. (1996). STATs: signal transducers and activators of transcription. Cell *84*, 331-334.

127. Imondi,R. and Kaprielian,Z. (2001). Commissural axon pathfinding on the contralateral side of the floor plate: a role for B-class ephrins in specifying the dorsoventral position of longitudinally projecting commissural axons. Development *128*, 4859-4871.

128. Ingham,P.W. (1998). Transducing Hedgehog: the story so far. EMBO J. *17*, 3505-3511.

129. Irving,C. and Mason,I. (1999). Regeneration of isthmic tissue is the result of a specific and direct interaction between rhombomere 1 and midbrain. Development *126*, 3981-3989.

130. Irving,C., Malhas,A., Guthrie,S., and Mason,I. (2002). Establishing the trochlear motor axon trajectory: role of the isthmic organiser and Fgf8. Development *129*, 5389-5398.

131. Jeong,Y. and Epstein,D.J. (2003). Distinct regulators of Shh transcription in the floor plate and notochord indicate separate origins for these tissues in the mouse node. Development *130*, 3891-3902.

132. Jessell,T.M. (2000). Neuronal specification in the spinal cord: inductive signals and transcriptional codes. Nat. Rev. Genet. *1*, 20-29.

133. Jiang,Y.J., Brand,M., Heisenberg,C.P., Beuchle,D., Furutani-Seiki,M., Kelsh,R.N., Warga,R.M., Granato,M., Haffter,P., Hammerschmidt,M., Kane,D.A., Mullins,M.C., Odenthal,J., van Eeden,F.J., and Nüsslein-Volhard,C. (1996). Mutations affecting neurogenesis and brain morphology in the zebrafish, *Danio rerio*. Development *123*, 205-216.

134. Jin,Z. and Strittmatter,S.M. (1997). Rac1 mediates collapsin-1-induced growth cone collapse. J. Neurosci. *17*, 6256-6263.

135. Jin,Z., Zhang,J., Klar,A., Chedotal,A., Rao,Y., Cepko,C.L., and Bao,Z.Z. (2003). Irx4-mediated regulation of Slit1 expression contributes to the definition of early axonal paths inside the retina. Development *130*, 1037-1048.

136. Johnson,R.L., Laufer,E., Riddle,R.D., and Tabin,C. (1994). Ectopic expression of Sonic hedgehog alters dorsal-ventral patterning of somites. Cell *79*, 1165-1173.

137. Johnston,J.B. (1913). The morphology of the septum, hippocampus and pallial commissures in reptiles and mammals. J. Comp. Neurol. *23*, 371-478.

138. Kaestner,K.H., Lee,K.H., Schlondorff,J., Hiemisch,H., Monaghan,A.P., and Schutz,G. (1993). Six members of the mouse *Fork head* gene family are developmentally regulated. Proc. Natl. Acad. Sci. U. S. A *90*, 7628-7631.

139. Kaestner,K.H., Hiemisch,H., Luckow,B., and Schutz,G. (1994). The HNF-3 gene family of transcription factors in mice: gene structure, cDNA sequence, and mRNA distribution. Genomics *20*, 377-385.

140. Kaestner,K.H., Schutz,G., and Monaghan,A.P. (1996). Expression of the winged helix genes fkh-4 and fkh-5 defines domains in the central nervous system. Mech. Dev. *55*, 221-230.

141. Kaestner,K.H., Knochel,W., and Martinez,D.E. (2000). Unified nomenclature for the winged helix/forkhead transcription factors. Genes Dev. *14*, 142-146.

142. Kaneko,Y., Kimura,T., Kishishita,M., Noda,Y., and Fujita,J. (1997). Cloning of *apg-2* encoding a novel member of heat shock protein 110 family. Gene *189*, 19-24.

143. Kaprielian,Z., Runko,E., and Imondi,R. (2001). Axon guidance at the midline choice point. Dev. Dyn. *221*, 154-181.

144. Karlstrom,R.O., Trowe,T., Klostermann,S., Baier,H., Brand,M., Crawford,A.D., Grunewald,B., Haffter,P., Hoffmann,H., Meyer,S.U., Muller,B.K., Richter,S., van Eeden,F.J., Nüsslein-Volhard,C., and Bonhoeffer,F. (1996). Zebrafish mutations affecting retinotectal axon pathfinding. Development *123*, 427-438.

145. Karlstrom,R.O., Talbot,W.S., and Schier,A.F. (1999). Comparative synteny cloning of zebrafish *you-too*: mutations in the Hedgehog target *gli2* affect ventral forebrain patterning. Genes Dev. *13*, 388-393.

146. Karlstrom,R.O., Tyurina,O.V., Kawakami,A., Nishioka,N., Talbot,W.S., Sasaki,H., and Schier,A.F. (2003). Genetic analysis of zebrafish gli1 and gli2 reveals divergent requirements for gli genes in vertebrate development. Development *130*, 1549-1564.

147. Katz,M.J., Lasek,R.J., and Silver,J. (1983). Ontophyletics of the nervous system: development of the corpus callosum and evolution of axon tracts. Proc. Natl. Acad. Sci. U.S.A. *80*, 5936-5940.

148. Kaufmann,E. and Knochel,W. (1996). Five years on the wings of fork head. Mech. Dev. *57*, 3-20.

149. Keino-Masu,K., Masu,M., Hinck,L., Leonardo,E.D., Chan,S.S., Culotti,J.G., and Tessier-Lavigne,M. (1996). Deleted in Colorectal Cancer (DCC) encodes a netrin receptor. Cell *87*, 175-185.

150. Kelly,P.D., Chu,F., Woods,I.G., Ngo-Hazelett,P., Cardozo,T., Huang,H., Kimm,F., Liao,L., Yan,Y.L., Zhou,Y., Johnson,S.L., Abagyan,R., Schier,A.F., Postlethwait,J.H., and Talbot,W.S. (2000). Genetic linkage mapping of zebrafish genes and ESTs. Genome Res. *10*, 558-567.

151. Kennedy,T.E., Serafini,T., de,l.T., Jr., and Tessier-Lavigne,M. (1994). Netrins are diffusible chemotropic factors for commissural axons in the embryonic spinal cord. Cell *78*, 425-435.

152. Keynes,R. and Lumsden,A. (1990). Segmentation and the origin of regional diversity in the vertebrate central nervous system. Neuron *4*, 1-9.

153. Keynes,R., Tannahill,D., Morgenstern,D.A., Johnson,A.R., Cook,G.M., and Pini,A. (1997). Surround repulsion of spinal sensory axons in higher vertebrate embryos. Neuron *18*, 889-897.

154. Kidd,T., Russell,C., Goodman,C.S., and Tear,G. (1998). Dosage-sensitive and complementary functions of Roundabout and Commissureless control axon crossing of the CNS midline. Neuron *20*, 25-33.

155. Kidd,T., Bland,KS., Goodman,CS. (1999). Slit is the midline repellent for the Robo receptor in *Drosophila*. Cell *19* (Mar), 96 (6), 785-94.

156. Kimmel,C.B., Warga,R.M., and Schilling,T.F. (1990). Origin and organization of the zebrafish fate map. Development *108*, 581-594.

157. Kimmel,C.B., Ballard,W.W., Kimmel,S.R., Ullmann,B., and Schilling,T.F. (1995). Stages of embryonic development of the zebrafish. Dev. Dyn. *203*, 253-310.

158. Kiss,J.Z. and Muller,D. (2001). Contribution of the neural cell adhesion molecule to neuronal and synaptic plasticity. Rev. Neurosci. *12*, 297-310.

159. Kitsukawa,T., Shimizu,M., Sanbo,M., Hirata,T., Taniguchi,M., Bekku,Y., Yagi,T., and Fujisawa,H. (1997). Neuropilin-semaphorin III/D-mediated chemorepulsive signals play a crucial role in peripheral nerve projection in mice. Neuron *19*, 995-1005.

160. Klambt,C., Jacobs,JR, Goodman,CS. (1991). Midline crossing in the midline of the *Drosophila* central nervous system: a model for the genetic analysis of cell fate, cell migration, and growth cone guidance. Cell *22* (Feb), 64 (4), 801-815.

161. Knoll,B. and Drescher,U. (2002). Ephrin-As as receptors in topographic projections. Trends Neurosci. *25*, 145-149.

162. Kolodziej,P.A., Timpe,L.C., Mitchell,K.J., Fried,S.R., Goodman,C.S., Jan,L.Y., and Jan,Y.N. (1996). *Frazzled* encodes a *Drosophila* member of the DCC immunoglobulin subfamily and is required for CNS and motor axon guidance. Cell *87*, 197-204.

163. Korzh,V., Edlund,T., and Thor,S. (1993). Zebrafish primary neurons initiate expression of the LIM homeodomain protein Isl-1 at the end of gastrulation. Development *118*, 417-425.

164. Kramer,S.G., Kidd,T., Simpson,J.H., and Goodman,C.S. (2001). Switching repulsion to attraction: changing responses to slit during transition in mesoderm migration. Science *292*, 737-740.

165. Krauss,S., Concordet,J.P., and Ingham,P.W. (1993). A functionally conserved homolog of the *Drosophila* segment polarity gene *hh* is expressed in tissues with polarizing activity in zebrafish embryos. Cell *75*, 1431-1444.

166. Kuwada,J.Y. and Bernhardt,R.R. (1990). Axonal outgrowth by identified neurons in the spinal cord of zebrafish embryos. Exp. Neurol. *109*, 29-34.

167. Kwok,C., Korn,R.M., Davis,M.E., Burt,D.W., Critcher,R., McCarthy,L., Paw,B.H., Zon,L.I., Goodfellow,P.N., and Schmitt,K. (1998). Characterization of whole genome radiation hybrid mapping resources for non-mammalian vertebrates. Nucleic Acids Res. *26*, 3562-3566.

168. Lai,C.S., Fisher,S.E., Hurst,J.A., Vargha-Khadem,F., and Monaco,A.P. (2001). A fork head domain gene is mutated in a severe speech and language disorder. Nature *413*, 519-523.

169. Lai,E., Prezioso,V.R., Tao,W.F., Chen,W.S., and Darnell,J.E., Jr. (1991). Hepatocyte nuclear factor 3 alpha belongs to a gene family in mammals that is homologous to the *Drosophila* homeotic gene *fork head*. Genes Dev. *5*, 416-427.

170. Lai,E., Clark,K.L., Burley,S.K., and Darnell,J.E., Jr. (1993). Hepatocyte nuclear factor 3/fork head or "winged helix" proteins: a family of transcription factors of diverse biologic function. Proc. Natl. Acad. Sci. U. S. A *90*, 10421-10423.

171. Landmesser,L., Dahm,L., Tang,J.C., and Rutishauser,U. (1990). Polysialic acid as a regulator of intramuscular nerve branching during embryonic development. Neuron *4*, 655-667.

172. Langelaan,J. (1908). On the development of the large commissures of the telencephalon in the human brain. Brain *31*, 221-241.

173. Lauderdale,J.D., Davis,N.M., and Kuwada,J.Y. (1997). Axon tracts correlate with netrin-1a expression in the zebrafish embryo. Mol. Cell Neurosci. *9*, 293-313.

174. Lee,J.S., Ray,R., and Chien,C.B. (2001). Cloning and expression of three zebrafish *roundabout* homologs suggest roles in axon guidance and cell migration. Dev. Dyn. *221*, 216-230.

175. Lee,S., Kim,J.H., Lee,C.S., Kim,J.H., Kim,Y., Heo,K., Ihara,Y., Goshima,Y., Suh,P.G., and Ryu,S.H. (2002). Collapsin response mediator protein-2 inhibits neuronal phospholipase D2 activity by direct interaction. J. Biol. Chem. *277*, 6542-6549.

176. Lewis,K.E. and Eisen,J.S. (2001). Hedgehog signaling is required for primary motoneuron induction in zebrafish. Development *128*, 3485-3495.

177. Lin,F., Hiesberger,T., Cordes,K., Sinclair,A.M., Goldstein,L.S., Somlo,S., and Igarashi,P. (2003). Kidney-specific inactivation of the KIF3A

subunit of kinesin-II inhibits renal ciliogenesis and produces polycystic kidney disease. Proc. Natl. Acad. Sci. U. S. A *100*, 5286-5291.

178. Lumsden,A. and Krumlauf,R. (1996). Patterning the vertebrate neuraxis. Science *274*, 1109-1115.

179. Luo,Y., Shepherd,I., Li,J., Renzi,M.J., Chang,S., and Raper,J.A. (1995). A family of molecules related to collapsin in the embryonic chick nervous system. Neuron *14*, 1131-1140.

180. Macdonald,R., Xu,Q., Barth,K.A., Mikkola,I., Holder,N., Fjose,A., Krauss,S., and Wilson,S.W. (1994). Regulatory gene expression boundaries demarcate sites of neuronal differentiation in the embryonic zebrafish forebrain. Neuron *13*, 1039-1053.

181. Macdonald,R., Scholes,J., Strähle,U., Brennan,C., Holder,N., Brand,M., and Wilson,S.W. (1997). The Pax protein Noi is required for commissural axon pathway formation in the rostral forebrain. Development *124*, 2397-2408.

182. Madden,K., Crowner,D., and Giniger,E. (1999). Lola has the properties of a master regulator of axon-target interaction for SNb motor axons of *Drosophila*. Dev. Biol. *213*, 301-313.

183. Maestrini,E., Tamagnone,L., Longati,P., Cremona,O., Gulisano,M., Bione,S., Tamanini,F., Neel,B.G., Toniolo,D., and Comoglio,P.M. (1996). A family of transmembrane proteins with homology to the MET-hepatocyte growth factor receptor. Proc. Natl. Acad. Sci. U. S. A *93*, 674-678.

184. Mann,F., Ray,S., Harris,W., and Holt,C. (2002). Topographic mapping in dorsoventral axis of the *Xenopus* retinotectal system depends on signaling through ephrin-B ligands. Neuron *35*, 461-473.

185. Manser,E., Leung,T., Salihuddin,H., Zhao,Z.S., and Lim,L. (1994). A brain serine/threonine protein kinase activated by Cdc42 and Rac1. Nature *367*, 40-46.

186. Marcus,R.C. and Easter,S.S., Jr. (1995). Expression of glial fibrillary acidic protein and its relation to tract formation in embryonic zebrafish (Danio rerio). J. Comp Neurol. *359*, 365-381.

187. Marx,M., Rutishauser,U., and Bastmeyer,M. (2001). Dual function of polysialic acid during zebrafish central nervous system development. Development *128*, 4949-4958.

188. Marszalek,J.R., Liu,X., Roberts,E.A., Chui,D., Marth,J.D., Williams,D.S., and Goldstein,L.S. (2000). Genetic evidence for selective transport of opsin and arrestin by kinesin-II in mammalian photoreceptors. Cell *102*, 175-187.

189. McMahon,A.P. (1994). Mouse development. Winged-helix in axial patterning. Curr. Biol. *4*, 903-906.

190. Mears,A.J., Jordan,T., Mirzayans,F., Dubois,S., Kume,T., Parlee,M., Ritch,R., Koop,B., Kuo,W.L., Collins,C., Marshall,J., Gould,D.B., Pearce,W., Carlsson,P., Enerback,S., Morissette,J., Bhattacharya,S., Hogan,B., Raymond,V., and Walter,M.A. (1998). Mutations of the forkhead/winged-helix

gene, FKHL7, in patients with Axenfeld-Rieger anomaly. Am. J. Hum. Genet. *63* , 1316-1328.

191. Meiniel,A., Meiniel,R., Didier,R., Creveaux,I., Gobron,S., Monnerie,H., and Dastugue,B. (1996). The subcommissural organ and Reissner's fiber complex. An enigma in the central nervous system? Prog. Histochem. Cytochem. *30*, 1-66.

192. Mendelson,B. (1986). Development of reticulospinal neurons of the zebrafish. II. Early axonal outgrowth and cell body position. J. Comp Neurol. *251*, 172-184.

193. Methot,N. and Basler,K. (2001). An absolute requirement for Cubitus interruptus in Hedgehog signaling. Development *128*, 733-742.

194. Meyer,A. and Malaga-Trillo,E. (1999). Vertebrate genomics: More fishy tales about *Hox* genes. Curr. Biol. *9*, R210-R213.

195. Miao,H., Wei,B.R., Peehl,D.M., Li,Q., Alexandrou,T., Schelling,J.R., Rhim,J.S., Sedor,J.R., Burnett,E., and Wang,B. (2001). Activation of EphA receptor tyrosine kinase inhibits the Ras/MAPK pathway. Nat. Cell Biol. *3*, 527-530.

196. Mihalkovics,V. (1877). Entwicklungsgeschichte des Gehirns: Nach Untesuchungen an hoheren Wurbeltieren und den Menschen. Leipzig: W Engelmann.

197. Mitchell,K.J., Doyle,J.L., Serafini,T., Kennedy,T.E., Tessier-Lavigne,M., Goodman,C.S., and Dickson,B.J. (1996). Genetic analysis of *netrin*

genes in *Drosophila*: Netrins guide CNS commissural axons and peripheral motor axons. Neuron *17*, 203-215.

198. Monnier,P.P., Beck,S.G., Bolz,J., and Henke-Fahle,S. (2001). The polysialic acid moiety of the neural cell adhesion molecule is involved in intraretinal guidance of retinal ganglion cell axons. Dev. Biol. *229*, 1-14.

199. Monnier,P.P., Sierra,A., Macchi,P., Deitinghoff,L., Andersen,J.S., Mann,M., Flad,M., Hornberger,M.R., Stahl,B., Bonhoeffer,F., and Mueller,B.K. (2002). RGM is a repulsive guidance molecule for retinal axons. Nature *419*, 392-395.

200. Müller,F., Albert,S., Blader,P., Fischer,N., Hallonet,M., and Strähle,U. (2000). Direct action of the nodal-related signal Cyclops in induction of *sonic hedgehog* in the ventral midline of the CNS. Development *127*, 3889-3897.

201. Müller,F., Blader,P., and Strähle,U. (2002). Search for enhancers: teleost models in comparative genomic and transgenic analysis of cis regulatory elements. Bioessays *24*, 564-572.

202. Mullins,M.C., Hammerschmidt,M., Haffter,P., and Nüsslein-Volhard,C. (1994). Large-scale mutagenesis in the zebrafish: In search of genes controlling development in a vertebrate. Curr. Biol. *4* , 189-202.

203. Myat,A., Henry,P., McCabe,V., Flintoft,L., Rotin,D., and Tear,G. (2002). *Drosophila* Nedd4, a ubiquitin ligase, is recruited by Commissureless to control cell surface levels of the Roundabout receptor. Neuron *35*, 447-459.

204. Nakano,M., Yamada,K., Fain,J., Sener,E.C., Selleck,C.J., Awad,A.H., Zwaan,J., Mullaney,P.B., Bosley,T.M., and Engle,E.C. (2001). Homozygous

mutations in *arix/phox2A* result in congenital fibrosis of the extraocular muscles type 2. Nat. Genet. *29*, 315-320.

205. Naruse,K., Fukamachi,S., Mitani,H., Kondo,M., Matsuoka,T., Kondo,S., Hanamura,N., Morita,Y., Hasegawa,K., Nishigaki,R., Shimada,A., Wada,H., Kusakabe,T., Suzuki,N., Kinoshita,M., Kanamori,A., Terado,T., Kimura,H., Nonaka,M., and Shima,A. (2000). A detailed linkage map of Medaka, *Oryzias latipes*: comparative genomics and genome evolution. Genetics *154*, 1773-1784.

206. Nasevicius,A. and Ekker,S.C. (2000). Effective targeted gene 'knockdown' in zebrafish. Nat. Genet. *26*, 216-220.

207. Neuhauss,S.C., Biehlmaier,O., Seeliger,M.W., Das,T., Kohler,K., Harris,W.A., and Baier,H. (1999). Genetic disorders of vision revealed by a behavioral screen of 400 essential loci in zebrafish. J. Neurosci. *19*, 8603-8615.

208. Niclou,S.P., Jia,L., and Raper,J.A. (2000). Slit2 is a repellent for retinal ganglion cell axons. J. Neurosci. *20*, 4962-4974.

209. O'Brien,S.J., Eisenberg,M., Miyamoto,M., Hedges,S., Kumar,D.E., Wilson,D.E., Menotti Raymond,M., Murphy,W.J., Nash,W.G. (1999). Genome maps 10. Comparative genomics. Mammalian radiations. Wall chart. *Science* 286, 463-478.

210. Oates,A.C., Bonkovsky,J.L., Irvine,D.V., Kelly,L.E., Thomas,J.B., and Wilks,A.F. (1998). Embryonic expression and activity of *doughnut*, a second RYK homolog in *Drosophila*. Mech. Dev. *78*, 165-169.

211. Odenthal,J. and Nüsslein-Volhard,C. (1998). *Fork head* domain genes in zebrafish. Dev. Genes Evol. *208*, 245-258.

212. Odenthal,J., van Eeden,F.J., Haffter,P., Ingham,P.W., and Nüsslein-Volhard,C. (2000). Two distinct cell populations in the floor plate of the zebrafish are induced by different pathways. Dev. Biol. *219*, 350-363.

213. Ono,K., Tomasiewicz,H., Magnuson,T., and Rutishauser,U. (1994). N-CAM mutation inhibits tangential neuronal migration and is phenocopied by enzymatic removal of polysialic acid. Neuron *13*, 595-609.

214. Oppenheimer,J.M. (1936). Transplantation experiments on developing teleosts (Fundulus and Perca). J. Exp. Zool. *72*, 409-437.

215. Orioli,D., Henkemeyer,M., Lemke,G., Klein,R., and Pawson,T. (1996). Sek4 and Nuk receptors cooperate in guidance of commissural axons and in palate formation. EMBO J. *15*, 6035-6049.

216. Osterfield,M., Kirschner,M.W., and Flanagan,J.G. (2003). Graded positional information. Interpretation for both fate and guidance. Cell *113*, 425-428.

217. Pani,L., Overdier,D.G., Porcella,A., Qian,X., Lai,E., and Costa,R.H. (1992). Hepatocyte nuclear factor 3 beta contains two transcriptional activation domains, one of which is novel and conserved with the *Drosophila* fork head protein. Mol. Cell Biol. *12*, 3723-3732.

218. Papan,C., Campos-Ortega,J.A. (1994). On the formation of the neural keel and neural tube in zebrafish. Roux's Arch. Dev. Biol. *203*, 178-186.

219. Penberthy,W.T., Shafizadeh,E., and Lin,S. (2002). The zebrafish as a model for human disease. Front Biosci. *7*, d1439-d1453.

220. Persson,M., Stamataki,D., te,W.P., Andersson,E., Bose,J., Ruther,U., Ericson,J., and Briscoe,J. (2002). Dorsal-ventral patterning of the spinal cord requires Gli3 transcriptional repressor activity. Genes Dev. *16*, 2865-2878.

221. Piperno,G. and Fuller,M.T. (1985). Monoclonal antibodies specific for an acetylated form of alpha-tubulin recognize the antigen in cilia and flagella from a variety of organisms. J. Cell Biol. *101*, 2085-2094.

222. Pittman,A. and Chien,C.B. (2002). Understanding dorsoventral topography: backwards and forwards. Neuron *35*, 409-411.

223. Pogoda,H.M., Solnica-Krezel,L., Driever,W., and Meyer,D. (2000). The zebrafish fork head transcription factor FoxH1/Fast1 is a modulator of nodal signaling required for organizer formation. Curr. Biol. *10*, 1041-1049.

224. Postlethwait,J.H., Johnson,S.L., Midson,C.N., Talbot,W.S., Gates,M., Ballinger,E.W., Africa,D., Andrews,R., Carl,T., Eisen,J.S. (1994). A genetic linkage map for the zebrafish. Science *264*, 699-703.

225. Postlethwait,J.H. and Talbot,W.S. (1997). Zebrafish genomics: from mutants to genes. Trends Genet. *13*, 183-190.

226. Postlethwait,J.H., Yan,Y.L., Gates,M.A., Horne,S., Amores,A., Brownlie,A., Donovan,A., Egan,E.S., Force,A., Gong,Z., Goutel,C., Fritz,A., Kelsh,R., Knapik,E., Liao,E., Paw,B., Ransom,D., Singer,A., Thomson,M., Abduljabbar,T.S., Yelick,P., Beier,D., Joly,J.S., Larhammar,D., Rosa,F., and . (1998). Vertebrate genome evolution and the zebrafish gene map. Nat. Genet. *18*, 345-349.

227. Postlethwait,J.H., Yan,Y.L., and Gates,M.A. (1999). Using random amplified polymorphic DNAs in zebrafish genomic analysis. Methods Cell Biol. *60*, 165-179.

228. Postlethwait,J.H., Woods,I.G., Ngo-Hazelett,P., Yan,Y.L., Kelly,P.D., Chu,F., Huang,H., Hill-Force,A., and Talbot,W.S. (2000). Zebrafish comparative genomics and the origins of vertebrate chromosomes. Genome Res. *10*, 1890-1902.

229. Puschel,A.W., Adams,R.H., and Betz,H. (1995). Murine semaphorin D/collapsin is a member of a diverse gene family and creates domains inhibitory for axonal extension. Neuron *14*, 941-948.

230. Rajagopalan,S., Vivancos, V., Nicolas,E., Dickson, BJ. (2000). Selecting a longitudinal pathway: Robo receptors specify the lateral position of axons in the *Drosophila* CNS. Cell *22*, 103 (7), 1033-45.

231. Ramón y Cajal. (1892). La retine des vertebres. La Cellule. *9*, 119-258.

232. Rastegar,S., Albert,S., Le,R., I, Fischer,N., Blader,P., Müller,F., and Strähle,U. (2002). A floor plate enhancer of the zebrafish netrin1 gene requires Cyclops (Nodal) signalling and the winged helix transcription factor FoxA2. Dev. Biol. *252*, 1-14.

233. Rauch, G-J., Granato, M. and Haffter (1997). A polymorphic line for genetic mapping using SSLPs on high percentage agarose gels. Technical Tips Online TO1208.

234. Rausa,F.M., Tan,Y., and Costa,R.H. (2003). Association between hepatocyte nuclear factor 6 (HNF-6) and FoxA2 DNA binding domains

stimulates FoxA2 transcriptional activity but inhibits HNF-6 DNA binding. Mol. Cell Biol. *23*, 437-449.

235. Rebagliati,M.R., Toyama,R., Haffter,P., and Dawid,I.B. (1998). *Cyclops* encodes a nodal-related factor involved in midline signaling. Proc. Natl. Acad. Sci. U.S.A. *95*, 9932-9937.

236. Reinhard,M., Jarchau,T., and Walter,U. (2001). Actin-based motility: stop and go with Ena/VASP proteins. Trends Biochem. Sci. *26*, 243-249.

237. Reissner,E (1860). Beitrage zur Kenntnis vom Bau des Ruckenmarks von *Petromyzon fluviatilis L.Arch.Anat. Physiol. 77,* 545-588.

238. Rhinn,M. and Brand,M. (2001). The midbrain-hindbrain boundary organizer. Curr. Opin. Neurobiol. *11*, 34-42.

239. Ringstedt,T., Braisted,J.E., Brose,K., Kidd,T., Goodman,C., Tessier-Lavigne,M., and O'Leary,D.D. (2000). Slit inhibition of retinal axon growth and its role in retinal axon pathfinding and innervation patterns in the diencephalon. J. Neurosci. *20*, 4983-4991.

240. Rolf,B., Bastmeyer,M., Schachner,M., and Bartsch,U. (2002). Pathfinding errors of corticospinal axons in neural cell adhesion molecule-deficient mice. J. Neurosci. *22*, 8357-8362.

241. Rosenzweig,M. and Garrity,P. (2002). Axon targeting meets protein trafficking: Comm takes Robo to the cleaners. Dev. Cell *3*, 301-302.

242. Ross,L.S., Parrett,T., and Easter,S.S., Jr. (1992). Axonogenesis and morphogenesis in the embryonic zebrafish brain. J. Neurosci. *12*, 467-482.

243. Rutishauser,U. (1989). Neural cell-to-cell adhesion and recognition. Curr. Opin. Cell Biol. *1*, 898-904.

244. Rutishauser,U. and Landmesser,L. (1996). Polysialic acid in the vertebrate nervous system: a promoter of plasticity in cell-cell interactions. Trends Neurosci. *19*, 422-427.

245. Sampath,K., Rubinstein,A.L., Cheng,A.M., Liang,J.O., Fekany,K., Solnica-Krezel,L., Korzh,V., Halpern,M.E., and Wright,C.V. (1998). Induction of the zebrafish ventral brain and floorplate requires Cyclops/Nodal signalling. Nature *395*, 185-189.

246. Sasaki,H. and Hogan,B.L. (1994). HNF-3β as a regulator of floor plate development. Cell *76*, 103-115.

247. Sasaki,H., Hui,C., Nakafuku,M., and Kondoh,H. (1997). A binding site for Gli proteins is essential for HNF-3β floor plate enhancer activity in transgenics and can respond to Shh *in vitro*. Development *124*, 1313-1322.

248. Saude,L., Woolley,K., Martin,P., Driever,W., and Stemple,D.L. (2000). Axis-inducing activities and cell fates of the zebrafish organizer. Development *127*, 3407-3417.

249. Savant-Bhonsale,S., Friese,M., McCoon,P., and Montell,D.J. (1999). A *Drosophila* Derailed homolog, *doughnut*, expressed in invaginating cells during embryogenesis. Gene *231*, 155-161.

250. Schauerte,H.E., van Eeden,F.J., Fricke,C., Odenthal,J., Strähle,U., and Haffter,P. (1998). Sonic hedgehog is not required for the induction of medial floor plate cells in the zebrafish. Development *125*, 2983-2993.

251. Schier,A.F., Neuhauss,S.C., Harvey,M., Malicki,J., Solnica-Krezel,L., Stainier,D.Y., Zwartkruis,F., Abdelilah,S., Stemple,D.L., Rangini,Z., Yang,H., and Driever,W. (1996). Mutations affecting the development of the embryonic zebrafish brain. Development *123*, 165-178.

252. Schier,A.F., Neuhauss,S.C., Helde,K.A., Talbot,W.S., and Driever,W. (1997). The *one-eyed pinhead* gene functions in mesoderm and endoderm formation in zebrafish and interacts with *no tail*. Development *124*, 327-342.

253. Schier,A.F. and Shen,M.M. (2000). Nodal signalling in vertebrate development. Nature *403*, 385-389.

254. Schier,A.F. (2001). Axis formation and patterning in zebrafish. Curr. Opin. Genet. Dev. *11*, 393-404.

255. Schmid,B., Furthauer,M., Connors,S.A., Trout,J., Thisse,B., Thisse,C., and Mullins,M.C. (2000). Equivalent genetic roles for *bmp7/snailhouse* and *bmp2b/swirl* in dorsoventral pattern formation. Development *127*, 957-967.

256. Schulte-Merker,S., van Eeden,F.J., Halpern,M.E., Kimmel,C.B., and Nüsslein-Volhard,C. (1994). *no tail* (*ntl*) is the zebrafish homologue of the mouse *T* (*Brachyury*) gene. Development *120*, 1009-1015.

257. Seeger,M., Tear,G., Ferres-Marco,D., Goodman,CS. (1993). Mutations affecting growth cone guidance in *Drosophila*: genes necessary for guidance toward or away from the midline. Neuron *10* (3), 409-26.

258. Seeger,M.A. and Beattie,C.E. (1999). Attraction versus repulsion: modular receptors make the difference in axon guidance. Cell *97*, 821-824.

259. Sekido,Y., Bader,S., Latif,F., Chen,J.Y., Duh,F.M., Wei,M.H., Albanesi,J.P., Lee,C.C., Lerman,M.I., and Minna,J.D. (1996). Human semaphorins A(V) and IV reside in the 3p21.3 small cell lung cancer deletion region and demonstrate distinct expression patterns. Proc. Natl. Acad. Sci. U.S.A. *93*, 4120-4125.

260. Serafini,T., Kennedy,T.E., Galko,M.J., Mirzayan,C., Jessell,T.M., and Tessier-Lavigne,M. (1994). The netrins define a family of axon outgrowth-promoting proteins homologous to *C. elegans* UNC-6. Cell *78*, 409-424.

261. Serafini,T., Colamarino,S.A., Leonardo,E.D., Wang,H., Beddington,R., Skarnes,W.C., and Tessier-Lavigne,M. (1996). Netrin-1 is required for commissural axon guidance in the developing vertebrate nervous system. Cell *87*, 1001-1014.

262. Shamah,S.M., Lin,M.Z., Goldberg,J.L., Estrach,S., Sahin,M., Hu,L., Bazalakova,M., Neve,R.L., Corfas,G., Debant,A., and Greenberg,M.E. (2001). EphA receptors regulate growth cone dynamics through the novel guanine nucleotide exchange factor Ephexin. Cell *105*, 233-244.

263. Shanmugalingam,S., Houart,C., Picker,A., Reifers,F., Macdonald,R., Barth,A., Griffin,K., Brand,M., and Wilson,S.W. (2000). *Ace/Fgf8* is required for forebrain commissure formation and patterning of the telencephalon. Development *127*, 2549-2561.

264. Shen,H., Illges,H., Reuter,A., and Stuermer,C. (2002). Cloning, expression, and alternative splicing of Neogenin1 in zebrafish. Mech. Dev. *118*, 219.

265. Shih,J. and Fraser,S.E. (1996). Characterizing the zebrafish organizer: microsurgical analysis at the early-shield stage. Development *122*, 1313-1322.

266. Shimoda,N., Knapik,E.W., Ziniti,J., Sim,C., Yamada,E., Kaplan,S., Jackson,D., de Sauvage,F., Jacob,H., and Fishman,M.C. (1999). Zebrafish genetic map with 2000 microsatellite markers. Genomics *58*, 219-232.

267. Shirasaki,R., Katsumata,R., and Murakami,F. (1998). Change in chemoattractant responsiveness of developing axons at an intermediate target. Science *279*, 105-107.

268. Shoji,W., Yee,C.S., and Kuwada,J.Y. (1998). Zebrafish semaphorin Z1a collapses specific growth cones and alters their pathway *in vivo*. Development *125*, 1275-1283.

269. Silver,J. (1993). Glia-neuron interactions at the midline of the developing mammalian brain and spinal cord. Perspect. Dev. Neurobiol. *1*, 227-236.

270. Simpson,J.H., Kidd,T., Bland,K.S., and Goodman,C.S. (2000). Short-range and long-range guidance by Slit and its Robo receptors. Robo and Robo2 play distinct roles in midline guidance. Neuron *28*, 753-766.

271. Sirotkin,H.I., Gates,M.A., Kelly,P.D., Schier,A.F., and Talbot,W.S. (2000). Fast1 is required for the development of dorsal axial structures in zebrafish. Curr. Biol. *10*, 1051-1054.

272. Solnica-Krezel,L., Schier,A.F., and Driever,W. (1994). Efficient recovery of ENU-induced mutations from the zebrafish germline. Genetics *136*, 1401-1420.

273. Spemann,H., and Mangold,H. (1924). Über die Induktion von Embryonalanlagen durch Implantation artfreuder Organisatoren. Wilhelm Roux Arch. Entw. Mech. Org. *100*, 599-638.

274. Sperry,RW. (1963). Chemoaffinity in the orderly growth of nerve fiber patterns and connections. Proc. Natl. Acad. Sci. U.S.A. *50*, 703-710.

275. Stein,E. and Tessier-Lavigne,M. (2001). Hierarchical organization of guidance receptors: silencing of Netrin attraction by Slit through a Robo/DCC receptor complex. Science *291*, 1928-1938.

276. Stickney,H.L., Schmutz,J., Woods,I.G., Holtzer,C.C., Dickson,M.C., Kelly,P.D., Myers,R.M., and Talbot,W.S. (2002). Rapid Mapping of Zebrafish Mutations With SNPs and Oligonucleotide Microarrays. Genome Res. *12*, 1929-1934.

277. Stoeckli,E.T., Sonderegger,P., Pollerberg,GE., Landmesser,LT. (1997). Interference with axonin-1 and NrCAM interactions unmasks a floor plate activity inhibitory for commissural axons. Neuron *18* (2), 209-221.

278. Stoeckli,E.T. and Landmesser,L.T. (1998). Axon guidance at choice points. Curr. Opin. Neurobiol. *8*, 73-79.

279. Storey,K.G., Crossley,J.M., De Robertis,E.M., Norris,W.E., and Stern,C.D. (1992). Neural induction and regionalisation in the chick embryo. Development *114*, 729-741.

280. Strähle,U., Blader,P., Henrique,D., and Ingham,P.W. (1993). *Axial*, a zebrafish gene expressed along the developing body axis, shows altered expression in cyclops mutant embryos. Genes Dev. *7*, 1436-1446.

281. Strähle,U., Fischer,N., and Blader,P. (1997). Expression and regulation of a Netrin homologue in the zebrafish embryo. Mech. Dev. *62*, 147-160.

282. Streisinger,G., Walker,C., Dower,N., Knauber,D., and Singer,F. (1981). Production of clones of homozygous diploid zebrafish (*Brachydanio rerio*). Nature *291*, 293-296.

283. Streisinger,G., Singer,F., Walker,C., Knauber,D., and Dower,N. (1986). Segregation analyses and gene-centromere distances in zebrafish. Genetics *112*, 311-319.

284. Suitsu,N. (1920). Comparative studies on the growth of the corpus callosum. (1920). J. Comp. Neurol. *32*, 35-60.

285. Summerton,J. (1999). Morpholino antisense oligomers: the case for an RNase H-independent structural type. Biochim. Biophys. Acta *1489*, 141-158.

286. Swiercz,J.M., Kuner,R., Behrens,J., and Offermanns,S. (2002). Plexin-B1 directly interacts with PDZ-RhoGEF/LARG to regulate RhoA and growth cone morphology. Neuron *35*, 51-63.

287. Taguchi,A., Wanaka,A., Mori,T., Matsumoto,K., Imai,Y., Tagaki,T., and Tohyama,M. (1996). Molecular cloning of novel leucine-rich repeat proteins and their expression in the developing mouse nervous system. Brain Res. Mol. Brain Res. *35*, 31-40.

288. Takahashi,T., Fournier,A., Nakamura,F., Wang,L.H., Murakami,Y., Kalb,R.G., Fujisawa,H., and Strittmatter,S.M. (1999). Plexin-neuropilin-1 complexes form functional semaphorin-3A receptors. Cell *99*, 59-69.

289. Takasu,M.A., Dalva,M.B., Zigmond,R.E., and Greenberg,M.E. (2002). Modulation of NMDA receptor-dependent calcium influx and gene expression through EphB receptors. Science *295*, 491-495.

290. Takeda,S., Yonekawa,Y., Tanaka,Y., Okada,Y., Nonaka,S., and Hirokawa,N. (1999). Left-right asymmetry and kinesin superfamily protein KIF3A: new insights in determination of laterality and mesoderm induction by kif3A-/- mice analysis. J. Cell Biol. *145*, 825-836.

291. Talbot,W.S. and Hopkins,N. (2000). Zebrafish mutations and functional analysis of the vertebrate genome. Genes Dev. *14*, 755-762.

292. Tamagnone,L., Artigiani,S., Chen,H., He,Z., Ming,G.I., Song,H., Chedotal,A., Winberg,M.L., Goodman,C.S., Poo,M., Tessier-Lavigne,M., and Comoglio,P.M. (1999). Plexins are a large family of receptors for transmembrane, secreted, and GPI-anchored semaphorins in vertebrates. Cell *99*, 71-80.

293. Tamagnone,L. and Comoglio,P.M. (2000). Signalling by semaphorin receptors: cell guidance and beyond. Trends Cell Biol. *10*, 377-383.

294. Taniguchi,M., Yuasa,S., Fujisawa,H., Naruse,I., Saga,S., Mishina,M., and Yagi,T. (1997). Disruption of semaphorin III/D gene causes severe abnormality in peripheral nerve projection. Neuron *19*, 519-530.

295. Tear,G., Harris,R., Sutaria,S., Kilomanski,K., Goodman,CS., Seeger,MA. (1996). Commissureless controls growth cone guidance across the CNS midline in *Drosophila* and encodes a novel transmembrane protein. Neuron *16* (3), 501-14.

296. Tear,G. (1999). Axon guidance at the central nervous system midline. Cell Mol. Life Sci. *55*, 1365-1376.

297. Tessier-Lavigne,M. and Goodman,C.S. (1996). The molecular biology of axon guidance. Science *274*, 1123-1133.

298. Thisse,B., Wright,C.V., and Thisse,C. (2000). Activin- and Nodal-related factors control antero-posterior patterning of the zebrafish embryo. Nature *403*, 425-428.

299. Tian,J., Yam,C., Balasundaram,G., Wang,H., Gore,A., and Sampath,K. (2003). A temperature-sensitive mutation in the nodal-related gene *cyclops* reveals that the floor plate is induced during gastrulation in zebrafish. Development *130*, 3331-3342.

300. Towbin,H., Staehelin,T., and Gordon,J. (1979). Electrophoretic transfer of proteins from polyacrylamide gels to nitrocellulose sheets: procedure and some applications. Proc. Natl. Acad. Sci. U. S. A *76*, 4350-4354.

301. Trevarrow,B., Marks,D.L., and Kimmel,C.B. (1990). Organization of hindbrain segments in the zebrafish embryo. Neuron *4*, 669-679.

302. Trowe,T., Klostermann,S., Baier,H., Granato,M., Crawford,A.D., Grunewald,B., Hoffmann,H., Karlstrom,R.O., Meyer,S.U., Müller,B., Richter,S., Nüsslein-Volhard,C., and Bonhoeffer,F. (1996). Mutations disrupting the ordering and topographic mapping of axons in the retinotectal projection of the zebrafish, *Danio rerio*. Development *123*, 439-450.

303. Tuzi,N.L. and Gullick,W.J. (1994). Eph, the largest known family of putative growth factor receptors. Br. J. Cancer *69*, 417-421.

304. van Eeden,F.J., Granato,M., Schach,U., Brand,M., Furutani-Seiki,M., Haffter,P., Hammerschmidt,M., Heisenberg,C.P., Jiang,Y.J., Kane,D.A., Kelsh,R.N., Mullins,M.C., Odenthal,J., Warga,R.M., Allende,M.L., Weinberg,E.S., and Nüsslein-Volhard,C. (1996). Mutations affecting somite formation and patterning in the zebrafish, *Danio rerio*. Development *123*, 153-164.

305. van Straaten,H.W. and Copp,A.J. (2001). Curly tail: a 50-year history of the mouse spina bifida model. Anat. Embryol. (Berl) *203*, 225-237.

306. Varela-Echavarria,A., Tucker,A., Puschel,A.W., and Guthrie,S. (1997). Motor axon subpopulations respond differentially to the chemorepellents netrin-1 and semaphorin D. Neuron *18*, 193-207.

307. Varga,Z.M., Amores,A., Lewis,K.E., Yan,Y.L., Postlethwait,J.H., Eisen,J.S., and Westerfield,M. (2001). Zebrafish *smoothened* functions in ventral neural tube specification and axon tract formation. Development *128*, 3497-3509.

308. Varlet,I., Collignon,J., and Robertson,E.J. (1997). *nodal* expression in the primitive endoderm is required for specification of the anterior axis during mouse gastrulation. Development *124*, 1033-1044.

309. Von Szily,A. (1912). Über die einleitenden Vorgange bei der ersten Entstehung der nervenfasern im nervous opticus. Graefes Arch. Opthalmol. *81*, 67-86.

310. Vos,P., Hogers,R., Bleeker,M., Reijans,M., van de,L.T., Hornes,M., Frijters,A., Pot,J., Peleman,J., and Kuiper,M. (1995). AFLP: a new technique for DNA fingerprinting. Nucleic Acids Res. *23*, 4407-4414.

311. Walker,C. (1999). Haploid screens and gamma-ray mutagenesis. Methods Cell Biol. *60*, 43-70.

312. Walsh,F.S., and Doherty,P. (1997). Neural cell adhesion molecules of the immunoglobulin superfamily: role in axon growth and guidance. Annu. Rev. Cell Dev. Biol. *13*, 425-456.

313. Wang,H., Long,Q., Marty,S.D., Sassa,S., and Lin,S. (1998). A zebrafish model for hepatoerythropoietic porphyria. Nat. Genet. *20*, 239-243.

314. Wang,X., Xiao,Y., Mou,Y., Zhao,Y., Blankesteijn,W.M., and Hall,J.L. (2002). A role for the beta-catenin/T-cell factor signaling cascade in vascular remodeling. Circ. Res. *90*, 340-347.

315. Weigel,D., Jurgens,G., Kuttner,F., Seifert,E., and Jackle,H. (1989). The homeotic gene *fork head* encodes a nuclear protein and is expressed in the terminal regions of the *Drosophila* embryo. Cell *57*, 645-658.

316. Westerfield,M. (1993). *The Zebrafish Book*: Eugene, Oregon: University of Oregon Press.

317. Westerfield,M. (1994). *The Zebrafish Book*, edition 2.1. Eugene, Oregon: University of Oregon Press.

318. Whitehead,J.L., Wang,S.Y., Bost-Usinger,L., Hoang,E., Frazer,K.A., and Burnside,B. (1999). Photoreceptor localization of the KIF3A and KIF3B

subunits of the heterotrimeric microtubule motor kinesin II in vertebrate retina. Exp. Eye Res. *69*, 491-503.

319. Wilkinson,D.G. (2001). Multiple roles of Eph receptors and ephrins in neural development. Nat. Rev. Neurosci. *2*, 155-164.

320. Wilson,S.W., Ross,L.S., Parrett,T., and Easter,S.S., Jr. (1990). The development of a simple scaffold of axon tracts in the brain of the embryonic zebrafish, *Brachydanio rerio*. Development *108*, 121-145.

321. Winberg,M.L., Noordermeer,J.N., Tamagnone,L., Comoglio,P.M., Spriggs,M.K., Tessier-Lavigne,M., and Goodman,C.S. (1998). Plexin A is a neuronal semaphorin receptor that controls axon guidance. Cell *95*, 903-916.

322. Winberg,M.L., Tamagnone,L., Bai,J., Comoglio,P.M., Montell,D., and Goodman,C.S. (2001). The transmembrane protein Off-track associates with Plexins and functions downstream of Semaphorin signaling during axon guidance. Neuron *32*, 53-62.

323. Winslow,J.W., Moran,P., Valverde,J., Shih,A., Yuan,J.Q., Wong,S.C., Tsai,S.P., Goddard,A., Henzel,W.J., Hefti,F., and . (1995). Cloning of AL-1, a ligand for an Eph-related tyrosine kinase receptor involved in axon bundle formation. Neuron *14*, 973-981.

324. Wong,K., Ren,X.R., Huang,Y.Z., Xie,Y., Liu,G., Saito,H., Tang,H., Wen,L., Brady-Kalnay,S.M., Mei,L., Wu,J.Y., Xiong,W.C., and Rao,Y. (2001). Signal transduction in neuronal migration: roles of GTPase activating proteins and the small GTPase Cdc42 in the Slit-Robo pathway. Cell *107*, 209-221.

325. Woo,K. and Fraser,S.E. (1995). Order and coherence in the fate map of the zebrafish nervous system. Development *121*, 2595-2609.

326. Woods,I.G., Kelly,P.D., Chu,F., Ngo-Hazelett,P., Yan,Y.L., Huang,H., Postlethwait,J.H., and Talbot,W.S. (2000). A comparative map of the zebrafish genome. Genome Res. *10*, 1903-1914.

327. Xiao,T., Shoji,W., Zhou,W., Su,F., and Kuwada,J.Y. (2003). Transmembrane Sema4E Guides Branchiomotor Axons to Their Targets in Zebrafish. J. Neurosci. *23*, 4190-4198.

328. Xu,Q., Alldus,G., Holder,N., and Wilkinson,D.G. (1995). Expression of truncated Sek-1 receptor tyrosine kinase disrupts the segmental restriction of gene expression in the *Xenopus* and zebrafish hindbrain. Development *121*, 4005-4016.

329. Xu,Q., Alldus,G., Macdonald,R., Wilkinson,D.G., and Holder,N. (1996). Function of the Eph-related kinase rtk1 in patterning of the zebrafish forebrain. Nature *381*, 319-322.

330. Yamada,T., Pfaff,S.L., Edlund,T., and Jessell,T.M. (1993). Control of cell pattern in the neural tube: motor neuron induction by diffusible factors from notochord and floor plate. Cell *73*, 673-686.

331. Yamamoto,M., Meno,C., Sakai,Y., Shiratori,H., Mochida,K., Ikawa,Y., Saijoh,Y., and Hamada,H. (2001). The transcription factor FoxH1 (FAST) mediates Nodal signaling during anterior-posterior patterning and node formation in the mouse. Genes Dev. *15*, 1242-1256.

332. Yan,Y.L., Hatta,K., Riggleman,B., and Postlethwait,J.H. (1995). Expression of a type II collagen gene in the zebrafish embryonic axis. Dev. Dyn. *203*, 363-376.

333. Yan,Y.L., Talbot,W.S., Egan,E.S., and Postlethwait,J.H. (1998). Mutant rescue by BAC clone injection in zebrafish. Genomics *50*, 287-289.

334. Yee,C.S., Chandrasekhar,A., Halloran,M.C., Shoji,W., Warren,J.T., and Kuwada,J.Y. (1999). Molecular cloning, expression, and activity of zebrafish semaphorin Z1a. Brain Res. Bull. *48*, 581-593.

335. Yoshikawa,S., Bonkowsky,J.L., Kokel,M., Shyn,S., and Thomas,J.B. (2001). The Derailed guidance receptor does not require kinase activity *in vivo*. J. Neurosci. *21*, Rapid Communication 119.

336. Yoshikawa,S., McKinnon,R.D., Kokel,M., and Thomas,J.B. (2003). Wnt-mediated axon guidance via the *Drosophila* Derailed receptor. Nature *422*, 583-588.

337. Yu,H.H., Araj,H.H., Ralls,S.A., and Kolodkin,A.L. (1998). The transmembrane Semaphorin Sema I is required in *Drosophila* for embryonic motor and CNS axon guidance. Neuron *20*, 207-220.

338. Yu,T.W. and Bargmann,C.I. (2001). Dynamic regulation of axon guidance. Nat. Neurosci. *4 Suppl*, 1169-1176.

339. Yu,T.W., Hao,J.C., Lim,W., Tessier-Lavigne,M., and Bargmann,C.I. (2002). Shared receptors in axon guidance: SAX-3/Robo signals via UNC-34/Enabled and a Netrin-independent UNC-40/DCC function. Nat. Neurosci. *5*, 1147-1154.

340. Yuan,W., Zhou,L., Chen,J.H., Wu,J.Y., Rao,Y., and Ornitz,D.M. (1999). The mouse Slit family: secreted ligands for Robo expressed in patterns that suggest a role in morphogenesis and axon guidance. Dev. Biol. *212*, 290-306.

341. Zallen,J.A., Yi,B.A., and Bargmann,C.I. (1998). The conserved immunoglobulin superfamily member SAX-3/Robo directs multiple aspects of axon guidance in *C. elegans*. Cell *92*, 217-227.

342. Zhang,J., Talbot,W.S., and Schier,A.F. (1998). Positional cloning identifies zebrafish one-eyed pinhead as a permissive EGF-related ligand required during gastrulation. Cell *92*, 241-251.

343. Zhong,T.P., Kaphingst,K., Akella,U., Haldi,M., Lander,E.S., and Fishman,M.C. (1998). Zebrafish genomic library in yeast artificial chromosomes. Genomics *48*, 136-138.

344. Zhou,L., Schnitzler,A., Agapite,J., Schwartz,L.M., Steller,H., and Nambu,J.R. (1997). Cooperative functions of the reaper and head involution defective genes in the programmed cell death of *Drosophila* central nervous system midline cells. Proc. Natl. Acad. Sci. U. S. A *94*, 5131-5136.

345. Zou,Y., Stoeckli,E., Chen,H., and Tessier-Lavigne,M. (2000). Squeezing axons out of the gray matter: a role for Slit and Semaphorin proteins from midline and ventral spinal cord. Cell *102*, 363-375.

9. Appendix

9.1 Mapping primers

Table 9.1.1 *Monorail* mapping primers on LG 17

SSLP	Position on MGH panel/cM	Forward primer (5'→3')	Reverse primer (5'→3')	Tü product size/bp
Z1490	15.1	TGGTGTCCATGTAAACGTGC	ACACTGCTGGAGGAGATGCT	135
Z22083	24.6	GCACATTGTAGCTCGCTCTG	CTCAGACCACCACCTGTCCT	195
Z22674	29.9	AAAGTCTTTAGGCCTTTTACAATGA	CGTTCCCAGATGCTTTCAAT	163
Z15738	34.2	TCTGAAACATTAGCCCAGGC	GGTGGCACAAAACCTGAAGT	—
Z24008	37.1	CCGTGAAGGTCGGTCTTTAA	GCGTTCAGCAGCACTATCAG	—
Z23501	39.2	GAAGCTTGGAGGATCAGTGC	GTCAAACTCTTCCACTCGCC	—
Z31650	40.8	AGATGCACCACACGACAAGA	CTGTGTGTTGGCTGCTCAGT	—
Z13557	40.9	AGCACTGCCTGATACCGTCT	TTGATGTGCTCTGCTTGGAC	254
Z9847	40.9	GGGCCAGACCAATTAGAACA	GTGTTGGCTGCTCAGTTCAA	215
Z21703	49.8	CACAATCAGATTAAAATCCGCA	ATCGCTGGAATTACCACCAC	139
Z21194	54.5	AGTTCACCTTGAGGCCCTTT	ATGCTTTTCTCTCTGCGCTC	165
Z3894	54.5	ACACGCTGTATGTCAGCTGC	CCCTCTCTGAGACAGTATGCG	—
Z14082	54.5	ACACGCTGTATGTCAGCTGC	CCCTCTCTGAGACAGTATGCG	—
Z4053	57.1	TGGCGACATCTGCGATGTTT	GGAAAGCGTCTGCCTCACGT	—
Z4862	75.2	GTCCACAGATGGACCGAAGT	TGATTCTGTCCTGAAAGAGCC	173
Z3123	78.7	CCTATGGGGAGTCCTGTGAACC	CTTCTGGCCTGTGCGGATTC	—

Table 9.1.2 *Shrink* mapping primers on LG 6

SSLP	Position on MGH panel/cM	Forward primer (5'→3')	Reverse primer (5'→3')	Tü product size/bp
Z6767	47.8	AGGCCGGTAGCAATAATCAA	CCCTTCCGTATTGGGAATTC	212
Z12094	49.0	ATCAGACCACAGACATGCCA	GCAATGACAGTTGGTTGACAA	—
Z53452	49.3	ACAGAGCTGGGTGCATCTCT	TGGGTAGGCTAAATTCTCCG	—
Z10183	51.3	CCGACATGGACAGACAATTG	TGTGTCCTGTTGGGGATACA	245
Z14826	53.6	ACTTTGCCCCCTCTTTTGTT	AATGTTCCAAAAGGCACAGG	—
Z22745	54.9	TGCTCAAACCAGCAACAGAC	CCCTCTGTTGACTAGTCCCC	216

Table 9.1.3 *Otter* mapping primers on LG 14

SSLP	Position on MGH panel/cM	Forward primer (5'→3')	Reverse primer (5'→3')	Tü product size/bp
Z7043	10.5	TGCACATTCCTTCCAGAACA	GCCAGAAAACTGAGCAGACC	185
Z9857	10.5	ACTCTCACGCATACACGCAC	CAGCTGATGTCCACATGATAGC	215
Z11513	10.5	AAAGTTTCCAGGGCAAAGGT	TTTCCATGTGTTGTGCCACT	180
Z5436	12.0	GATAAATGGAGGACGGCAGA	TTTTTCCGTAGAGGGTGTGG	—
Z20072	12.0	ACTGTGTGCACATCACCTCC	CTGGCGCTCACACTGTATGT	178
Z8873	16.7	AAGACACACATGCAAAAGCG	TCTCTGGCTGTCATTGTGCT	—
Z12087	21.3	TGGAGGGAGAGATGATCCAC	AATGCTGAAAATGCAAACCA	—
Z1536	21.4	GTGGCTGTAATGCGTTCAGA	GCACACATCTGGGGAAAACT	213
Z3259	21.4	TGATAATTGCAGGGGGCTAG	TGATCCACAGCGAATAGTGC	—
Z8435	27.4	TTTGCCTCTTTTCTGAGGGA	ACGCATTGCAACCAATAACA	152
Z7030	32.9	ACAGGAATTGGCAGTCATCC	GATGAACCCTTGACCCTCAA	129
Z5435	34.6	CCTTGTGCCCCTCAAATG	AACAGTCATGGGAGGGAATG	—
Z22107	58.3	AGCGTTAGTGTGACAGGGCT	TTTTACAGCGGGGCTTACAC	129

Table 9.1.4 *Eisspalte* mapping primers on LG 14

SSLP	Position on MGH panel/cM	Forward primer (5'→3')	Reverse primer (5'→3')	Tü product size/bp
Z5435	34.6	CCTTGTGCCCCTCAAATG	AACAGTCATGGGAGGGAATG	—
Z22128	49.8	GGAGCAGGAATTCATTTCCA	GTGGTCCATGAGTGCATCTG	270
Z23266	51.3	GCAGCGTAAATCTTGGACAA	GCACATATTTCATCCTCGGC	—
Z9057	52.5	CAGAAACATTCCATGTGCCA	TCCACCCATTTGGCATATCT	144
Z1226	60.6	GTGTTGACATATGGCCCTCC	GCCGAGGCAAATATTTTCAA	—
Z4701	64.0	CAGACTCCAGCCGTATGGAT	GAGCCGCTCTCTTCTCTTGA	—
Z31366	65.2	TAGCGTAACTGACTGGCTGC	ACCATAACGAGGTTTGTGCC	—
Z15804	66.8	TAGCGTAACTGACTGGCTGC	GTTTGTGCCAAAGCAGAACA	—
Z6011	80.1	TCCCCACCAGGATATAGGAA	TGATTTACAGCCATGTCGGA	168
Z6666	80.1	TGCTGCTGATGATGTGACAA	TTTAATAGGTCACAGCACACGC	157
Z6756	80.1	TGATTTACAGCCATGTCGGA	CCTATGAGTGTCCCCACCAG	181
Z3984	84.8	TGACATGTGCTCATGCTTGA	CCACAAAAACCACATGATGG	—
Z27137	90.8	TGGTCTCCTGGAAGTTTGCT	TTAGCTTCACGCTGTCATGC	—
Z1801	91.9	ATTCAGCAGCCGAGCAGA	TCGACATGGGTAACGAGAGA	—

The annealing temperature of all mapping primers is 60 °C
— = Tü product size not determined
Source:
Position of SSLP on MGH panel from http://zfin.org
SSLP sequences and product sizes from http://zebrafish.mgh.harvard.edu

9.2 Sequencing primers

Table 9.2.1 *foxA1* gene primers (GenBank accession number AF052250)

Primer name	Sequence (5'→3')	GC content (%)	Tm (°C)
F7REV2	GATGTATTGAGAACAGGCC	47	44
F7FWD2	TCCTCCATAATGTTGGGCG	52	46
Fkd 7 fwd1	CTGCATGTGCACGAGCTGTGGATTTCCTC	55	59
Fkd 7 fwd2	ATGTTGGGCGCAGTGAAAATGGAAGGAC	50	56
Fkd 7 rev1	CAGTTCCTTTTGCACCAAGTGCATGCC	51	56
Fkd 7 rev2	CGTGGCAATGACTACGATGTATTGAGAAC	44	55
fkd7	CTCCCATGACGAACAGCAG	57	48
fkd7 2	ATGGCGTTCAGGTTGGACG	57	48
fkd7 3	AGTAGGAGCCTTTTCCCGG	57	48
fkd7 4	GTTTGCCTCTGGTCTGTCG	57	48
FKD7 FWD	ATGTGCACGAGCTGTGGATTTCCTC	52	54
FKD7 REV	GTTCCTTTTGCACCAAGTGCATGCC	52	54
Fkd 7 fwd (F)	TGCGACAAAAAGTTGCCCG	52	46
Fkd 7 fwd (C)	GATGTATTGAGAACAGGCC	47	44
FKD7FWD	TACTACCGTCAGAACCAGC	52	46
FKD7FWD2	TTACTCCTTCAACCACCCG	52	46
fkd7 fwd	ACCCCTACACCAGCATGAG	57	48
fkd7 fwd2	TGCGACAAAAAGTTGCCCG	52	46

Table 9.2.2 *foxA2* gene primers

GenBank accession number NM_130949

Coding sequence region 181-1410 bp.

Primer name (position in sequence/bp)	Sequence (5'→3')	GC content (%)	Tm (°C)
Axial reverse (306)	CCGGACATAGTCATGTAAGTG	47	47
Axial genomic fwd (585)	CAGATCGAGAGATCCGAAGAC	49	49
Axial genomic rev (798)	CGGAGAGCGCGGAACTTTCAG	61	53
AXIAL FWD2 (123)	TACAGGCATTTCTCGTGTGGGGAAGCG	55	58
AXIAL REV2 (1383)	GTTTAGGAAGAGTTCAGGATGGGCCTGGAG	53	59
AXIAL FWD1 (174)	TTCCAGGATGCTCGGTGCTGTCAAAATGG	51	58
AXIAL REV1 (1403)	GTCACAAGGTCCAAGAGAGTTTAGGAAG	46	55
axial fwd3 (366)	GAACATGTCCTATGTCAACAC	42	45
axial fwd4 (526)	CTAACCTCGTACAGCAACATG	47	47
axial fwd5 (774)	AGCAATCACCCAGTAAGATGC	47	47
axial fwd6 (936)	ACTAAGCAAGGATCCGAGTCG	52	49
axial fwd7 (1055)	TGTCTGACATGAAGTCGGGTC	52	49
axial fwd8 (1168)	CTGAAGCCAGAACATCACTAC	47	47
axial rev2 (1214)	TGCTCCGAGGACATTAGGTTG	52	49
axial rev3 (1055)	ACCCGACTTCATGTCAGACAG	52	49
axial rev4 (915)	TTCTTATCGCACTTGAAGCGC	47	47
axial rev5 (579)	GGATCTCTCGATCTGTTTATG	42	45
axial rev6 (366)	GTGTTGACATAGGACATGTTC	42	45

Table 9.3 *foxA2* mapping, restriction digest and genescan primers

Primer name	Sequence (5'→3')	Tm (°C)
axial polymorphism 1	GACATACGAGCAAGTGATGCA	47
axial polymorphism 2	GCGAAAAAAGTCCAAATAACA	41
axial modified fwd	CTAATAACCATGGCCATCCTG	47
axial modified rev	TCTCGGAGCTGCTGTTTGATC	49
axial labelled	FAM-TCTCGGAGCTGCTGTTTGATC	59

9.4 Websites used: URLs and description of contents

- **Zebrafish Genome Resources on NCBI**

  http://www.ncbi.nlm.nih.gov/genome/guide/D_rerio.html

  Zebrafish meiotic maps, radiation hybrid maps, mutagenesis projects

- **NCBI Map Viewer**

  http://www.ncbi.nlm.nih.gov/cgi-bin/Entrez/map_search?chr=zfish.inf

  Graphical representation of integrated zebrafish genetic and RH maps

- **Zebrafish Information Network (ZFIN)**

  http://zfin.org

  Searches for mutant lines, wild-types, genes, gene expression data, mapping panels and genetic markers including cloned genes, RAPDs, SSLPs, RFLPs, STSs, ESTs and mapped mutations.

  Anatomical atlas provides detailed images of zebrafish developmental stages and allows annotation of gene expression data.

- **Microsatellite marker database**

  http://zebrafish.mgh.harvard.edu/

  Search for marker sequence, PCR primers, BLAST results, mapping information and strain product size.

- **Regions of conserved synteny between human and zebrafish**

  http://zebrafish.stanford.edu/genome/refmaps/refhomology/Table2.html

- **Zebrafish orthologues of human genes**

  http://134.174.23.160/HumanblastZebrafish/

- **Ensembl Trace Archive**

  http://www.trace.ensembl.org/

  http://www.sanger.ac.uk/Projects/D_rerio/mapping.shtml

  Access of genomic sequence data from the Sanger Institute